PragueMedical
REPORT

(Sborník lékařský)

Reviews

Primary Scientific Studies

Case Reports

Instructions to Authors

Contents

D

C

B

E

Fig. 7.

B

C

A

Fig. 6.

B

A

Fig. 8.

C

B

A

B

Fig. 2.

D

A

D

E

Fig. 9.

A

E

Prognostic Significance of the Coagulation and Complement Systems in Critical COVID-19 Infection

Amitabha Ray[1], Kristen A. K. Winter[1], Dayalu S. L. Naik[2], Chuku Okorie[3]

[1]College of Medical Science, Alderson Broaddus University, Philippi, United States;
[2]National Institute of Traditional Medicine (ICMR), Belagavi, India;
[3]Union County College, Plainfield, United States

Abstract: Infection with the SARS-CoV-2 virus (COVID-19 disease) can cause a wide range of clinical situations – from an asymptomatic state to fatal outcomes. In cases of serious clinical manifestations, the underlying mechanisms involve a number of immune cells and stromal cells as well as their products such as pro-inflammatory interleukin-6 and tumour necrosis factor-alpha that ultimately cause the cytokine storm. The situation of overproduction of pro-inflammatory cytokines is somewhat similar to, though in a mild form, health conditions in obesity and related metabolic disorders like type-2 diabetes, which are also considered important risk factors for severe illness in COVID-19. Interestingly, neutrophils perhaps play a significant role in this pathogenesis. On the other hand, it is thought that COVID-19-related critical illness is associated with pathological hyperactivity of the complement system and coagulopathy. Although the precise molecular interactions between the complement and coagulation systems are not clear, we observe an intimate cross-talk between these two systems in critically ill COVID-19 patients. It is believed that both of these biological systems are connected with the cytokine storm in severe COVID-19 disease and actively participate in this vicious cycle. In order to hinder the pathological progression of COVID-19, a number of anticoagulation agents and complement inhibitors have been used with varying success. Among these drugs, low molecular weight heparin enoxaparin, factor Xa inhibitor apixaban, and complement C5 inhibitor eculizumab have been commonly used in patients with COVID-19. Our overall experience might help us in the future to tackle any such conditions.

Mailing Address: Assoc. Prof. Amitabha Ray, MD., PhD., College of Medical Science, Alderson Broaddus University, 101 College Hill Drive, Philippi, WV 26416, United States; Phone: 1 304 457 6587; Fax: 1 304 457 6308; e-mails: ray.amit213@gmail.com, raya@ab.edu

Introduction

In the latest coronavirus (COVID-19) pandemic, where the causative agent SARS-CoV-2 has been spreading and evolving currently in a milder form, an important pathogenesis-related issue is the understanding of the specific role of the immune system. Although only a small percentage of COVID-19 patients usually develop serious clinical manifestations, different studies have reported a condition of hyper-inflammation or cytokine storm that could produce a grave condition, the acute respiratory distress syndrome (ARDS) (de la Rica et al., 2020). It is believed that imbalanced production of various cytokines and their dysregulated or excess activities are responsible for the adverse clinical outcomes; and this cytokine storm can affect other organs besides the lungs, leading to multi-organ failure.

Perhaps, one of the most important cytokines, which may participate prominently in the above-mentioned hyper-inflammation, is interleukin-6 (IL-6). Interestingly, in one study, the mean IL-6 concentration was shown to be 2.9-fold higher in patients with complicated COVID-19 than patients with uncomplicated illness (Coomes and Haghbayan, 2020). IL-6 is a pleiotropic cytokine, mainly produced by a number of stromal cells and immune cells, including monocytes or macrophages, and it has multifaceted effects on inflammation and immune responses. Many investigators believe that SARS-CoV-2 induces the biosynthesis of IL-6 along with other pro-inflammatory cytokines, which are the significant mediators for lung injury, disease severity, and mortality (Hedrick et al., 2020). On the other hand, pro-inflammatory cytokines such as IL-6 and tumour necrosis factor α (TNF-α) probably play a significant role in obesity and insulin resistance (Bastard et al., 2006). Remarkably, both obesity and insulin resistance (or type-2 diabetes) are considered as risk factors for the development of severe disease, and mortality in SARS-CoV-2 infection (Cevik et al., 2020).

Studies have shown cooperation between IL-6 and neutrophil functions (Fielding et al., 2008; Mateer et al., 2018). In a study in Italy, bronchoalveolar lavage was examined from 33 adult patients with SARS-CoV-2 infection (Pandolfi et al., 2020). The patients admitted to the intensive care unit (ICU) showed higher IL-6 and IL-8 levels, as well as a marked increase in neutrophils and decreased lymphocyte count. Similarly, another study on 364 patients with COVID-19 from Wuhan, China (from this place, SARS-CoV-2 spread) found higher blood levels of IL-6 and neutrophils among severe and critical patients compared to patients with mild symptoms (Li et al., 2020). Of note, Godkin and Humphreys (2020) have commented that the elevated level of neutrophils along with the raised concentrations of IL-6, IL-10, and C-reactive protein (CRP) suggest a very significant role of innate cells (like neutrophils) in the pathogenesis of severe disease in SARS-CoV-2 infection. Consequently, it could be assumed that neutrophils may intensify disease-associated injury (Borges et al., 2020). Moreover, besides the movement to the site of inflammation for phagocytosis of pathogenic agents including viruses, neutrophils can

modify the adaptive immune responses by supporting bidirectional cross-talk with T-lymphocytes.

The neutrophil to lymphocyte ratio (NLR) is an indicator of inflammation. Several studies have demonstrated that an increase in NLR was associated with a higher risk for disease severity and death among COVID-19 patients (Basbus et al., 2020; Liu et al., 2020; Tatum et al., 2020). On the other hand, activated neutrophils can release neutrophil extracellular traps (NETs) that are net-like structures composed of chromosomal DNA, histones, and cytoplasmic proteins, including enzymes like myeloperoxidase (MPO) and neutrophil elastase. Interestingly, NETs confine invading microorganisms. However, the overproduction of NETs induces lung injury (Grabcanovic-Musija et al., 2015). After analysing the production of NETs from 32 patients with COVID-19, the investigators concluded a possible detrimental role of NETs in the disease course (Veras et al., 2020). Specifically, they detected higher concentration of NETs in tracheal aspirate, lung tissue, and plasma. Interestingly, a study on 25 patients with COVID-19 in Greece observed that complement activation potentiated the NETs and thrombotic pathway during SARS-CoV-2 infection (Skendros et al., 2020). Of note, complement components C3a and C5a activate neutrophils, monocytes, endothelial cells, and platelets leading to the release of pro-inflammatory cytokines that promotes coagulopathy (Lim and Mcrae, 2021). Furthermore, analyses of clinical specimens from critical COVID-19 patients revealed that complement proteins were upregulated along with IL-6 (which is possibly a marker of disease severity) (D'Alessandro et al., 2020; Alosaimi et al., 2021). A precise knowledge of SARS-CoV-2 infection-related different factors, e.g., immune cells, complement components, pro-inflammatory cytokines, and coagulation proteases, as well as their interactions, would be helpful to understand the underlying pathology of disease severity.

The complement system in COVID-19

We know that complement proteins have a vital function in the immune system in order to protect our health against different pathogenic microorganisms; however, its hyperactivity or disturbances in its normal function can cause tissue damage. Unlike the high mortality rate of MERS-CoV infection (approximately 35%), lower disease severity and death rates have been noticed in COVID-19 cases. It is important to remember that a significant role of the complement system was detected in MERS-CoV infection. Of note, apart from the latest outbreak of SARS-CoV-2, the two other recent outbreaks were due to similar coronaviruses – SARS-CoV (or SARS-CoV-1) and MERS-CoV, which started in China and Saudi Arabia, respectively. Nonetheless, in a study on a DPP4 transgenic (hDPP4-Tg) mouse model (with MERS-CoV infection), the investigators observed that MERS-CoV infection induced over-activation of complement components, which perhaps contributed to pyroptosis, i.e., inflammatory apoptosis, and overall hyper-inflammation (Jiang et al., 2019). In another study on C57BL/6J mice, the investigators utilised C3

knockout/null (C3$^{-/-}$) mice of the matching genetic background (Gralinski et al., 2018). It is notable that the principal complement component C3 plays a central role in complement activation pathways. However, in this study, mice were infected with SARS-CoV-1. Compared to C57BL/6J control mice, the investigators noticed that SARS-CoV-1-infected C3$^{-/-}$ mice displayed significantly less disease severity and a reduced amount of respiratory dysfunction in spite of equivalent viral loads in the lungs of both controls and C3$^{-/-}$ mice. Interestingly, a smaller quantity of neutrophils and monocytes were present in the lungs of C3$^{-/-}$ mice in comparison with C56BL/6J control mice. Furthermore, a reduced amount of lung damage, as well as diminished levels of cytokines were found in both lung tissue and serum samples of C3$^{-/-}$ mice relative to controls. Consequently, this study explained that the involvement of the complement system was associated with lung injury, disease severity, and a systemic pro-inflammatory reaction in cases with SARS-CoV-1 infection (Gralinski et al., 2018). With these above-mentioned examples, it could be said that the complement system also has a significant role in the immune response to SARS-CoV-2 infection, disease severity, and associated hyper-inflammation that adversely affects the functions of multiple organs.

Generally, we know that the complement system functions through 3 pathways: the classical, lectin, and alternative pathways. However, there is another extrinsic pathway where coagulation-related proteases such as thrombin, factor XIIa, plasmin, as well as kallikrein are involved (Figure 1). Moreover, it has been believed that the coagulation factors Xa and XIa, and also plasmin may cleave both C5 and C3, and intensely generate C5a and C3a (i.e., anaphylatoxins) (Amara et al., 2008). It is worth mentioning that initial studies have suggested that the complement system plays a key role in the coagulopathy of severe COVID-19 (Lo et al., 2020). After
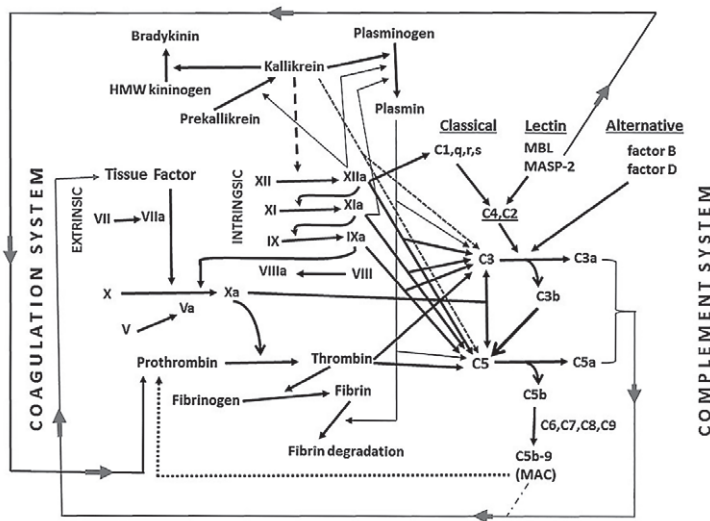
Figure 1 – Interactions between the complement and coagulation systems (MBL – mannose-binding lectin; MASP-2 – mannan-binding lectin serine protease-2; MAC – membrane attack complex [terminal complement complex, i.e., C5b + C6 + C7 + C8 + C9]).

analysing post-mortem lung tissue samples from 5 patients with severe COVID-19 characterised by respiratory failure, the investigators observed significant deposits of terminal complement components C5b-9 (membrane attack complex/MAC), C4d (a split product), and mannose binding lectin (MBL)-associated serine protease (MASP-2) in the microvasculature, along with systemic activation of the complement pathways (Magro et al., 2020). Perhaps, the normal functions of the complement system could be imbalanced in response to the overstimulation of different immune-associated cells such as neutrophils and monocytes or macrophages. Conversely, complement components such as anaphylatoxins (C3a and C5a) and opsonins (C3b, C1q, MBL) can also influence macrophage responses (Bohlson et al., 2014).

The coagulation system in COVID-19

Overall, the complement system's functional abnormalities can cause a number of health problems such as recurrent microbial infections, autoimmune diseases, hereditary angioedema, and atypical haemolytic-uremic syndrome (aHUS) (Tichaczek-Goska, 2012). Activated complement components may mediate hyper-inflammation, coagulation, and tissue damage – all these pathological features can be seen in critical patients with SARS-CoV-2 infection (Figure 2). As mentioned earlier, the presence of coagulopathy is a common feature of severe COVID-19 (Gómez-Mesa et al., 2021). A study on 148 patients with COVID-19 noticed that
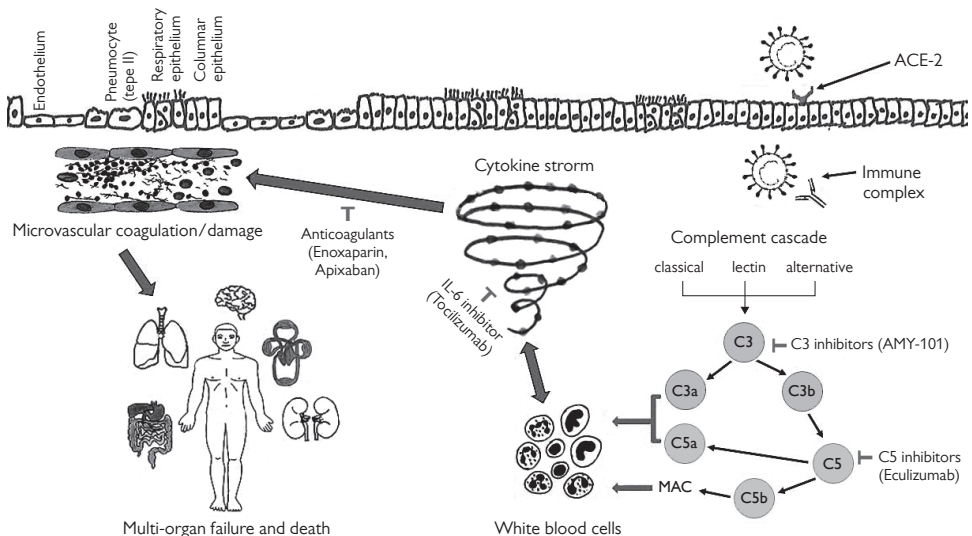
Figure 2 – Inflammatory response via complement activation in COVID-19 disease (ACE-2 – angiotensin converting enzyme-2 [receptor for the SARS-CoV-2 viral entry]; C3a and C5a – anaphylatoxins, primarily induce pro-inflammatory responses; MAC – membrane attack complex; cytokine storm – associated with the elevated levels of several cytokines that include interleukin-1β [IL-1β], IL-6, TNF-α, and macrophage inflammatory protein [MIP]).

the high plasma levels of soluble MAC (or sC5b-9) correlated with von Willebrand factor (vWF) and paralleled disease severity, but these levels diminished during disease remission (Cugno et al., 2021). Another study on 25 patients showed higher plasma levels of NETs, and sC5b-9, as well as increased tissue factor (TF) activity in patients (Skendros et al., 2020). Moreover, patients' neutrophils displayed elevated TF expression and released NETs carrying active TF. In a study conducted by D'Alessandro et al. (2020), several peptides related to both the complement and coagulation systems were increased in COVID-19 patients' sera. The study included 33 COVID-19-positive patients and 16 control subjects (SARS-CoV-2 negative by nasopharyngeal swab). On the other hand, a study examined blood samples from 102 COVID-19-positive patients and 26 negative controls from New York. The investigators applied RNA sequencing and high-resolution mass spectrometry to record 219 molecular features that are relevant to COVID-19 status and severity (Overmyer et al., 2021). They observed increased expression of genes and/or proteins associated with the neutrophil function (like MPO – linked to NETs formation), neutrophil degranulation, platelet activation, vWF, and complement activation. Similarly, a study on 31 SARS-CoV-2 infected patients from Berlin identified 27 potential biomarker expressions, which are connected with disease severity (Messner et al., 2020). Importantly, these biomarkers included complement components of both the classical and alternative pathways (like C1r and CFB), the coagulation system (like fibrinogen), acute-phase reactants (like CRP), and pro-inflammatory cytokine signalling (like IL-6).

COVID-19-related microangiopathy and thrombotic condition
As a part of innate immunity, MBL is a protein that has lectin domains, which can bind to some special carbohydrate groups on the surface of various microorganisms including viruses and activate the complement system. MBL belongs to the collectin protein family that also includes lung surfactant protein A (SP-A) and D (SP-D) (Turner, 2003). In a Swedish study on a cohort of 65 critically ill COVID-19 patients, it was observed that COVID-19 patients had elevated plasma MBL levels compared to healthy controls (n=72) (Eriksson et al., 2020). Furthermore, patients who developed thromboembolic complications (n=9, 14%) had significantly elevated MBL levels than patients without thrombotic problems. Interestingly, MBL was strongly correlated to plasma D-dimer levels (a marker of coagulopathy/degradation product of blood clots in fibrinolysis), but did not exhibit any association with the degree of inflammation. On the other hand, in a study on lung tissue sections from 12 autopsies who died of the severe COVID-19 disease, the investigators documented that dilated vessels of both the venous and arterial system were mostly devoid of viable endothelium (and pneumocytes) and showed focal thrombosis (Magro et al., 2021). Additionally, immunohistochemical staining revealed endothelial and subendothelial deposition of C3d, C4d, and/or C5b-9 (MAC) in the microvasculature of all examined cases, but none of the controls.

Of note, complement component C3's final degradation product is C3d that can augment immune responses, and C4's split product is C4d (from C4b). Similar histopathological findings were also recorded in an *in vivo* experimental model (SARS-CoV-2-infected rhesus macaques). In this study, infected lung tissue sections displayed considerable macrophage infiltration, prominent changes in vascular morphology along with endothelialitis, and the presence of increased vWF (Aid et al., 2020). In addition, the investigators observed increased blood levels of several pro-inflammatory cytokines, complement components, and coagulation factors including platelet activation in infected macaques.

In a study in Spain, the investigators analysed the data from 19 COVID-19 patients admitted to ICU and observed higher levels of fibrinogen and D-dimer among patients at admission (Ibañez et al., 2021). The authors suggested that the primary source of D-dimer could be the lungs. Unlike our typical ideas about sepsis-induced coagulopathy, COVID-19-linked coagulopathy is dissimilar in many aspects. For instance, coagulation parameters such as activated partial thromboplastin time (aPTT), prothrombin time (PT), and platelet count among COVID-19 patients usually display a normal range (Hadid et al., 2021). In contrast, a majority of COVID-19 patients show higher levels of fibrinogen, which exhibit a relationship with IL-6. However, an increased level of D-dimer has been frequently linked with critical illness and mortality, i.e., prognosis (Hadid et al., 2021).

In a study wherein 400 hospitalised COVID-19 patients from the Massachusetts area were evaluated, the venous thromboembolism (VTE) rate was 4.8%, the rate of overall thrombotic complication was 9.5%, and the overall bleeding complication rate was 4.8% (Al-Samkari et al., 2020). Furthermore, a study in China analysed the data of 107 COVID-19 patients; in comparison to patients with mild infection (n=56), severe cases (n=51) had coagulation dysfunction, higher levels of fibrin degradation product and D-dimer, and severe systemic inflammation (Qi et al., 2021). In addition, the patient's D-dimer level was positively correlated with CRP and IL-6. Remarkably, in a meta-analysis, the authors reviewed 2,139 COVID-19 patients from 16 observational studies, and they noticed that coagulation dysfunction was commonly linked with severe cases, elevated mean D-dimer, and higher mortality (Xiang et al., 2021).

Pathological links between the complement and coagulation systems
Like the studies of Magro and her colleagues, which showed activation of complement components and an accompanying triggering of pro-coagulant status in severe COVID-19 disease (Magro et al., 2020, 2021), a number of literature also have suggested a connection between the complement and coagulation pathways in this disease (Chauhan et al., 2020; Ghebrehiwet and Peerschke, 2020; Lo et al., 2020). Interestingly, both complement and coagulation systems work through a common mechanism – sequential amplification of enzyme cascades as a consequence of zymogen activation; and a potential cross-talk exists between these two primitive

biological systems (Figure 1). The shared participation of both complement and coagulation systems has been noticed in diseases such as paroxysmal nocturnal haemoglobinuria (PNH), antiphospholipid syndrome, and aHUS (Dzik, 2019). It is notable that aetiologically, haemolytic-uremic syndrome (HUS) is different from aHUS. Strikingly, HUS is usually linked to Shiga toxin-producing *Escherichia coli* (O157:H7); but this aetiological factor is not associated with aHUS. The formation of thrombi in the renal blood vessels is an important feature in aHUS, along with other pathologies such as complement over-activation, thrombocytopenia, haemolytic anemia, and kidney failure.

Several reports revealed serious complications that were triggered by SARS-CoV-2 infection in patients with a history of aHUS or development of aHUS-like clinical features in COVID-19 patients (Kurian et al., 2021; Gill et al., 2022; Korotchaeva et al., 2022; Leone et al., 2022; Suzuki et al., 2022). Furthermore, the aforementioned reports generally observed a beneficial role of eculizumab, a C5-blocking monoclonal antibody, in the treatment of these patients. On the other hand, a number of reports documented antiphospholipid syndrome or the presence of antiphospholipid antibodies (aPLs) in COVID-19 patients (Yasri and Wiwanitkit, 2020; Zhang et al., 2020; Hollerbach et al., 2021). It may be worth mentioning that antiphospholipid syndrome is characterised by an increased risk of abnormal blood clot formation. Nevertheless, Zhang et al. (2020) recorded coagulopathy and aPLs in their critically ill patients. In another study, Xiao et al. (2020) detected aPLs in 47% (31/66) of critically ill COVID-19 patients' sera, whereas the said antibodies were not present in COVID-19 patients who were not in a critical state (n=13). In addition, Hollerbach et al. (2021) suggested a causative effect of aPLs in coagulopathy of COVID-19. Similarly, Hines et al. (2021) confirmed a diagnosis of PNH in acute COVID-19 infection, and they concluded that COVID-19 spike proteins could trigger the complement components of the alternative pathway, which might cause cellular injuries such as haemolysis, endothelial lesions, and end-organ damage. Moreover, a study in Italy on PNH patients at the time of COVID-19 outbreak concluded that treatment with complement inhibitors (C5 inhibitors – eculizumab, ravulizumab, and crovalimab, as well as factor B inhibitor – iptacopan) might be advantageous in the reduction of thrombo-inflammation, and overall prevention of SARS-CoV-2 infection and related disease severity (Barcellini et al., 2021).

The role of complement inhibitors
Eculizumab is one of the most commonly used complement inhibitors in the treatment of COVID-19 disease. It is a monoclonal antibody, and it inhibits the cleavage of C5 into C5a and C5b and the generation of MAC. It is reasonable to consider that preventing MAC formation could block the chain of subsequent inflammatory responses such as stimulation of inflammatory cells, cytokine storm, and coagulopathy in COVID-19 disease progression (Figure 2). In a study in Italy, 4 COVID-19 patients with severe pneumonia or ARDS were treated

with eculizumab (900 mg intravenously/I.V., up to 4 weekly infusions) along with anticoagulant enoxaparin 4,000 IU/day subcutaneously (Diurno et al., 2020). Successful recovery occurred in all patients, with a decline in inflammatory markers, including CRP level. In another study in France, 45 patients with severe COVID-19 disease received standard care, and 35 were treated with standard treatment protocol plus eculizumab in ICU. For the eculizumab group, the survival rate was 82.9% as compared to 62.2% without eculizumab (Annane et al., 2020). Clearly, a favourable health condition was recorded in patients treated with eculizumab. On the other hand, in a study wherein 8 COVID-19 patients were treated with eculizumab (1 to 3 doses of 900 mg I.V., once a week) in Brazil, and 3 COVID-19 patients with ARDS were treated with compstatin-based C3-targeted AMY-101 (5 mg/kg/daily, I.V. infusion) in Italy (Mastellos et al., 2020). Of note, by binding with C3, cyclic peptide compstatin hinders convertase formation, cleavage of C3, and complement activation. AMY-101 has been derived from Cp40, a 3rd-generation compstatin analogue. Nevertheless, the investigators noticed that both C3 and C5 inhibitors showed an anti-inflammatory response (decline in IL-6 and CRP levels) and noticeable improvement in lung function (Mastellos et al., 2020). Furthermore, a report documented marked improvement of all parameters within two days after the start of AMY-101 treatment in a patient with severe ARDS caused by SARS-CoV-2 infection (Mastaglio et al., 2020). Like eculizumab, another C5 inhibitor ravulizumab, which is used for the treatment of two complement-linked disorders – PNH and aHUS, exhibited diminished levels of serum free C5 in 22 patients with severe COVID-19 disease (McEneny-King et al., 2021). Therefore, overall, complement inhibition displayed significant clinical improvement and therapeutic benefit in COVID-19 patients with serious illnesses.

Anticoagulants in COVID-19
The state of coagulopathy, which is linked with endothelial dysfunction and diffuse microvascular thrombi formation or disseminated intravascular coagulation, displays poor prognosis in COVID-19 cases. In these patients, enoxaparin and apixaban are commonly used anticoagulants. Drugs such as enoxaparin and dalteparin belong to the group of low molecular weight heparin (LMWH), whereas apixaban inhibits free and clot-bound factor Xa and the activity of prothrombinase that catalyses the conversion of prothrombin to thrombin. Interestingly, some investigators have demonstrated that apixaban may also inhibit the activity of SARS-CoV-2 protease M^{pro}, which is associated with the viral replication and pathogenic potentiality (Chaves et al., 2022). Briefly, the results of selected clinical studies on anticoagulant therapy in COVID-19 have been discussed in Table 1.

Conclusion
The COVID-19 pandemic has increased our knowledge and seriousness about the problems of coronavirus disease and relevant pathologies, which may be

Table 1 – Selected studies on anticoagulation for COVID-19 patients

Investigators and place of study	Subjects	Findings in brief
Barco et al. (2022) (Switzerland and Germany)	Outpatients 50 years or older; enoxaparin group (n=234), no thromboprophylaxis group (n=238)	Enoxaparin did not reduce early hospitalisations and deaths
Joanico-Morales et al. (2022) (Mexico)	Patients received enoxaparin – 60 mg (n=44) and 40 mg (n=156)	60 mg dose was associated with a lower risk of death
Morici et al. (2022) (Italy)	Comparing 40 mg BID (n=91) vs. 40 mg OD (n=92) enoxaparin	OD enoxaparin was associated with higher incidence of VTE compared to BID dose. No DVT development, independently of enoxaparin dosing
Abdelwahab et al. (2021) (Egypt)	Control (no aspirin/enoxaparin, n=36), aspirin alone (n=31), enoxaparin alone (n=123), and aspirin-enoxaparin group (n=35)	Concomitant use of aspirin and enoxaparin demonstrated promising results
Albisinni et al. (2022) (Italy)	Enoxaparin was provided to 90/141 patients in either prophylactic dose (n=65) or therapeutic dose (n=25)	No significant difference between patients without anticoagulants and those on prophylactic or therapeutic dose
Assiri et al. (2021) (Saudi Arabia)	Patients were treated with various drugs such as enoxaparin (n=99), dexamethasone (n=93), favipiravir (n=67), and tocilizumab (n=37)	Enoxaparin significantly reduced the length of ICU stay and mortality in patients aged 50–75
Cardillo et al. (2021) (Italy)	Comparing the outcomes between inpatients who used enoxaparin (n=62) and fondaparinux (n=38) as thromboprophylaxis	No significant differences in clinical outcomes between these two groups
Martinelli et al. (2021) (Italy)	Patients on standard prophylaxis dosage of enoxaparin (40 mg daily, n=151) were compared with those who received high doses (1 mg/kg BID, n=127)	Patients treated with high enoxaparin dosages displayed a reduction of mortality, clinical deterioration, and VTE compared to standard dosage
Pawlowski et al. (2021) (United States)	Clinical outcomes at 28 days were compared between patients who received unfractionated heparin (n=441) and patients who received enoxaparin (n=166)	Enoxaparin was associated with lower mortality compared to unfractionated heparin
Sadeghipour et al. (2021) (Iran)	Comparison between intermediate-dose enoxaparin (1 mg/kg daily, n=276) and standard-dose (40 mg daily, n=286), among adult patients admitted to ICU	Results did not show any significant differences

Deitelzweig et al. (2022) (United States)	A total of 7,869 patients with nonvalvular atrial fibrillation and COVID-19 were included: among these patients, 6,676 continued apixaban (discontinuers = 1193)	Patients who discontinued apixaban had a higher risk of hospitalisation and thrombotic events compared to those who continued apixaban
Ananworanich et al. (2022) (United States)	Adults with mild symptoms and at high risk for disease progression – either rivaroxaban 10 mg OD (n=246) or placebo (n=251)	No impact of rivaroxaban on disease progression
Kumar et al. (2022) (India)	Hospitalised patients with mild or moderate disease received either rivaroxaban (10 mg or 15 mg OD, n=115) or enoxaparin (40 mg or 60 mg OD, n=113)	Rivaroxaban was superior to enoxaparin for prophylactic coagulopathy management
Mohamed et al. (2022) (Egypt)	Patients with moderate disease (pneumonia without hypoxia) – enoxaparin group (0.5 mg/kg BID, n=66) and rivaroxaban group (10 mg OD, n=58)	No significant differences were observed between these two groups
Ramacciotti et al. (2022) (Brazil)	Patients were randomly assigned to receive rivaroxaban (n=160) or without anticoagulation therapy (n=160). During hospitalisation, all patients received thromboprophylaxis with standard doses of heparin	Patients with rivaroxaban for 35 days improved clinical outcomes compared to non-extended thromboprophylaxis

apixaban and rivaroxaban – direct-acting oral anticoagulants (DOACs); enoxaparin – low molecular weight heparin (LMWH) and administered subcutaneously; favipiravir – an antiviral used in influenza; fondaparinux – causes antithrombin III-mediated inhibition of factor Xa; tocilizumab – monoclonal antibody against IL-6 receptor; high risk for COVID-19 – aged ≥ 65 years, and with a chronic disease, e.g., lung disease, heart disease, hypertension, cancer, and diabetes (which requires adequate daily management), or obesity; BID – two times a day; DVT – deep vein thrombosis; ICU – intensive care unit; OD – once daily; VTE – venous thromboembolism

helpful in the future as well. This multi-system disease behaves differently during its progression through different stages, viz. viral entry and replication, dissemination, widespread inflammation, and thrombotic microangiopathy/multi-organ damage. The disease processes are linked with several other health problems such as obesity and related metabolic disorders, chronic lung diseases, and immunodeficiency conditions, as well as various body systems including different components of the circulatory system such as endothelium, coagulation factors, and complement proteins. However, the precise understanding of the interplay between the complement and coagulation pathways and their status in coronavirus disease is important to interpret several issues, such as the exact nature of systemic inflammation and the pertinent roles of various cytokines. Accordingly, the favourable treatment strategies could be designed in relation to proper timings and appropriate combination of drugs in order to maximize the therapeutic efficacy.

References

Abdelwahab, H. W., Shaltout, S. W., Sayed Ahmed, H. A., Fouad, A. M., Merrell, E., Riley, J. B., Salama, R., Abdelrahman, A. G., Darling, E., Fadel, G., Elfar, M. S. A., Sabry, K., Shah, J., Amin, H., Nieman, G. F., Mishriky, A., Aiash, H. (2021) Acetylsalicylic acid compared with enoxaparin for the prevention of thrombosis and mechanical ventilation in COVID-19 patients: A retrospective cohort study. *Clin. Drug Investig.* **41**, 723–732.

Aid, M., Busman-Sahay, K., Vidal, S. J., Maliga, Z., Bondoc, S., Starke, C., Terry, M., Jacobson, C. A., Wrijil, L., Ducat, S., Brook, O. R., Miller, A. D., Porto, M., Pellegrini, K. L., Pino, M., Hoang, T. N., Chandrashekar, A., Patel, S., Stephenson, K., Bosinger, S. E., Andersen, H., Lewis, M. G., Hecht, J. L., Sorger, P. K., Martinot, A. J., Estes, J. D., Barouch, D. H. (2020) Vascular disease and thrombosis in SARS-CoV-2-infected rhesus macaques. *Cell* **183**, 1354–1366.

Albisinni, R., Vitrone, M., Ursi, M. P., Spiezia, S., Salemme, A., Florio, L. L., Boccia, F., Iossa, D., Zampino, R., Atripaldi, L., Squillante, F., Maturo, N., Franganza, F., Severino, S., Punzi, R., Fiorentino, G. (2022) Clinical evaluation of the safety and efficacy of enoxaparin in patients with COVID-19. *Blood Transfus.* **20**, 495–504.

Alosaimi, B., Mubarak, A., Hamed, M. E., Almutairi, A. Z., Alrashed, A. A., AlJuryyan, A., Enani, M., Alenzi, F. Q., Alturaiki, W. (2021) Complement anaphylatoxins and inflammatory cytokines as prognostic markers for COVID-19 severity and in-hospital mortality. *Front. Immunol.* **12**, 668725.

Al-Samkari, H., Karp Leaf, R. S., Dzik, W. H., Carlson, J. C. T., Fogerty, A. E., Waheed, A., Goodarzi, K., Bendapudi, P. K., Bornikova, L., Gupta, S., Leaf, D. E., Kuter, D. J., Rosovsky, R. P. (2020) COVID-19 and coagulation: Bleeding and thrombotic manifestations of SARS-CoV-2 infection. *Blood* **136**, 489–500.

Amara, U., Rittirsch, D., Flierl, M., Bruckner, U., Klos, A., Gebhard, F., Lambris, J. D., Huber-Lang, M. (2008) Interaction between the coagulation and complement system. *Adv. Exp. Med. Biol.* **632**, 71–79.

Ananworanich, J., Mogg, R., Dunne, M. W., Bassyouni, M., David, C. V., Gonzalez, E., Rogalski-Salter, T., Shih, H., Silverman, J., Medema, J., Heaton, P. (2022) Randomized study of rivaroxaban vs placebo on disease progression and symptoms resolution in high-risk adults with mild coronavirus disease 2019. *Clin. Infect. Dis.* **75**, e473–e481.

Annane, D., Heming, N., Grimaldi-Bensouda, L., Frémeaux-Bacchi, V., Vigan, M., Roux, A. L., Marchal, A., Michelon, H., Rottman, M., Moine, P. (2020) Eculizumab as an emergency treatment for adult patients with severe COVID-19 in the intensive care unit: A proof-of-concept study. *EClinicalMedicine* **28**, 100590.

Assiri, A., Iqbal, M. J., Mohammed, A., Alsaleh, A., Assiri, A., Noor, A., Nour, R., Khobrani, M. (2021) COVID-19 related treatment and outcomes among COVID-19 ICU patients: A retrospective cohort study. *J. Infect. Public Health* **14**, 1274–1278.

Barcellini, W., Fattizzo, B., Giannotta, J. A., Quattrocchi, L., Aydin, S., Barone, F., Carbone, C., Pomponi, F., Metafuni, E., Beggiato, E., Sica, S., Di Bona, E., Lanza, F., Notaro, R., Iori, A. P. (2021) COVID-19 in patients with paroxysmal nocturnal haemoglobinuria: An Italian multicentre survey. *Br. J. Haematol.* **194**, 854–856.

Barco, S., Voci, D., Held, U., Sebastian, T., Bingisser, R., Colucci, G., Duerschmied, D., Frenk, A., Gerber, B., Götschi, A., Konstantinides, S. V., Mach, F., Robert-Ebadi, H., Rosemann, T., Simon, N. R., Spechbach, H., Spirk, D., Stortecky, S., Vaisnora, L., Righini, M., Kucher, N. (2022) Enoxaparin for primary thromboprophylaxis in symptomatic outpatients with COVID-19 (OVID): A randomised, open-label, parallel-group, multicentre, phase 3 trial. *Lancet Haematol.* **9**, e585–e593.

Basbus, L., Lapidus, M. I., Martingano, I., Puga, M. C., Pollán, J. (2020) Neutrophil to lymphocyte ratio as a prognostic marker in COVID-19. *Medicina (B. Aires)* **80**, 31–36 (Suppl. 3). (in Spanish)

Bastard, J. P., Maachi, M., Lagathu, C., Kim, M. J., Caron, M., Vidal, H., Capeau, J., Feve, B. (2006) Recent advances in the relationship between obesity, inflammation, and insulin resistance. *Eur. Cytokine Netw.* **17**, 4–12.

Ray A.; Winter K. A. K.; Naik D. S. L.; Okorie C.

Bohlson, S. S., O'Conner, S. D., Hulsebus, H. J., Ho, M. M., Fraser, D. A. (2014) Complement, c1q, and c1q-related molecules regulate macrophage polarization. *Front. Immunol.* **5**, 402.

Borges, L., Pithon-Curi, T. C., Curi, R., Hatanaka, E. (2020) COVID-19 and neutrophils: The relationship between hyperinflammation and neutrophil extracellular traps. *Mediators Inflamm.* **2020**, 8829674.

Cardillo, G., Viggiano, G. V., Russo, V., Mangiacapra, S., Cavalli, A., Castaldo, G., Agrusta, F., Bellizzi, A., Amitrano, M., Iannuzzo, M., Sacco, C., Lodigiani, C., Fontanella, A., Di Micco, P. (2021) Antithrombotic and anti-inflammatory effects of fondaparinux and enoxaparin in hospitalized COVID-19 patients: The FONDENOXAVID study. *J. Blood Med.* **12**, 69–75.

Cevik, M., Kuppalli, K., Kindrachuk, J., Peiris, M. (2020) Virology, transmission, and pathogenesis of SARS-CoV-2. *BMJ* **371**, m3862.

Chauhan, A. J., Wiffen, L. J., Brown, T. P. (2020) COVID-19: A collision of complement, coagulation and inflammatory pathways. *J. Thromb. Haemost.* **18**, 2110–2117.

Chaves, O. A., Sacramento, C. Q., Fintelman-Rodrigues, N., Temerozo, J. R., Pereira-Dutra, F., Mizurini, D. M., Monteiro, R. Q., Vazquez, L., Bozza, P. T., Castro-Faria-Neto, H. C., Souza, T. M. L. (2022) Apixaban, an orally available anticoagulant, inhibits SARS-CoV-2 replication and its major protease in a non-competitive way. *J. Mol. Cell Biol.* **14**, mjac039.

Coomes, E. A., Haghbayan, H. (2020) Interleukin-6 in Covid-19: A systematic review and meta-analysis. *Rev. Med. Virol.* **30**, 1–9.

Cugno, M., Meroni, P. L., Gualtierotti, R., Griffini, S., Grovetti, E., Torri, A., Lonati, P., Grossi, C., Borghi, M. O., Novembrino, C., Boscolo, M., Uceda Renteria, S. C., Valenti, L., Lamorte, G., Manunta, M., Prati, D., Pesenti, A., Blasi, F., Costantino, G., Gori, A., Bandera, A., Tedesco, F., Peyvandi, F. (2021) Complement activation and endothelial perturbation parallel COVID-19 severity and activity. *J. Autoimmun.* **116**, 102560.

D'Alessandro, A., Thomas, T., Dzieciatkowska, M., Hill, R. C., Francis, R. O., Hudson, K. E., Zimring, J. C., Hod, E. A., Spitalnik, S. L., Hansen, K. C. (2020) Serum proteomics in COVID-19 patients: Altered coagulation and complement status as a function of IL-6 level. *J. Proteome Res.* **19**, 4417–4427.

de la Rica, R., Borges, M., Gonzalez-Freire, M. (2020) COVID-19: In the eye of the cytokine storm. *Front. Immunol.* **11**, 558898.

Deitelzweig, S., Zhu, J., Jiang, J., Luo, X., Keshishian, A., Ferri, M., Rosenblatt, L., Schuler, P., Gutierrez, C., Dhamane, A. D. (2022) Impact of apixaban treatment discontinuation on the risk of hospitalization among patients with nonvalvular atrial fibrillation and COVID-19. *Curr. Med. Res. Opin.* **38**, 1891–1896.

Diurno, F., Numis, F. G., Porta, G., Cirillo, F., Maddaluno, S., Ragozzino, A., De Negri, P., Di Gennaro, C., Pagano, A., Allegorico, E., Bressy, L., Bosso, G., Ferrara, A., Serra, C., Montisci, A., D'Amico, M., Schiano Lo Morello, S., Di Costanzo, G., Tucci, A. G., Marchetti, P., Di Vincenzo, U., Sorrentino, I., Casciotta, A., Fusco, M., Buonerba, C., Berretta, M., Ceccarelli, M., Nunnari, G., Diessa, Y., Cicala, S., Facchini, G. (2020) Eculizumab treatment in patients with COVID-19: Preliminary results from real life ASL Napoli 2 Nord experience. *Eur. Rev. Med. Pharmacol. Sci.* **24**, 4040–4047.

Dzik, S. (2019) Complement and coagulation: Cross talk through time. *Transfus. Med. Rev.* **33**, 199–206.

Eriksson, O., Hultström, M., Persson, B., Lipcsey, M., Ekdahl, K. N., Nilsson, B., Frithiof, R. (2020) Mannose-binding lectin is associated with thrombosis and coagulopathy in critically ill COVID-19 patients. *Thromb. Haemost.* **120**, 1720–1724.

Fielding, C. A., McLoughlin, R. M., McLeod, L., Colmont, C. S., Najdovska, M., Grail, D., Ernst, M., Jones, S. A., Topley, N., Jenkins, B. J. (2008) IL-6 regulates neutrophil trafficking during acute inflammation via STAT3. *J. Immunol.* **181**, 2189–2195.

Ghebrehiwet, B., Peerschke, E. I. (2020) Complement and coagulation: Key triggers of COVID-19-induced multiorgan pathology. *J. Clin. Invest.* **130**, 5674–5676.

Gill, J., Hebert, C. A., Colbert, G. B. (2022) COVID-19-associated atypical hemolytic uremic syndrome and use of eculizumab therapy. *J. Nephrol.* **35**, 317–321.

Godkin, A., Humphreys, I. R. (2020) Elevated interleukin-6, interleukin-10 and neutrophil : lymphocyte ratio as identifiers of severe coronavirus disease 2019. *Immunology* **160**, 221–222.

Gómez-Mesa, J. E., Galindo-Coral, S., Montes, M. C., Muñoz Martin, A. J. (2021) Thrombosis and coagulopathy in COVID-19. *Curr. Probl. Cardiol.* **46**, 100742.

Grabcanovic-Musija, F., Obermayer, A., Stoiber, W., Krautgartner, W. D., Steinbacher, P., Winterberg, N., Bathke, A. C., Klappacher, M., Studnicka, M. (2015) Neutrophil extracellular trap (NET) formation characterises stable and exacerbated COPD and correlates with airflow limitation. *Respir. Res.* **16**, 59.

Gralinski, L. E., Sheahan, T. P., Morrison, T. E., Menachery, V. D., Jensen, K., Leist, S. R., Whitmore, A., Heise, M. T., Baric, R. S. (2018) Complement activation contributes to severe acute respiratory syndrome coronavirus pathogenesis. *mBio* **9**, e01753-18.

Hadid, T., Kafri, Z., Al-Katib, A. (2021) Coagulation and anticoagulation in COVID-19. *Blood Rev.* **47**, 100761.

Hedrick, T. L., Murray, B. P., Hagan, R. S., Mock, J. R. (2020) COVID-19: Clean up on IL-6. *Am. J. Respir. Cell Mol. Biol.* **63**, 541–543.

Hines, A., Hakim, N., Barrientos, J. (2021) COVID-19 infection presenting as paroxysmal nocturnal hemoglobinuria. *Clin. Case Rep.* **9**, e04636.

Hollerbach, A., Müller-Calleja, N., Pedrosa, D., Canisius, A., Sprinzl, M. F., Falter, T., Rossmann, H., Bodenstein, M., Werner, C., Sagoschen, I., Münzel, T., Schreiner, O., Sivanathan, V., Reuter, M., Niermann, J., Galle, P. R., Teyton, L., Ruf, W., Lackner, K. J. (2021) Pathogenic lipid-binding antiphospholipid antibodies are associated with severity of COVID-19. *J. Thromb. Haemost.* **19**, 2335–2347.

Ibañez, C., Perdomo, J., Calvo, A., Ferrando, C., Reverter, J. C., Tassies, D., Blasi, A. (2021) High D dimers and low global fibrinolysis coexist in COVID19 patients: What is going on in there? *J. Thromb. Thrombolysis* **51**, 308–312.

Jiang, Y., Li, J., Teng, Y., Sun, H., Tian, G., He, L., Li, P., Chen, Y., Guo, Y., Li, J., Zhao, G., Zhou, Y., Sun, S. (2019) Complement receptor C5aR1 inhibition reduces pyroptosis in hDPP4-transgenic mice infected with MERS-CoV. *Viruses* **11**, 39.

Joanico-Morales, B., Gaspar-Chamu, A. D., Salgado-Jiménez, M. L. Á., Rodríguez-Echeverría, G. (2022) Enoxaparin dose associated with decreased risk of death in COVID-19. *Rev. Med. Inst. Mex. Seguro Soc.* **60**, 33–39. (in Spanish)

Korotchaeva, J., Chebotareva, N., Andreeva, E., Sorokin, Y., McDonnell, V., Stolyarevich, E., Moiseev, S. (2022) Thrombotic microangiopathy triggered by COVID-19: case reports. *Nephron* **146**, 197–202.

Kumar, D., Kaimaparambil, V., Chandralekha, S., Lalchandani, J. (2022) Oral rivaroxaban in the prophylaxis of COVID-19 induced coagulopathy. *J. Assoc. Physicians India* **70**, 11–12.

Kurian, C. J., French, Z., Kukulich, P., Lankiewicz, M., Ghimire, S., Maarouf, O. H., Rizk, S., Rhoades, R. (2021) Case series: Coronavirus disease 2019 infection as a precipitant of atypical hemolytic uremic syndrome: Two case reports. *J. Med. Case Rep.* **15**, 587.

Leone, V. F., Imeraj, A., Gastoldi, S., Mele, C., Liguori, L., Condemi, C., Ruggenenti, P., Remuzzi, G., Carrara, C. (2022) Case report: Tackling complement hyperactivation with eculizumab in atypical hemolytic uremic syndrome triggered by COVID-19. *Front. Pharmacol.* **13**, 842473.

Li, Q., Xie, Y., Cui, Z., Tang, S., Yuan, B., Huang, H., Hu, Y., Wang, Y., Zhou, M., Shi, C. (2020) Analysis of peripheral blood IL-6 and leukocyte characteristics in 364 COVID-19 patients of Wuhan. *Front. Immunol.* **11**, 559716.

Lim, M. S., Mcrae, S. (2021) COVID-19 and immunothrombosis: Pathophysiology and therapeutic implications. *Crit. Rev. Oncol. Hematol.* **168**, 103529.

Liu, Y., Du, X., Chen, J., Jin, Y., Peng, L., Wang, H. H. X., Luo, M., Chen, L., Zhao, Y. (2020) Neutrophil-to-lymphocyte ratio as an independent risk factor for mortality in hospitalized patients with COVID-19. *J. Infect.* **81**, e6–e12.

Lo, M. W., Kemper, C., Woodruff, T. M. (2020) COVID-19: Complement, coagulation, and collateral damage. *J. Immunol.* **205**, 1488–1495.

Magro, C., Mulvey, J. J., Berlin, D., Nuovo, G., Salvatore, S., Harp, J., Baxter-Stoltzfus, A., Laurence, J. (2020) Complement associated microvascular injury and thrombosis in the pathogenesis of severe COVID-19 infection: A report of five cases. *Transl. Res.* **220**, 1–13.

Magro, C. M., Mulvey, J., Kubiak, J., Mikhail, S., Suster, D., Crowson, A. N., Laurence, J., Nuovo, G. (2021) Severe COVID-19: A multifaceted viral vasculopathy syndrome. *Ann. Diagn. Pathol.* **50**, 151645.

Martinelli, I., Ciavarella, A., Abbattista, M., Aliberti, S., De Zan, V., Folli, C., Panigada, M., Gori, A., Artoni, A., Ierardi, A. M., Carrafiello, G., Monzani, V., Grasselli, G., Blasi, F., Peyvandi, F. (2021) Increasing dosages of low-molecular-weight heparin in hospitalized patients with Covid-19. *Intern. Emerg. Med.* **16**, 1223–1229.

Mastaglio, S., Ruggeri, A., Risitano, A. M., Angelillo, P., Yancopoulou, D., Mastellos, D. C., Huber-Lang, M., Piemontese, S., Assanelli, A., Garlanda, C., Lambris, J. D., Ciceri, F. (2020) The first case of COVID-19 treated with the complement C3 inhibitor AMY-101. *Clin. Immunol.* **215**, 108450.

Mastellos, D. C., Pires da Silva, B. G. P., Fonseca, B. A. L., Fonseca, N. P., Auxiliadora-Martins, M., Mastaglio, S., Ruggeri, A., Sironi, M., Radermacher, P., Chrysanthopoulou, A., Skendros, P., Ritis, K., Manfra, I., Iacobelli, S., Huber-Lang, M., Nilsson, B., Yancopoulou, D., Connolly, E. S., Garlanda, C., Ciceri, F., Risitano, A. M., Calado, R. T., Lambris, J. D. (2020) Complement C3 vs C5 inhibition in severe COVID-19: Early clinical findings reveal differential biological efficacy. *Clin. Immunol.* **220**, 108598.

Mateer, S. W., Mathe, A., Bruce, J., Liu, G., Maltby, S., Fricker, M., Goggins, B. J., Tay, H. L., Marks, E., Burns, G., Kim, R. Y., Minahan, K., Walker, M. M., Callister, R. C., Foster, P. S., Horvat, J. C., Hansbro, P. M., Keely, S. (2018) IL-6 drives neutrophil-mediated pulmonary inflammation associated with bacteremia in murine models of colitis. *Am. J. Pathol.* **188**, 1625–1639.

McEneny-King, A. C., Monteleone, J. P. R., Kazani, S. D., Ortiz, S. R. (2021) Pharmacokinetic and pharmacodynamic evaluation of ravulizumab in adults with severe coronavirus disease 2019. *Infect. Dis. Ther.* **10**, 1045–1054.

Messner, C. B., Demichev, V., Wendisch, D., Michalick, L., White, M., Freiwald, A., Textoris-Taube, K., Vernardis, S. I., Egger, A. S., Kreidl, M., Ludwig, D., Kilian, C., Agostini, F., Zelezniak, A., Thibeault, C., Pfeiffer, M., Hippenstiel, S., Hocke, A., von Kalle, C., Campbell, A., Hayward, C., Porteous, D. J., Marioni, R. E., Langenberg, C., Lilley, K. S., Kuebler, W. M., Mülleder, M., Drosten, C., Suttorp, N., Witzenrath, M., Kurth, F., Sander, L. E., Ralser, M. (2020) Ultra-high-throughput clinical proteomics reveals classifiers of COVID-19 infection. *Cell Syst.* **11**, 11-24.e4.

Mohamed, A. S., Ahmad, H. M., Abdul-Raheem, A. S. A., Kamel, F. M. M., Khames, A., Mady, A. F. (2022) Thromboprophylaxis and clinical outcomes in moderate COVID-19 patients: A comparative study. *Res. Social Adm. Pharm.* **18**, 4048–4055.

Morici, N., Podda, G., Birocchi, S., Bonacchini, L., Merli, M., Trezzi, M., Massaini, G., Agostinis, M., Carioti, G., Saverio Serino, F., Gazzaniga, G., Barberis, D., Antolini, L., Grazia Valsecchi, M., Cattaneo, M. (2022) Enoxaparin for thromboprophylaxis in hospitalized COVID-19 patients: The X-COVID-19 randomized trial. *Eur. J. Clin. Invest.* **52**, e13735.

Overmyer, K. A., Shishkova, E., Miller, I. J., Balnis, J., Bernstein, M. N., Peters-Clarke, T. M., Meyer, J. G., Quan, Q., Muehlbauer, L. K., Trujillo, E. A., He, Y., Chopra, A., Chieng, H. C., Tiwari, A., Judson, M. A., Paulson, B., Brademan, D. R., Zhu, Y., Serrano, L. R., Linke, V., Drake, L. A., Adam, A. P., Schwartz, B. S., Singer, H. A., Swanson, S., Mosher, D. F., Stewart, R., Coon, J. J., Jaitovich, A. (2021) Large-scale multi-omic analysis of COVID-19 severity. *Cell Syst.* **12**, 23-40.e7.

Pandolfi, L., Fossali, T., Frangipane, V., Bozzini, S., Morosini, M., D'Amato, M., Lettieri, S., Urtis, M., Di Toro, A., Saracino, L., Percivalle, E., Tomaselli, S., Cavagna, L., Cova, E., Mojoli, F., Bergomi, P., Ottolina, D., Lilleri, D., Corsico, A. G., Arbustini, E., Colombo, R., Meloni, F. (2020) Broncho-alveolar inflammation in COVID-19 patients: A correlation with clinical outcome. *BMC Pulm. Med.* **20**, 301.

Pawlowski, C., Venkatakrishnan, A. J., Kirkup, C., Berner, G., Puranik, A., O'Horo, J. C., Badley, A. D., Soundararajan, V. (2021) Enoxaparin is associated with lower rates of mortality than unfractionated heparin in hospitalized COVID-19 patients. *EClinicalMedicine* **33**, 100774.

Qi, X., Kong, H., Ding, W., Wu, C., Ji, N., Huang, M., Li, T., Wang, X., Wen, J., Wu, W., Wu, M., Huang, C., Li, Y., Liu, Y., Tang, J. (2021) Abnormal coagulation function of patients with COVID-19 is significantly related to hypocalcemia and severe inflammation. *Front. Med. (Lausanne)* **8**, 638194.

Ramacciotti, E., Barile Agati, L., Calderaro, D., Aguiar, V. C. R., Spyropoulos, A. C., de Oliveira, C. C. C., Lins Dos Santos, J., Volpiani, G. G., Sobreira, M. L., Joviliano, E. E., Bohatch Júnior, M. S., da Fonseca, B. A. L., Ribeiro, M. S., Dusilek, C., Itinose, K., Sanches, S. M. V., de Almeida Araujo Ramos, K., de Moraes, N. F., Tierno, P. F. G. M. M., de Oliveira, A. L. M. L., Tachibana, A., Chate, R. C., Santos, M. V. B., de Menezes Cavalcante, B. B., Moreira, R. C. R., Chang, C., Tafur, A., Fareed, J., Lopes, R. D. (2022) Rivaroxaban versus no anticoagulation for post-discharge thromboprophylaxis after hospitalisation for COVID-19 (MICHELLE): An open-label, multicentre, randomised, controlled trial. *Lancet* **399(10319)**, 50–59.

Sadeghipour, P., Talasaz, A. H., Rashidi, F., Sharif-Kashani, B., Beigmohammadi, M. T., Farrokhpour, M., Sezavar, S. H., Payandemehr, P., Dabbagh, A., Moghadam, K. G., Jamalkhani, S., Khalili, H., Yadollahzadeh, M., Riahi, T., Rezaeifar, P., Tahamtan, O., Matin, S., Abedini, A., Lookzadeh, S., Rahmani, H., Zoghi, E., Mohammadi, K., Sadeghipour, P., Abri, H., Tabrizi, S., Mousavian, S. M., Shahmirzaei, S., Bakhshandeh, H., Amin, A., Rafiee, F., Baghizadeh, E., Mohebbi, B., Parhizgar, S. E., Aliannejad, R., Eslami, V., Kashefizadeh, A., Kakavand, H., Hosseini, S. H., Shafaghi, S., Ghazi, S. F., Najafi, A., Jimenez, D., Gupta, A., Madhavan, M. V., Sethi, S. S., Parikh, S. A., Monreal, M., Hadavand, N., Hajighasemi, A., Maleki, M., Sadeghian, S., Piazza, G., Kirtane, A. J., Van Tassell, B. W., Dobesh, P. P., Stone, G. W., Lip, G. Y. H., Krumholz, H. M., Goldhaber, S. Z., Bikdeli, B. (2021) Effect of intermediate-dose vs standard-dose prophylactic anticoagulation on thrombotic events, extracorporeal membrane oxygenation treatment, or mortality among patients with COVID-19 admitted to the intensive care unit: The INSPIRATION randomized clinical trial. *JAMA* **325**, 1620–1630.

Skendros, P., Mitsios, A., Chrysanthopoulou, A., Mastellos, D. C., Metallidis, S., Rafailidis, P., Ntinopoulou, M., Sertaridou, E., Tsironidou, V., Tsigalou, C., Tektonidou, M., Konstantinidis, T., Papagoras, C., Mitroulis, I., Germanidis, G., Lambris, J. D., Ritis, K. (2020) Complement and tissue factor-enriched neutrophil extracellular traps are key drivers in COVID-19 immunothrombosis. *J. Clin. Invest.* **130**, 6151–6157.

Suzuki, K., Nagaharu, K., Hachiya, K., Nishimura, K., Matsumoto, T., Tawara, I. (2022) A hemolytic episode following COVID-19 in a case with atypical hemolytic uremic syndrome. *Rinsho Ketsueki* **63**, 224–228.

Tatum, D., Taghavi, S., Houghton, A., Stover, J., Toraih, E., Duchesne, J. (2020) Neutrophil-to-lymphocyte ratio and outcomes in Louisiana COVID-19 patients. *Shock* **54**, 652–658.

Tichaczek-Goska, D. (2012) Deficiencies and excessive human complement system activation in disorders of multifarious etiology. *Adv. Clin. Exp. Med.* **21**, 105–114.

Turner, M. W. (2003) The role of mannose-binding lectin in health and disease. *Mol. Immunol.* **40**, 423–429.

Veras, F. P., Pontelli, M. C., Silva, C. M., Toller-Kawahisa, J. E., de Lima, M., Nascimento, D. C., Schneider, A. H., Caetité, D., Tavares, L. A., Paiva, I. M., Rosales, R., Colón, D., Martins, R., Castro, I. A., Almeida, G. M., Lopes, M. I. F., Benatti, M. N., Bonjorno, L. P., Giannini, M. C., Luppino-Assad, R., Almeida, S. L., Vilar, F., Santana, R., Bollela, V. R., Auxiliadora-Martins, M., Borges, M., Miranda, C. H., Pazin-Filho, A., da Silva, L. L. P., Cunha, L. D., Zamboni, D. S., Dal-Pizzol, F., Leiria, L. O., Siyuan, L., Batah, S., Fabro, A., Mauad, T., Dolhnikoff, M., Duarte-Neto, A., Saldiva, P., Cunha, T. M.,

Ray A.; Winter K. A. K.; Naik D. S. L.; Okorie C.

Alves-Filho, J. C., Arruda, E., Louzada-Junior, P., Oliveira, R. D., Cunha, F. Q. (2020) SARS-CoV-2-triggered neutrophil extracellular traps mediate COVID-19 pathology. *J. Exp. Med.* **217**, e20201129.

Xiang, G., Hao, S., Fu, C., Hu, W., Xie, L., Wu, Q., Li, S., Liu, X. (2021) The effect of coagulation factors in 2019 novel coronavirus patients: A systematic review and meta-analysis. *Medicine (Baltimore)* **100**, e24537.

Xiao, M., Zhang, Y., Zhang, S., Qin, X., Xia, P., Cao, W., Jiang, W., Chen, H., Ding, X., Zhao, H., Zhang, H., Wang, C., Zhao, J., Sun, X., Tian, R., Wu, W., Wu, D., Ma, J., Chen, Y., Zhang, D., Xie, J., Yan, X., Zhou, X., Liu, Z., Wang, J., Du, B., Qin, Y., Gao, P., Lu, M., Hou, X., Wu, X., Zhu, H., Xu, Y., Zhang, W., Li, T., Zhang, F., Zhao, Y., Li, Y., Zhang, S. (2020) Antiphospholipid antibodies in critically ill patients with COVID-19. *Arthritis Rheumatol.* **72**, 1998–2004.

Yasri, S., Wiwanitkit, V. (2020) COVID-19, antiphospholipid syndrome and thrombosis. *Clin. Appl. Thromb. Hemost.* **26**, 1076029620931927.

Zhang, Y., Xiao, M., Zhang, S., Xia, P., Cao, W., Jiang, W., Chen, H., Ding, X., Zhao, H., Zhang, H., Wang, C., Zhao, J., Sun, X., Tian, R., Wu, W., Wu, D., Ma, J., Chen, Y., Zhang, D., Xie, J., Yan, X., Zhou, X., Liu, Z., Wang, J., Du, B., Qin, Y., Gao, P., Qin, X., Xu, Y., Zhang, W., Li, T., Zhang, F., Zhao, Y., Li, Y., Zhang, S. (2020) Coagulopathy and antiphospholipid antibodies in patients with Covid-19. *N. Engl. J. Med.* **382**, e38.

The Neuropsychiatric Aspect of the Chronic Viral Hepatitis

Tatyana Vasiliyevna Polukchi[1,2], Gulzhan Narkenovna Abuova[2], Yelena Alekseevna Slavko[1]
[1]Department of Gastroenterology, Asfendiyarov Kazakh National Medical University, Almaty, Republic of Kazakhstan;
[2]Department of Infectious Diseases and Dermatovenerology, South Kazakhstan Medical Academy, Shymkent, Republic of Kazakhstan

Abstract: Chronic viral hepatitis is a systemic disease characterized by a wide range of extrahepatic manifestations, such as cognitive impairment, chronic fatigue, sleep disorders, depression, anxiety and a decrease in quality of life. This article presents a summary of the main theories and hypotheses about the occurrence of cognitive impairment, features of treatment of patients with chronic viral hepatitis. Often, extrahepatic manifestations can outstrip the clinical manifestations of liver damage itself, which requires the use of additional diagnostic and treatment methods, and they can also significantly change the treatment tactics and prognosis of the disease. Changes in neuropsychological parameters and cognitive impairments are often recorded in patients with chronic viral hepatitis at stages characterized by the absence of significant liver fibrosis and liver cirrhosis. These changes usually occur regardless of the genotype of the infection and in the absence of structural damage to the brain. The purpose of this review is to study the main aspects of the formation of cognitive impairment in patients with chronic hepatitis, cirrhosis of viral etiology.

Mailing Address: Tatyana Vasiliyevna Polukchi, MD., Department of Infectious Diseases and Dermatovenerology, South Kazakhstan Medical Academy, Zhybek-Zholy Street 1/1, 160019, Shymkent, Republic of Kazakhstan; Phone: +7 747 983 83 88; e-mail: tatyana_polukchi@mail.ru

Introduction

In the structure of chronic liver diseases, one of the significant places is assigned to viral hepatitis, which affect the lives of hundreds of millions of people around the world and are the main cause of steadily progressive morbidity and mortality (Torre et al., 2021). According to the latest estimates, more than 257 million people in the world have active viral hepatitis B (HBV) infection, but according to some authors, the number of infected patients reaches 350 million, chronic viral hepatitis accounts for more than 185 million patients, more than 20 million people have chronic viral hepatitis D (HDV) infection (Conde et al., 2017; Komas et al., 2018; Lanini et al., 2019). Prolonged persistence of viral hepatitis B, C and D can lead to the chronization of infection and subsequently lead to transformation into fibrosis and cirrhosis (Conde et al., 2017; Komas et al., 2018). However, at present, chronic viral hepatitis is a systemic disease characterized by a wide range of extrahepatic manifestations, including a number of neurological conditions (Monaco et al., 2015). In patients with chronic viral hepatitis, a number of symptoms are detected in 50% of cases, such as depression, anxiety, sleep disorders, fatigue and neurocognitive disorders, including impaired executive function, working memory, information processing speed, change of attitudes, decision-making and fluency of speech, which significantly affect the quality of life of patients (Adinolfi et al., 2015; Monaco et al., 2015; Yeoh et al., 2018; Tagliapietra and Monaco, 2020). Various scientists have noted the fact that depression, in particular, can be a reaction to increased psychosocial stress, as well as to the physical symptoms of a progressive existing disease (Yeoh et al., 2018). At the same time, patients at an early stage of the disease with minimal liver inflammation may have more pronounced symptoms of depression and fatigue than in the general population of patients (Yeoh et al., 2018). Characteristic neurocognitive deficiency can occur at an early stage of infection and has no connection with depression or encephalopathy, does not depend on the severity of the disease, the rate of replication of the virus, as well as on the stage of liver fibrosis, the genotype of the virus, the absence of visible structural damage to the brain (Monaco et al., 2015; Pawełczyk, 2016; Yeoh et al., 2018).

Chronic viral hepatitis and nervous system

Patients infected with chronic viral hepatitis have numerous extrahepatic manifestations, such as symptoms of central and peripheral nervous system disorders that develop at various times after infection. Hepatitis B and C viruses can directly have a neurotoxic effect on the brain. These processes are based on complex mechanisms associated with both the direct impact of the virus on brain cells and tissues, and with indirect effects resulting from the impact of the virus on the immune system or as a result of the use of antiviral therapy (Ferenci and Staufer, 2008). According to various authors, cognitive function disorders and neuropsychiatric disorders are registered in almost 50% of patients with chronic viral hepatitis, which do not depend on the severity of liver disease or the rate of

replication of viral hepatitis C (HCV) infection. In addition, symptoms such as fatigue, sleep disorders, depression and decreased quality of life are usually associated with neurocognitive changes in patients even with non-cirrhotic chronic HCV infection, regardless of the stage of liver fibrosis, infecting genotype or in the absence of structural damage to the brain and abnormal signals when using conventional magnetic resonance imaging (MRI) the brain (Adinolfi et al., 2015). Chronic viral hepatitis not only the central nervous system can be affected, but also the peripheral one, which leads to the formation of a wide variety of clinical manifestations, such as cerebrovascular phenomena, encephalopathy, myelitis, encephalomyelitis and cognitive disorders. Moreover, HCV infection is known to cause both motor and sensory peripheral neuropathy in the context of mixed cryoglobulinemia, which has recently been recognized as an independent risk factor for stroke (Wu et al., 2015; Sonavane et al., 2018). Approximately 1% of all cases of acute inflammatory demyelinating polyneuropathy associated with viral hepatitis B. Guillain-Barre syndrome is a surprisingly clinically diverse disease with characteristic variants characterized by an immuno-mediated attack on the components of the peripheral nervous system (Sonavane et al., 2018). Recent studies have shown that hepatitis C virus and Parkinson's disease have a common overexpression of inflammatory biomarkers due to the fact that HCV infection may release inflammatory cytokines that may play a role in the pathogenesis of Parkinson's disease (Wu et al., 2015).

Cognitive impairment and chronic viral hepatitis
According to WHO (World Health Organization) data, over 20 million people worldwide have dementia and cognitive impairment, moreover, the number of new cases of diseases is steadily increasing both in senile and elderly people, and in people of working age (Groppell et al., 2019). According to forecasts, the incidence of dementia is expected to increase from 35 million to 70 million by 2030 (Groppell et al., 2019). In turn, cognitive impairments include a decrease in memory, mental performance and other cognitive functions compared to the individual norm. Changes in neuropsychological parameters and cognitive impairments are often recorded in patients with chronic viral hepatitis, at stages characterized by the absence of significant liver fibrosis and liver cirrhosis. These changes usually occur regardless of the genotype of HCV infection and in the absence of structural damage to the brain or a pathological signal when using conventional magnetic resonance imaging (MRI) of the brain (Ferenci and Staufer, 2008). Researchers note that chronic HCV infection itself can cause moderate cognitive impairment, even in the absence of cirrhosis-related hepatic encephalopathy (Yeoh et al., 2018). Patients with chronic viral hepatitis may have impaired memory, attention, executive function, and processing speed at the non-cirrhotic stage of the disease (Yeoh et al., 2018). In addition to neurocognitive disorders, patients with chronic viral hepatitis may experience a number of symptoms, such as depression and fatigue, which worsen the quality of life (Yeoh et al., 2018). Depression in this case can

serve as a response to psychosocial stress and physical symptoms of progressive HCV-infection or concomitant diseases. However, even patients at an early stage of HCV-infection with minimal inflammation or concomitant liver disease report more symptoms of depression and fatigue than the general population. Similarly, specific cognitive impairments occur at an early stage of HCV-infection and do not depend on the presence of depression or encephalopathy (Lowry et al., 2016; Yeoh et al., 2018). Depression and cognitive impairment may be associated with the neurotoxicity of chronic viral hepatitis itself (Adinolfi et al., 2015). Thus, in studies in which interferon-free therapy was used in patients with chronic viral hepatitis, it was found that patients of this category have neuropsychiatric symptoms such as fatigue, insomnia, anxiety, depression and cognitive dysfunction, supporting hypotheses about the neurotoxicity of HCV infection (Gritsenko and Hughes, 2015). According to recent data, clinical and subclinical manifestations of cognitive dysfunction may be detected in 50% of chronic viral hepatitis patients (Barreira et al., 2019).

Risk factors of cognitive impairment
The high level of substance abuse and the prevalence of mental disorders among HCV-infected patients are important factors associated with cognitive impairments that jeopardize adherence and effectiveness of treatment (Więdłocha et al., 2017). Various authors have established a possible relationship in patients with chronic viral hepatitis between gender and cognitive functions. For example, a recent study found that the female gender apparently affects depression, anxiety and some indicators of cognitive functions in patients with chronic viral hepatitis before treatment (Barreira et al., 2019). Chronic viral hepatitis can also cause long-term brain dysfunction, which significantly worsens the quality of life and may even persist after the elimination of the virus (Dirks et al., 2017). With chronic HBV-infection, the quality of life may also be worsened due to the appearance of fatigue, cognitive impairment and sleep disorders (Wang et al., 2019).

Pathogenesis of the cognitive impairment
The theory of the appearance of cognitive impairment in patients at the terminal stage of liver disease is a generally recognized fact. It is known that ammonia is a toxic metabolite present in the blood in relatively low concentrations in a healthy individual, however, even a small increase in its concentration has an adverse effect on the body, and in particular on the brain (Fletcher and McKeating, 2012). Excessive intake of ammonia through the blood-brain barrier leads to depletion of the amount of glutamate, simultaneously leading to excessive accumulation of glutamine in brain tissues, resulting in swelling and swelling of astrocytes, a decrease in gamma-aminobutyric acid and dysfunction of transmembrane electrolyte transfer, thereby contributing to the deterioration of chemical neurotransmission (Fletcher and McKeating, 2012). Ineffective neutralization of ammonia leads to a decrease in the amount of α-ketoglutarate (which is a metabolite of glutamate), suppression

of transamination and a decrease in the synthesis of neurotransmitters (Fletcher and McKeating, 2012). This pathological cascade of reactions, simultaneously with an increase in alkalosis with excessive concentration of ammonia, contribute to increased hypoxia and hypoenergesis of astrocytes, neurons, resulting in the formation of hepatic encephalopathy (Fletcher and McKeating, 2012). However, recent studies indicate that one third of patients with chronic viral hepatitis have cognitive impairment in the absence of liver cirrhosis, at the same time, their connection with laboratory parameters, viral load and genotype is excluded (Wozniak et al., 2016). There is information explaining the possible pathogenesis of the direct effect of hepatitis viruses on brain cells, as a result of which these symptoms appear. It is assumed that neurobiological changes occur as a result of infiltration of the brain by induced cytokines and through the direct neuropathic action of viral particles of chronic viral hepatitis penetrating the blood-brain barrier (Yeoh et al., 2018). Changes that occur in the brain under the action of viral particles lead to increased inflammatory reactions, changes in the level of neurotransmitters, hormonal regulation and the release of neurotoxic substances, which subsequently lead to abnormal neural conduction and functioning in areas of the brain responsible for affective reactions, emotional processing, motivation, attention and concentration (Fletcher and McKeating, 2012; Yeoh et al., 2018). Despite the fact that direct-acting antiviral drugs lead to high rates of elimination of viral agents, intracerebral changes are not regressed, as a result of which the symptoms of neurocognitive deficiency persist (Fletcher and McKeating, 2012; Yeoh et al., 2018). On the other hand, according to the results of the recent study, it was found that replication of chronic viral hepatitis viruses can take place both on the surface of endothelial cells of the blood-brain barrier, and inside, due to the expression of known receptor molecules such as (LDLR, CD81, claudin-1, occludin, and scavenger receptor-B1) (Fletcher et al., 2012). According to these data, theoretically, hepatitis viruses can lead to obstructive vascular disorders, due to the direct involvement of brain vessels in chronic inflammation (Fletcher et al., 2012). The generally recognized facts of the pathogenesis of cognitive disorders in chronic viral hepatitis is the strengthening of the host's immune response, in which autoantibodies, immune complexes and cryoglobulins are produced (Fletcher et al., 2012). But there are alternative mechanisms of cognitive impairment in patients with chronic viral hepatitis, including the release of viral RNA in microglial cells and astrocytes (Fletcher et al., 2012). Researchers have suggested that hepatitis viruses have the ability to penetrate into the brain and multiply in the endothelial cells of the brain, which characterizes their independent life and pathogenic role in the development of cognitive deficits (Fletcher and McKeating, 2012; Fletcher et al., 2012). Despite the expansion of the clinical range of syndromes in chronic viral hepatitis, the exact pathophysiological mechanisms of cognitive impairment are still poorly understood. On the one hand, the detection of defects in the central serotonergic and dopaminergic neurotransmission of patients with cognitive disorders and mild

course of the disease suggests a possible role of chronic viral hepatitis viruses in inducing dysfunction of selective aminergic systems (Weissenborn et al., 2006). On the other hand, patients undergoing interferon therapy the appearance of depression correlates with the depletion of serotonin in platelets, possibly due to the effectiveness of antidepressants that inhibit serotonin reuptake (Stasi et al., 2014). There are other putative mechanisms of cognitive deficits associated with cytokines released during systemic or immune activation of the brain (Stasi et al., 2014). In recent studies, it was found that patients with mild HCV-infection during magnetic resonance spectroscopy have a pronounced dysfunction of choline and creatinine metabolism in the basal ganglia and white matter of the brain compared with patients without a history of hepatitis. In comparison with the process observed in hepatic encephalopathy, higher concentrations of cerebral choline were recorded in patients in this study, which ultimately serves as evidence of the effect on cognitive functions (Stasi et al., 2014).

Chronic fatigue
Chronic fatigue is an important clinical finding in patients with chronic hepatitis virus infection. Fatigue, according to foreign researchers, has 2 main types – central and peripheral, which can occur both in combination and separately (Golabi et al., 2017). Central fatigue is characterized by a lack of self-motivation and can manifest itself in both physical and mental activity. Peripheral fatigue is classically manifested by neuromuscular dysfunction and muscle weakness. Therefore, the difference is often considered as the difference between intention (central fatigue) and ability (peripheral fatigue) (Golabi et al., 2017). Fatigue is characterized as a multi-level structure, the division of which into central and peripheral fatigue makes it possible to better assess the condition and identify potential causes and correlations. The liver occupies a central place in the pathogenesis of peripheral and central fatigue, which, according to researchers, depends on the regulation of energy and crosstalk between the intestine, liver, muscles and brain (Gerber et al., 2019). Fatigue in liver diseases in most cases manifests itself as central fatigue, which does not correlate with traditional markers of activity or with the severity of the disease (Swain, 2006). There is a certain consensus on the nature, mechanisms and degree of immune dysfunction in this pathology, characterized by slightly increased indicators of pro-inflammatory and anti-inflammatory cytokines, such as interleukin-1 (IL), interleukin-6 and tumour necrosis factor (TNF-α), as well as a violation of the function of natural killer cells and a change in the amount of T-lymphocytes (Torgrimson-Ojerio et al., 2014). Several previous studies have also attempted to establish a link between fatigue and various biomarkers, such as IL-6 and TNF-α in cytokine assays. According to the results of the study, no association of TNF-α with fatigue was recorded, while IL-6 and cortisol were reported to be positively associated with fatigue (Jang et al., 2018a). However, other fatigue studies have established a significant negative correlation with cortisol in patients with HBV,

however, a significant positive correlation has been observed with IL-6 and TNF-α. Cortisol, IL-6, and TNF-α were associated with levels of perceived fatigue, especially cognitive impairment in patients with HBV infection. The characteristic of fatigue in patients with chronic liver disease was noted as central fatigue (Wang et al., 2019). Some studies have shown that fatigue is a true and specific sign of HDV-infection that negatively affects the quality of life, while a significant proportion of fatigue in HBV is associated with the presence of autonomic dysfunction (Ekerfors et al., 2019). Other studies have found that muscle dysfunction is a key mechanism of chronic fatigue syndrome. It is noted that the appearance of fatigue in patients directly depended on low muscle performance and a decrease in the level of physical activity, which can serve as a potential for the treatment of chronic fatigue syndrome (Jang et al., 2018a). A recent content analysis revealed that the overall level of cognitive impairment and chronic fatigue syndrome in chronic HCV-infection had a significant negative correlation with age. Consequently, emotional and psychosocial problems associated with fatigue may be more common in patients with chronic viral hepatitis than physical problems (Jang et al., 2018b). Chronic fatigue is also very common in the terminal stage of liver disease, recent studies have shown its connection with physical activity in patients with cirrhosis of the liver, so when conducting a 6-minute walking test in patients, its indicators showed low and a high degree of shortness of breath was found, which were associated with chronic fatigue syndrome (Ahboucha et al., 2008). Chronic fatigue syndrome is also present in a significant number of patients after liver transplantation (21.5%), and almost half of patients suffer from severe fatigue (45.0%). The related factors of the appearance of chronic fatigue syndrome after liver transplantation are still unclear and complex, which requires additional information to reduce the course of the syndrome and improve the quality of life of recipients (Lima et al., 2019). In patients with liver cirrhosis, chronic fatigue syndrome is a common complaint and can be considered as a debilitating symptom that negatively affects the quality of life, and also has a strong correlation with depressive symptoms and quality of life (Hong et al., 2015). However, studies to assess fatigue in patients with chronic viral hepatitis are very limited.

Anxiety and depression
The prevalence of anxiety and depression in patients with chronic viral hepatitis, according to various authors, varies from 37 to 83% (Adinolfi et al., 2017). Patients with chronic viral hepatitis are characterized by the dominance of negative emotions, communication difficulties, a high degree of asthenization, difficulties in obtaining psychological help and social support (Aktuğ Demir et al., 2013; Yeoh et al., 2018). In patients with chronic viral hepatitis, depression is a possible reaction to increased psychosocial stress, to the presence of physical symptoms of progression of chronic viral hepatitis, or to existing concomitant diseases (Tamayo et al., 2016). However, researchers have found that patients even in the early stages of

the disease with minimal liver inflammation or concomitant diseases report more pronounced symptoms of depression and fatigue than in the general population (Fletcher and McKeating, 2012; Zayed et al., 2018; Egmond et al., 2020). The presence of concomitant pathology in patients with chronic hepatitis increases the risk of developing mental complications (Fletcher et al., 2012; Zayed et al., 2018; Egmond et al., 2020). However, according to other authors, depression was not detected in the early stages of the disease, although the fact was noted that in patients with chronic viral hepatitis, depressive mood and cognitive fatigue were critical psychosocial mediators of a decrease in the quality of life (Zayed et al., 2018). Depression is a frequent disorder detected in one third of patients with chronic viral hepatitis C and its prevalence is estimated to be 1.5–4.0 times higher than in patients with chronic infection caused by the hepatitis B virus (Zayed et al., 2018). Currently, an increasing number of studies are focused only on the study of depression, but not on anxiety, although its presence can also significantly correlate with the quality of life associated with health in patients with chronic viral hepatitis (Fletcher and McKeating, 2012).

Modern diagnostic capabilities of cognitive disorders
As is known, neuropsychiatric disorders and neurocognitive dysfunction are registered in almost 50% of patients with chronic viral hepatitis, regardless of the severity of liver disease or the frequency of HCV-infection replication. Fatigue, sleep disturbance, depression and decreased quality of life are usually associated with neurocognitive changes in patients with non-cirrhotic stage of chronic HCV-infection, regardless of the stage of liver fibrosis and the type of virus genotype (Monaco et al., 2015). These manifestations usually occur in the absence of structural brain damage or signal pathology when using conventional MRI of the brain, although metabolic and microstructural changes can be detected with its help (Monaco et al., 2015). It is assumed that chronic viral hepatitis causes neurodegenerative changes through low-severity neuroinflammation, which suggests cortical atrophy. Some researchers have not found a link between fatigue and the thickness of the cortical layer. The total difference in the volume of white and gray matter of the brain was also not detected (Hjerrild et al., 2016). Other researchers also did not establish a connection between chronic viral hepatitis and the volume of gray matter of the brain obtained from 3T neuroimaging. Although a cluster of endothelial cells is reported to be associated with the primary and secondary somatosensory cortex, as well as the temporal and occipital lobes in patients with chronic viral hepatitis. At the same time, a higher average value of endothelial cells in the upper parietal part, adjusted for the average shift in frames, was associated with improved memory and attention indicators, but not with fatigue, depression, viral load or the level of liver fibrosis among patients. These results, according to the researchers, suggest a compensatory mechanism in chronic viral hepatitis and explain the ambiguous results in the literature on cognitive deficits in infected people (Kharabian Masouleh et al.,

2017). HCV-infection affecting the central nervous system (CNS) can lead to various manifestations, such as anxiety, depression, cognitive impairment and vasculitis. In a recent study, patients with HCV-infection were evaluated using the Wexler Adult Intelligence Scale, the Wexler Memory Scale, the Beck Depression Scale and computed tomography (CT) with single-photon emission. The aim of the study was to identify subclinical CNS lesions in patients with chronic viral hepatitis with and without systemic vasculitis. According to the results of the study, it was found that the indicators of the memory scale were lower in HCV patients with vasculitis compared to patients without vasculitis, while block tests and comprehension tests, the indicators of the Beck scale did not differ significantly in both groups. The test scores in patients with and without cirrhosis did not differ significantly. However, some patients had different patterns of cerebral hypoperfusion during CT, while all of them had associated vasculitis, which indicates the possibility of vasculitis developing neuropsychiatric lesions in patients with chronic viral hepatitis (Zayed et al., 2018). An attempt was also made to assess whether neuropsychological disorders in patients infected with chronic viral hepatitis are accompanied by structural changes in the brain, through extensive neuropsychological testing and the use of cranial MRI. The data obtained indicated structural changes in the brains of patients with chronic viral hepatitis. The data obtained indicated structural changes in the brains of patients with chronic HCV-infection. Disorders of the cerebelloalamocortical regions and contours connecting the projections of the cerebellum with the prefrontal cortex through the thalamus, according to the researchers, indicated cognitive dysfunction observed in these patients (Prell et al., 2019). Chronic viral hepatitis can often manifest as a noticeable impairment of attention and executive functions associated with neuropsychiatric symptoms. Neuroimaging methods show the predominance of frontal cortical striated structures and their connections, systems that regulate the interaction between emotional and motivational regulation, executive and motor functions. Unlike metabolic and hepatic encephalopathy, direct brain involvement is observed as an inflammatory reaction in these structures. There is still uncertainty about the clinical significance of this inflammation, and in various studies contradictory data have been obtained on its harmful or protective effects on cognitive functions. According to current hypotheses of brain circuits, altered function is also observed in distant structures associated with the frontal cortical-striatal network, in the absence of signs of inflammation. There is scant evidence for the reversibility of post-treatment imaging changes and their potential use as a biomarker to consider starting treatment. Since effective and well-tolerated treatments are currently available, imaging biomarkers can help clinicians assess cognitive impairment in chronic viral hepatitis (Tagliapietra and Monaco, 2020). The role of HCV hepatitis virus co-infection in cognitive impairment in patients infected with human immunodeficiency virus (HIV) is still being discussed, and there is no functional assessment of neuroimaging on this issue. A recent pilot study demonstrates that there are statistically significant differences in

the types of connections. Thus, it was found that in HCV, the involved areas were the pallidum, the brain stem, lobules 1 and 10 lobes of the right cerebellum. Enlarged frontal-striated dysfunctions have already been reported as consequences of HCV-infection and they may reflect an additive effect. Changes in the cerebellum are associated with HIV-infection, but not with HCV, which indicates a synergistic effect of HCV-infection in the functional modification of the brain associated with HIV (Corgiolu et al., 2018). Several studies have demonstrated evidence of moderate neurocognitive impairment in various areas of ability among a subgroup of people infected with HCV, the severity and exact neurocognitive domains vary depending on the literature, for example, some researchers found only general moderate cognitive impairment in a cohort of HCV-infected patients with specific learning disabilities compared to seronegative participants (Corgiolu et al., 2018). Other evidence suggests that some people infected with HCV may have more diffuse neurocognitive deficits in neuropsychological areas associated with prefrontal systems, including deficits in complex information processing, motor skills, and executive functions. Moreover, approximately 30% of people infected with HCV had difficulties with the test, which required mental flexibility, abstract thinking and concept formation (Posada et al., 2010). It was found that HCV-infection was associated with mild deficiency when performing tasks that assessed inhibition of speech response and fluency of speech. Thus, mild neurocognitive disorders are observed among a subgroup of people with HCV even in the absence of severe liver disease (Posada et al., 2010). In the light of contradictory results in the literature, various complex batteries of tests are used by foreign researchers to study cognitive disorders. The Wexler reading test for adults is a widely used word recognition test, with the help of which it is possible to assess the initial cognitive abilities before the disease (Huckans et al., 2015). It is also possible to use a battery of neuropsychological assessment (NAB), characterized as a well-tested complex set of subtests evaluating a number of cognitive areas, including the modules attention, memory and executive functions, each of which consists of several subtests related to this area. Based on demographically adjusted norms (age, gender, education), standard scores are derived for each subtest, and standard indexes are defined as the total performance indicators for the subtests for each module (Huckans et al., 2015). It is reported about the use of psychiatric questionnaires to identify cognitive impairments in patients with chronic viral hepatitis. The Beck depression scale well confirms the criteria for the severity of depression, consisting of 21 points with which two factors of the disease can be determined, the first of which is the somatic factor (loss of energy, changes in sleep patterns, irritability, changes in appetite, difficulty concentrating, fatigue, loss of interest in sex), and the cognitive affective factor (sadness, pessimism, failure in the past, guilt, sense of punishment, self-dislike, self-criticism, thoughts of suicide, crying, excitement, uselessness) (Bjelland et al., 2002; Zimmerman et al., 2015). Fatigue Severity Scale (FSS) is a 9-point fatigue severity scale previously confirmed for use in patients with HCV, multiple sclerosis

and other chronic diseases (Gavrilov et al., 2018). Although there are many measurement tools available to assess fatigue, there is no tool that can provide both specificity and sensitivity for measuring fatigue. The lack of a tool is part of the problem that leads to underestimation, recognition and treatment of fatigue in patients. Part of the problem is that the tools currently used do not adequately reflect the complexity and dimension of fatigue. None of the commonly used tools addresses all aspects of fatigue. Commonly assessed areas include: descriptions or characteristics of fatigue, feelings of distress associated with fatigue, suspected causes of fatigue, and effects of fatigue. It is important to understand which fatigue components are being evaluated and which fatigue components should be evaluated. Since there are no tools that would cover all these components, it is important for researchers to consider what fatigue is, which is relevant to the current study or patient, and use it to select a specific measure (Gavrilov et al., 2018). When assessing the severity of anxiety, it is possible to use a generalized inventory of anxiety disorders consisting of 18 items (Bjelland et al., 2002). Another equally effective method of diagnosing anxiety and depression is the Hospital Anxiety and Depression Scale (HADS). It is characterized as a tool that measures mental stress among somatic patients. It consists of two subscales: the anxiety subscale (HADS-D A) and the depression subscale (HADS-D D). Each consists of seven questions and must be analysed independently. Higher values indicate a greater deterioration. The average values on the anxiety and depression scales were presented (0–21 n per scale, ≤7 n = normal, ≥11 n = noteworthy symptoms) (Gerber et al., 2019). Cognitive and physical weakness are common in patients with cirrhosis. There is evidence of the use of a combined assessment (MoCA-CFS) developed using the Montreal Cognitive Assessment (MoCA) to assess the severity of hepatic encephalopathy. The MoCA-CFS composite score makes it possible to predict the deterioration of health-related and all-cause quality of life indicators within 6 months. Recent data confirm the prognostic value of the "multidimensional" weakness tool for predicting adverse clinical outcomes and emphasize the potential of a multifaceted approach to therapy aimed at cognitive impairment, physical weakness and depression (Ney et al., 2018).

Conclusion
There is evidence of a wide range of neuropsychiatric disorders at various stages of fibrosis, including early in patients with chronic viral hepatitis. The difficulty of diagnosing cognitive impairment in chronic viral hepatitis is due to the fact that the currently used wide range of neuropsychological tests does not fully reflect the degree and features of cognitive dysfunction in this category of patients. The use of modern diagnostic criteria helps to improve the diagnosis of neuropsychiatric disorders in patients with chronic viral hepatitis, which may be an indication for timely therapeutic measures aimed at improving the quality of life in this category of patients.

References

Adinolfi, L. E., Nevola, R., Lus, G., Restivo, L., Guerrera, B., Romano, C., Zampino, R., Rinaldi, L., Sellitto, A., Giordano, M., Marrone, A. (2015) Chronic hepatitis C virus infection and neurological and psychiatric disorders: An overview. *World J. Gastroenterol*. **21(8)**, 2269–2280.

Adinolfi, L. E., Nevola, R., Rinaldi, L., Romano, C., Giordano, M. (2017) Chronic hepatitis C virus infection and depression. *Clin. Liver Dis.* **21(3)**, 517–534.

Ahboucha, S., Butterworth, R. F., Pomier-Layrargues, G., Vincent, C., Hassoun, Z., Baker, G. B. (2008) Neuroactive steroids and fatigue severity in patients with primary biliary cirrhosis and hepatitis C. *Neurogastroenterol. Motil.* **20(6)**, 671–679.

Aktuğ Demir, N., Çelik, M., Kölgelier, S., Sümer, S., Aksöz, S., Demir, L. S., İnkaya, A. Ç. (2013) Comparison of the level of depression and anxiety in inactive hepatitis B carriers and chronic hepatitis B patients. *Turk Psikiyatri Derg.* **24(4)**, 248–252. (in Turkish)

Barreira, D. P., Marinho, R. T., Bicho, M., Flores, I., Fialho, R., Ouakinin, S. (2019) Hepatitis C pretreatment profile and gender differences: Cognition and disease severity effects. *Front. Psychol.* **10**, 2317.

Bjelland, I., Dahl, A. A., Haug, T. T., Neckelmann, D. (2002) The validity of the Hospital Anxiety and Depression Scale. An updated literature review. *J. Psychosom. Res.* **52(2)**, 69–77.

Conde, I., Vinaixa, C., Berenguer, M. (2017) Hepatitis C-related cirrhosis. Current status. Cirrosis por hepatitis C. Estado actual. *Medicina Clínica* **148(2)**, 78–85.

Corgiolu, S., Barberini, L., Suri, J. S., Mandas, A., Costaggiu, D., Piano, P., Zaccagna, F., Lucatelli, P., Balestrieri, A., Saba, L. (2018) Resting-state functional connectivity MRI analysis in human immunodeficiency virus and hepatitis C virus co-infected subjects. A pilot study. *Eur. J. Radiol.* **102**, 220–227.

Dirks, M., Pflugrad, H., Haag, K., Tillmann, H. L., Wedemeyer, H., Arvanitis, D., Hecker, H., Tountopoulou, A., Goldbecker, A., Worthmann, H., Weissenborn, K. (2017) Persistent neuropsychiatric impairment in HCV patients despite clearance of the virus?! *J. Viral Hepat.* **24(7)**, 541–550.

Egmond, E., Mariño, Z., Navines, R., Oriolo, G., Pla, A., Bartres, C., Lens, S., Forns, X., Martin-Santos, R. (2020) Incidence of depression in patients with hepatitis C treated with direct-acting antivirals. *Braz. J. Psychiatry* **42(1)**, 72–76.

Ekerfors, U., Sunnerhagen, K. S., Westin, J., Jakobsson Ung, E., Marschall, H. U., Josefsson, A., Simrén, M. (2019) Muscle performance and fatigue in compensated chronic liver disease. *Scand. J. Gastroenterol.* **54(7)**, 925–933.

Ferenci, P., Staufer, K. (2008) Depression in chronic hepatitis: The virus, the drug, or the ethnic background? *Liver Int.* **28(4)**, 429–431.

Fletcher, N. F., McKeating, J. A. (2012) Hepatitis C virus and the brain. *J. Viral Hepat.* **19(5)**, 301–306.

Fletcher, N. F., Wilson, G. K., Murray, J., Hu, K., Lewis, A., Reynolds, G. M., Stamataki, Z., Meredith, L. W., Rowe, I. A., Luo, G., Lopez-Ramirez, M. A., Baumert, T. F., Weksler, B., Couraud, P. O., Kim, K. S., Romero, I. A., Jopling, C., Morgello, S., Balfe, P., McKeating, J. A. (2012) Hepatitis C virus infects the endothelial cells of the blood-brain barrier. *Gastroenterology* **142(3)**, 634–643.e6.

Gavrilov, Y. V., Shkilnyuk, G. G., Valko, P. O., Stolyarov, I. D., Ivashkova, E. V., Ilves, A. G., Nikiforova, I. G., Shchelkova, O. Y., Vasserman, L. I., Vais, E. E., Valko, Y. (2018) Validation of the Russian version of the Fatigue Impact Scale and Fatigue Severity Scale in multiple sclerosis patients. *Acta Neurol. Scand.* **138(5)**, 408–416.

Gerber, L. H., Weinstein, A. A., Mehta, R., Younossi, Z. M. (2019) Importance of fatigue and its measurement in chronic liver disease. *World J. Gastroenterol.* **25(28)**, 3669–3683.

Golabi, P., Sayiner, M., Bush, H., Gerber, L. H., Younossi, Z. M. (2017) Patient-reported outcomes and fatigue in patients with chronic hepatitis C infection. *Clin. Liver Dis.* **21(3)**, 565–578.

Gritsenko, D., Hughes, G. (2015) Ledipasvir/sofosbuvir (Harvoni): Improving options for hepatitis C virus infection. *P T* **40(4)**, 256–276.

Groppell, S., Soto-Ruiz, K. M., Flores, B., Dawkins, W., Smith, I., Eagleman, D. M., Katz, Y. (2019) A rapid, mobile neurocognitive screening test to aid in identifying cognitive impairment and dementia (BrainCheck): Cohort study. *JMIR Aging* **2(1)**, e12615.

Hjerrild, S., Renvillard, S. G., Leutscher, P., Sørensen, L. H., Østergaard, L., Eskildsen, S. F., Videbech, P. (2016) Reduced cerebral cortical thickness in non-cirrhotic patients with hepatitis C. *Metab. Brain Dis.* **31(2)**, 311–319.

Hong, K., Kim, H., Lee, J. M., Lee, K. W., Yi, N. J., Lee, H. W., Choi, Y., Suh, S. W., Hong, S. K., Yoon, K. C., Kim, H. S., Suh, K. S. (2015) Fatigue and related factors after liver transplantation. *Korean J. Hepatobiliary Pancreat. Surg.* **19(4)**, 149–153.

Huckans, M., Fuller, B., Wheaton, V., Jaehnert, S., Ellis, C., Kolessar, M., Kriz, D., Anderson, J. R., Berggren, K., Olavarria, H., Sasaki, A. W., Chang, M., Flora, K. D., Loftis, J. M. (2015) A longitudinal study evaluating the effects of interferon-alpha therapy on cognitive and psychiatric function in adults with chronic hepatitis C. *J. Psychosom. Res.* **78(2)**, 184–192.

Jang, Y., Boo, S., Yoo, H. (2018a) Hepatitis B virus infection: Fatigue-associated illness experiences among Koreans. *Gastroenterol. Nurs.* **41(5)**, 388–395.

Jang, Y., Kim, J. H., Lee, H., Lee, K., Ahn, S. H. (2018b) A quantile regression approach to explain the relationship of fatigue and cortisol, cytokine among Koreans with hepatitis B. *Sci. Rep.* **8(1)**, 16434.

Kharabian Masouleh, S., Herzig, S., Klose, L., Roggenhofer, E., Tenckhoff, H., Kaiser, T., Thöne-Otto, A., Wiese, M., Berg, T., Schroeter, M. L., Margulies, D. S., Villringer, A. (2017) Functional connectivity alterations in patients with chronic hepatitis C virus infection: A multimodal MRI study. *J. Viral Hepat.* **24(3)**, 216–225.

Komas, N. P., Ghosh, S., Abdou-Chekaraou, M., Pradat, P., Al Hawajri, N., Manirakiza, A., Laghoe, G. L., Bekondi, C., Brichler, S., Ouavéné, J. O., Sépou, A., Yambiyo, B. M., Gody, J. C., Fikouma, V., Gerber, A., Abeywickrama Samarakoon, N., Alfaiate, D., Scholtès, C., Martel, N., Le Gal, F., Lo Pinto, H., Amri, I., Hantz, O., Durantel, D., Lesbordes, J. L., Gordien, E., Merle, P., Drugan, T., Trépo, C., Zoulim, F., Cortay, J. C., Kay, A. C., Dény, P. (2018) Hepatitis B and hepatitis D virus infections in the Central African Republic, twenty-five years after a fulminant hepatitis outbreak, indicate continuing spread in asymptomatic young adults. *PLoS Negl. Trop. Dis.* **12(4)**, e0006377.

Lanini, S., Ustianowski, A., Pisapia, R., Zumla, A., Ippolito, G. (2019) Viral hepatitis: Etiology, epidemiology, transmission, diagnostics, treatment, and prevention. *Infect. Dis. Clin. North Am.* **33(4)**, 1045–1062.

Lima, Y. B., Magalhães, C. B. A., Garcia, J. H. P., Viana, C. F. G., Prudente, G. F. G., Pereira, E. D. B. (2019) Association between fatigue and exercise capacity in patients with chronic liver disease awaiting liver transplantation. *Arq. Gastroenterol.* **56(3)**, 252–255.

Lowry, D., Burke, T., Galvin, Z., Ryan, J. D., Russell, J., Murphy, A., Hegarty, J., Stewart, S., Crowe, J. (2016) Is psychosocial and cognitive dysfunction misattributed to the virus in hepatitis C infection? Select psychosocial contributors identified. *J. Viral Hepat.* **23(8)**, 584–595.

Monaco, S., Mariotto, S., Ferrari, S., Calabrese, M., Zanusso, G., Gajofatto, A., Sansonno, D., Dammacco, F. (2015) Hepatitis C virus-associated neurocognitive and neuropsychiatric disorders: Advances in 2015. *World J. Gastroenterol.* **21(42)**, 11974–11983.

Ney, M., Tangri, N., Dobbs, B., Bajaj, J., Rolfson, D., Ma, M., Ferguson, T., Bhardwaj, P., Bailey, R. J., Abraldes, J., Tandon, P. (2018) Predicting hepatic encephalopathy-related hospitalizations using a composite assessment of cognitive impairment and frailty in 355 patients with cirrhosis. *Am. J. Gastroenterol.* **113(10)**, 1506–1515.

Pawełczyk, A. (2016) Consequences of extrahepatic manifestations of hepatitis C viral infection (HCV). *Postepy Hig. Med. Dosw. (Online)* **70**, 349–359. (in Polish)

Polukchi T. V.; Abuova G. N.; Slavko Y. A.

Posada, C., Moore, D. J., Woods, S. P., Vigil, O., Ake, C., Perry, W., Hassanein, T. I., Letendre, S. L., Grant, I.; HIV Neurobehavioral Research Center Group (2010) Implications of hepatitis C virus infection for behavioral symptoms and activities of daily living. *J. Clin. Exp. Neuropsychol.* **32(6)**, 637–644.

Prell, T., Dirks, M., Arvanitis, D., Braun, D., Peschel, T., Worthmann, H., Schuppner, R., Raab, P., Grosskreutz, J., Weissenborn, K. (2019) Cerebral patterns of neuropsychological disturbances in hepatitis C patients. *J. Neurovirol.* **25(2)**, 229–238.

Sonavane, A. D., Saigal, S., Kathuria, A., Choudhary, N. S., Saraf, N. (2018) Guillain-Barré syndrome: Rare extra-intestinal manifestation of hepatitis B. *Clin. J. Gastroenterol.* **11(4)**, 312–314.

Stasi, C., Rosselli, M., Zignego, A. L., Laffi, G., Milani, S. (2014) Serotonin and its implication in the side-effects of interferon-based treatment of patients with chronic viral hepatitis: Pharmacological interventions. *Hepatol. Res.* **44(1)**, 9–16.

Swain, M. G. (2006) Fatigue in liver disease: Pathophysiology and clinical management. *Can. J. Gastroenterol.* **20(3)**, 181–188.

Tagliapietra, M., Monaco, S. (2020) Neuroimaging findings in chronic hepatitis C virus infection: Correlation with neurocognitive and neuropsychiatric manifestations. *Int. J. Mol. Sci.* **21(7)**, 2478.

Tamayo, A., Shah, S. R., Bhatia, S., Chowdhury, A., Rao, P. N., Dinh, P., Knox, S. J., Gaggar, A., Subramanian, G. M., Mohan, V. G., Sood, A., Mehta, R., Sarin, S. K. (2016) Correlates of disease-specific knowledge among patients with chronic hepatitis B or hepatitis C infection in India. *Hepatol. Int.* **10(6)**, 988–995.

Torgrimson-Ojerio, B., Ross, R. L., Dieckmann, N. F., Avery, S., Bennett, R. M., Jones, K. D., Guarino, A. J., Wood, L. J. (2014) Preliminary evidence of a blunted anti-inflammatory response to exhaustive exercise in fibromyalgia. *J. Neuroimmunol.* **277(1–2)**, 160–167.

Torre, P., Aglitti, A., Masarone, M., Persico, M. (2021) Viral hepatitis: Milestones, unresolved issues, and future goals. *World J. Gastroenterol.* **27(28)**, 4603–4638.

Wang, H., Zhou, Y., Yan, R., Ru, G. Q., Yu, L. L., Yao, J. (2019) Fatigue in chronic hepatitis B patients is significant and associates with autonomic dysfunction. *Health Qual. Life Outcomes* **17(1)**, 130.

Więdłocha, M., Marcinowicz, P., Sokalla, D., Stańczykiewicz, B. (2017) The neuropsychiatric aspect of the HCV infection. *Adv. Clin. Exp. Med.* **26(1)**, 167–175.

Weissenborn, K., Ennen, J. C., Bokemeyer, M., Ahl, B., Wurster, U., Tillmann, H., Trebst, C., Hecker, H., Berding, G. (2006) Monoaminergic neurotransmission is altered in hepatitis C virus infected patients with chronic fatigue and cognitive impairment. *Gut* **55(11)**, 1624–1630.

Wozniak, M. A., Lugo Iparraguirre, L. M., Dirks, M., Deb-Chatterji, M., Pflugrad, H., Goldbecker, A., Tryc, A. B., Worthmann, H., Gess, M., Crossey, M. M., Forton, D. M., Taylor-Robinson, S. D., Itzhaki, R. F., Weissenborn, K. (2016) Apolipoprotein E-ε4 deficiency and cognitive function in hepatitis C virus-infected patients. *J. Viral Hepat.* **23(1)**, 39–46.

Wu, W. Y., Kang, K. H., Chen, S. L., Chiu, S. Y., Yen, A. M., Fann, J. C., Su, C. W., Liu, H. C., Lee, C. Z., Fu, W. M., Chen, H. H., Liou, H. H. (2015) Hepatitis C virus infection: A risk factor for Parkinson's disease. *J. Viral Hepat.* **22(10)**, 784–791.

Yeoh, S. W., Holmes, A. C. N., Saling, M. M., Everall, I. P., Nicoll, A. J. (2018) Depression, fatigue and neurocognitive deficits in chronic hepatitis C. *Hepatol. Int.* **12(4)**, 294–304.

Zayed, H. S., Amin, A., Alsirafy, S., Elsayed, N. D., Abo Elfadl, S., Nasreldin, M., Enaba, D., Nawito, Z. (2018) Psychiatric and functional neuroimaging abnormalities in chronic hepatitis C virus patients: Is vasculitis a contributing factor? *Arab J. Gastroenterol.* **19(2)**, 71–75.

Zimmerman, M., Clark, H. L., Multach, M. D., Walsh, E., Rosenstein, L. K., Gazarian, D. (2015) Have treatment studies of depression become even less generalizable? A review of the inclusion and exclusion criteria used in placebo-controlled antidepressant efficacy trials published during the past 20 years. *Mayo Clin. Proc.* **90(9)**, 1180–1186.

Vascular Anatomy and Variations of the Anterior Abdominal Wall – Significance in Abdominal Surgery

Stoyan Kostov[1], Svetla Dineva[2,3], Yavor Kornovski[1], Stanislav Slavchev[1], Yonka Ivanova[1], Angel Yordanov[4]

[1]Department of Gynecology, University Hospital "Saint Anna", Medical University of Varna, Varna, Bulgaria;
[2]Diagnostic Imaging Department, Medical University of Sofia, Sofia, Bulgaria;
[3]National Cardiology Hospital, Sofia, Bulgaria;
[4]Department of Gynecologic Oncology, Medical University Pleven, Pleven, Bulgaria

Abstract: Detailed knowledge of the human anatomy is an integral part of every surgical procedure. The majority of surgery related complications are due to a failure to possess appropriate knowledge of human anatomy. However, surgeons pay less attention of the anatomy of the anterior abdominal wall. It is composed of nine abdominal layers, which are composed of fascias, muscles, nerves, and vessels. Many superficial and deep vessels and their anastomoses supply the anterior abdominal wall. Moreover, anatomical variations of these vessels are often presented. Intraoperative and postoperative complications associated with entry and closure of the anterior abdominal wall could compromise the best surgical procedure. Therefore, sound knowledge of the vascular anatomy of the anterior abdominal wall is fundamental and a prerequisite to having a favourable quality of patient care. The purpose of the present article is to describe and delineate the vascular anatomy and variations of the anterior abdominal wall and its application in abdominal surgery. Consequently, the most types of abdominal incisions and laparoscopic accesses will be discussed. Furthermore, the possibility of vessels injury related to different types of incisions and accesses will be outlined in detail. Morphological characteristics and distribution pattern of the vascular system of the anterior abdominal wall is illustrated by using figures either from open surgery, different types of imaging modalities or embalmed cadaveric dissections. Oblique skin incisions in the upper or lower abdomen such as McBurney, Chevron and Kocher are not the topic of the present article.

Mailing Address: Assoc. Prof. Angel Yordanov, Department of Gynecologic Oncology, Medical University Pleven, Bul Georgi Kochev 8A, 5800 Pleven, Bulgaria; e-mail: angel.jordanov@gmail.com

Introduction

The anterior abdominal wall (AAW) is limited superiorly by the xiphoid process and costal arch, and inferiorly by the inguinal ligament, bones of the pubis and the iliac crest (Arslan, 2005). It is composed of nine abdominal layers, which consist of fascias, muscles, nerves and vessels (Mahadevan, 2006). Rich arterial and venous anastomoses from the superficial and deep vessels of the AAW are present (Gray et al., 2005; Netter, 2014). Therefore, physicians from surgical specialties regarding abdominal procedures should be familiar with the anatomy of the AAW. Moreover, surgeons should anticipate the types of surgical procedures that will be performed and possible complicated aspects related to the abdominal incision and the procedure. Knowledge of AAW anatomy is crucial to prevent iatrogenic vessels injury and to enhance repair in order to reduce the risk of incisional hernias or wound dehiscence. Additionally, the development and further evolution of the laparoscopic surgery emphasizes the essential and thorough understanding of the vascular anatomy of the AAW (Baggish and Karram, 2006). The goal of the present article is to delineate the AAW vessels anatomy and its application in abdominal surgery. Consequently, the majority of types of abdominal incisions and laparoscopic accesses will be presented. Furthermore, the possibility of vessels injury related to different types of accesses will be outlined in detail. Oblique skin incisions in the upper and lower abdomen such as McBurney, Chevron and Kocher are not the topic of the present article.

Methodology

The review and consensus process between authors was completed from March 2022 to December 2022. A comprehensive literature searches of studies (articles written in English and German) associated with AAW vessels anatomy, variations and abdominal incisions was performed. A computer-based extensive review of the MEDLINE, PubMed, EMBASE, and SciSearch databases was conducted. We used the following keywords and Medical Subject Headings (Mesh) terms: "anterior abdominal wall", "anatomy", "vessels", "artery", "vein", "variation", "incisions", "trocar", "complication", "hematoma". References from the selected papers were scanned for identifying other related articles. Additional information and figures from previous surgical procedures, different types of imaging modalities and anatomical studies on cadavers performed by authors were used for the preparation of the article. The anatomical terms used in the paper conform to the Terminologia Anatomica (Whitmore, 1999). Given the review nature of the article, no institutional review board or ethics committee approval was required.

Regions of the anterior abdominal wall

The AAW could be divided by into four quadrants by imaginary lines, which pass vertically and horizontally to the umbilicus (Farthing, 2018). The quadrants divide the anterior abdomen into the right and left upper and lower quadrants. Additionally,
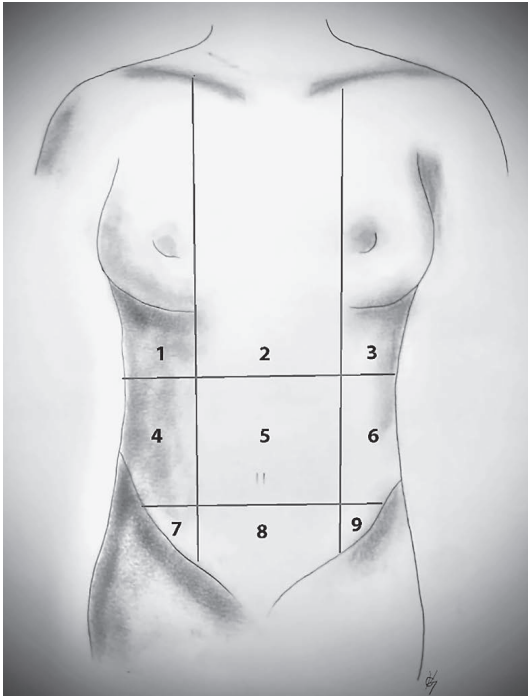
Figure 1 – The nine regions of the AAW (anterior abdominal wall). 1, 3 – right and left hypochondriac (located under the right and left costal margin). 4, 6 – right and left lumbar (on the right and left side of the abdomen). 7, 8 – right and left iliac (over the right and left iliac region). 8 – hypogastric (lower central abdomen – suprapubic). 2 – epigastric region (upper central abdomen). 5 – umbilical region.

the AAW could be separated into 9 regions, which are created by two vertical lines (through the midline of each clavicle) and two horizontal lines (one through the costal margin and one through the transtubercular plane). The regions are: right/left hypochondriac, right/left lumbar, right/left iliac, umbilical, hypogastric and epigastric (Gray et al., 2005; Netter, 2014). The nine regions are illustrated in Figure 1. This separation helps physicians accurately to describe the pathological conditions in the AAW (Arslan, 2005).

Layers of the anterior abdominal wall
The AAW from superficial to deep consists of the following nine layers: skin, subcutaneous fat, superficial fascia (Camper's fascia and Scarpa's fascia), external oblique muscle, internal oblique muscle, transversus abdominis muscle, transversalis fascia, preperitoneal adipose and areolar tissue, and parietal peritoneum (Mahadevan, 2006; Farthing, 2018). Some of the layers are shown in Figure 2.

   The superficial fascia consists of two additional fascial layers – Camper's fascia and Scarpa's fascia. The Camper's fascia is a soft and movable adipose layer subjacent to the dermis, which inferior prolongation unites within the superficial fascia covering the labia majora. Additionally, the Camper's fascia passes above the inguinal ligament (without attaching to it) and continues with the superficial fascia of the thigh (Gray et al., 2005; Mahadevan, 2006; Netter, 2014; Farthing, 2018).

Kostov S.; Dineva S.; Kornovski Y.; Slavchev S.; Ivanova Y.; Yordanov A.
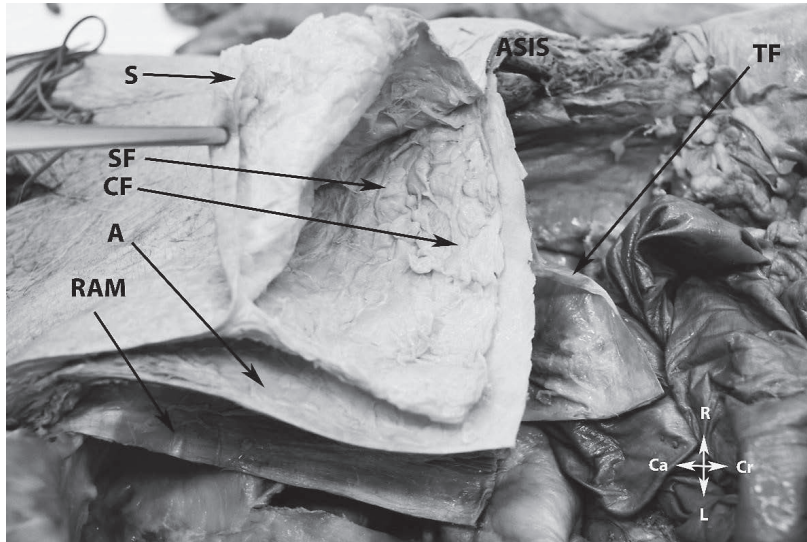
Figure 2 – The majority of the layers of anterior abdominal wall (embalmed cadaver – right pelvic sidewall).
S – skin; SF – subcutaneous fat; CF – Camper's fascia; A – aponeurosis of rectus abdominis muscle;
RAM – rectus abdominis muscle; TF – transversalis fascia; ASIS – anterior superior iliac spine; Cr – cranial;
Ca – caudal; R – right; L – left.

Camper's fascia divides the skin from the muscles and plays an important role as a protector and an insulator to the deep organs of the abdomen (MacKay et al., 2022). Camper's fascia is often used as a marker for identifying superficial epigastric vessels, as they are located between the Scarpa's and Camper's fascia. Moreover, the latter has implication during inguinofemoral lymphadenectomy, as superficial inguinal lymph nodes are also located between these two superficial fascial layers. The incision is performed just deep to the Camper's fascia. The fascia has also applications during wound closure after cesarean section. The space between two superficial fascial layers is a potential source of postoperative wound complications such as dehiscence, seroma and fluid accumulation. Therefore, studies showed that approximation of Camper's fascia during wound closure was associated with lower rate of dehiscence and incisional hernias (Bohman et al., 1994; Hodgson et al., 2000; Mian et al., 2014).

The Scarpa's is a dense collagenous connective tissue layer, which lies below the Camper's fascia. It is thinner than Camper's fascia, especially in inferior direction. This Scarpa fascia is also known as Thompson's fascia. Superiorly, it continues with the retromammary fascia, whereas inferiorly with the superficial fascia covering the perineum. The continuation of the Scarpa's fascia to the perineum is known as Colles' fascia. The Scarpa's fascia is firmly attached to the linea alba, perineum and inguinal ligament. It passes below the ligament and continues with the fascia lata of

the thigh (Reardon et al., 2004; Mahadevan, 2006; Farthing, 2018; Joshi and Duong, 2022).

A muscular-aponeurotic layer consists of the following anatomical structures – the external oblique muscles, the internal oblique muscles, the rectus abdominis muscles, the transversus abdominis muscles, the pyramidalis muscles, the rectus sheath and the linea alba. The pyramidalis muscles are inconstant and could be absent (Taylor and Daniel, 1975; Stern and Nahai, 1992; Yüksel and Yüksel, 1995; Arslan, 2005; Gagnon and Blondeell, 2006; Fukaya et al., 2011; Tubbs et al., 2016; Ogami et al., 2017; Zubler et al., 2021).

The linea alba is located at the midline (medial to the rectus abdominis muscle) from the xiphoid process to the symphysis pubis. It is formed from the aponeuroses of the external, internal and transversus abdominis muscles. The linea alba is significantly thicker above the umbilicus as the rectus abdominis muscles lie closer from one other, whereas below the umbilicus the linea alba narrows progressively as the muscles diverge from one other. At the lower AAW, the linea alba has two attachments – one to the symphysis pubis and the other behind rectus muscles to the posterior surface of the pubic crest (also known as "adminiculum lineae albae" (Arslan, 2005; Gray et al., 2005; Mahadevan, 2006; Netter, 2014).

The umbilicus is a result from the remnants of the umbilical cord. The base of the umbilicus is the thinnest part of the AAW. It is located in the linea alba, but its position depends on the body mass index of the patients. Generally, in adults it is located at the level of the disc between the 3th and 4th lumbar vertebral body. The abdominal aorta bifurcation is located 2 cm inferior to the umbilicus. The
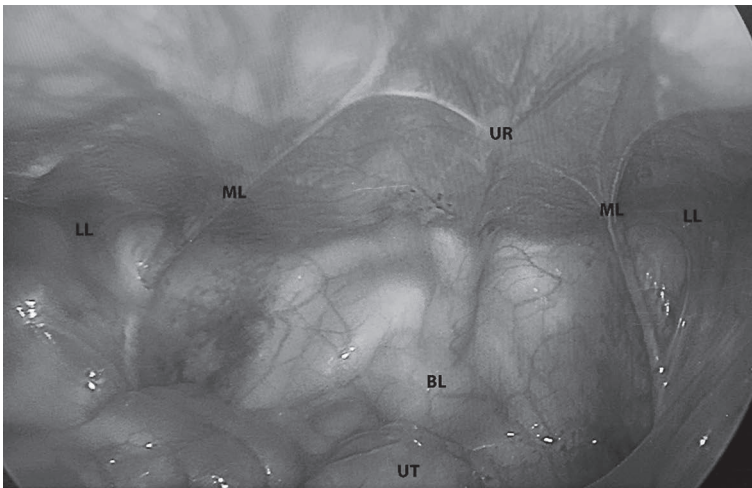
Figure 3 – Ligament of the anterior abdominal wall (laparoscopic surgery). UR – urachus remnant, median umbilical ligament; ML – medial umbilical ligament (obliterated umbilical arteries); LL – lateral ligament (inferior epigastric artery/vein); BL – bladder; UT – uterus.

following ligaments attach to the umbilicus – median (urachus remnant), medial (obliterated umbilical arteries), lateral (inferior epigastric artery/vein) and the falciforme ligament (Arslan, 2005; Gray et al., 2005; Mahadevan, 2006; Netter, 2014) (Figure 3).

The rectus sheath is an aponeurotic sheath that surrounds the rectus abdominis muscle. It is formed by two sublayers – anterior and posterior. The anterior is derived from two adherent layers – one of aponeurosis of the external oblique muscle and the other from the anterior aponeurosis of the internal oblique muscle. The posterior layer of the rectus sheath is formed from the posterior aponeurosis of the internal oblique muscle and the aponeurosis of the transversus abdominis (Arslan, 2005; Mahadevan, 2006). However, that particular layer arrangement of the rectus sheath exists only below the arcuate line (5 cm below the umbilicus). Above that line, the anterior aponeurosis of the internal oblique muscle and the aponeurosis of the transverse muscle pass completely anterior to the rectus abdominis muscle. Therefore, the posterior wall of the rectus abdominis sheath is absent above that line, and the transversalis fascia lies just below the muscle (Gray et al., 2005; Netter, 2014).

The transversalis fascia of the AAW is located between the inner surface of transversus abdominis and the preperitoneal fat. It contributes to the posterior wall of the rectus sheath. Although it is a relatively thin layer, in the lower part of the anterior abdominal wall is less expansive, especially at the level of the inguinal region, where it becomes thicker and dense. The fascia attaches to the iliac crest, the posterior margin of the inguinal ligament, to the pecten pubis and to the conjoint tendon. At the level of the deep inguinal ring, the round ligament of the uterus passes through the transversalis fascia (Arslan, 2005; Gray et al., 2005; Mahadevan, 2006; Netter, 2014).

The preperitoneal fat is located between the transversalis fascia and the parietal peritoneum. Its thickness depends on body mass index of the patient, but in the lower part of the AAW, the preperitoneal fat is always thicker. Below the umbilicus, the preperitoneal fast is divided into two layers (anterior and posterior) by the umbilical prevesical aponeurosis (fascia prevesicalis). The letter represents a triangle with a posterior broad base formed by the fascia of the bladder. The anterior vertex of the triangle fuses with the transversalis fascia at the level of the umbilicus. The space near the bladder, which is located between the umbilical prevesical aponeurosis and transversal fascia, is called Retzius space (Gray et al., 2005; Mahadevan, 2006; Netter, 2014).

The parietal peritoneum is the last posterior layer of the AAW. It is loosely attached to the AAW due to the existence of the preperitoneal fat. However, the parietal peritoneum is dense and firmly attached to the umbilicus, linea alba, inferior surface of the diagraph and the posterior wall of the inguinal canal. At the lower and posterior part of the AAW, the parietal peritoneum passes though the iliac fossa without joining to the inguinal ligament. Contrary, the transversalis fascias attaches
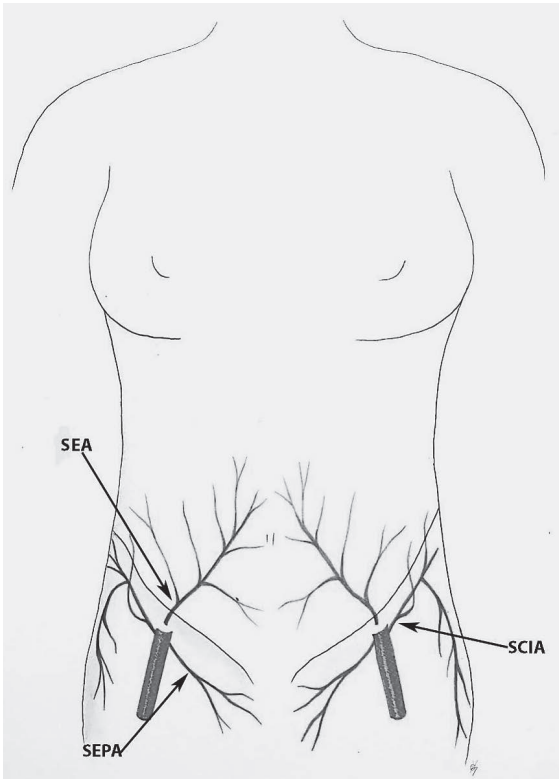
Figure 4 – Superficial arteries of the anterior abdominal wall. SEA – superficial epigastric artery; SCIA – superficial circumflex iliac artery; SEPA – superficial external pudendal artery.

to the inguinal ligament. As a result of that divergation between the fascia and the peritoneum, a potential space could be encountered – the Bogros space (Gray et al., 2005; La Falce et al., 2006; Netter, 2014).

Superficial arteries of the anterior abdominal wall
The superficial arteries of the AAW are the following: superficial epigastric artery (SEA), superficial circumflex iliac artery (SCIA), superficial external pudendal artery (SEPA). These arteries are illustrated in Figure 4.

Superficial epigastric artery
The superficial epigastric artery (SEA) arises from the common femoral artery 2–3 cm below the inguinal ligament. It then proceeds superiorly and laterally from the femoral triangle and then crosses the inguinal ligament at its midpoint. Initially it is located deep to Scarpa's fascia. Subsequently, above the inguinal ligament, the SEA is located superomedially and continues in the subcutaneous fat by piercing the Scarpa's fascia (Reardon et al., 2004; Gagnon and Blondeell, 2006). The SEA is located laterally and deeper than its venous counterpart is. The medial branches of

the artery anastomose with the branches of intercostal arteries, superficial and deep circumflex iliac arteries, whereas lateral branches anastomose with the branches of superior and inferior epigastric arteries (Reardon et al., 2004).

Anatomical variations and discussion
SEA variations differ according to different anatomical studies. Fathi et al. (2008) performed 40 dissections on 20 preserved or fresh male cadavers. Authors reported that in 57.9% of the cases, the SEA originated directly from a common femoral artery. Some studies found that the SEA could be absent in approximately one third of the population (Taylor and Daniel, 1975; Gagnon and Blondeell, 2006; Fukaya et al., 2011). A large ascending branch or multiple small branches from the SCIA replaced the absent SEA (Taylor and Daniel, 1975; Stern and Nahai, 1992; Reardon et al., 2004; Gagnon and Blondeell, 2006; Fukaya et al., 2011). However, other studies reported a presence of the SEA in 90, 94 and 95% of the examined cadavers, respectively (Reardon et al., 2004; Rozen et al., 2010). SEA could arise in a common trunk with the SCIA, SEPA and deep circumflex iliac artery (Taylor and Daniel, 1975; Stern and Nahai, 1992; Reardon et al., 2004; Gagnon and Blondeell, 2006; Fukaya et al., 2011). Fukaya et al. (2011) found a common trunk between SEA and SCIA in 36.4% of cases. Reardon et al. (2004) reported that the SEA shared a common trunk with the SCIA, SEPA and deep circumflex iliac artery in 70, 35 and 20% of cases, respectively. In rare cases, the artery could arise from the pudendal artery or deep femoral artery (Yüksel and Yüksel, 1995; Tubbs et al., 2016). Yüksel and Yüksel (1995) reported a case of SCIA and SEA arising in a common stem from the deep femoral artery.

Superficial circumflex iliac artery
In the majority of cases, the SCIA originates from the lateral aspect of the femoral artery at the level of the SEA (sometimes in a common trunk) (Figure 5). It then perforates laterally the deep fascia of the thigh and proceeds parallel to the inguinal ligament. The SCIA has a lateral course forward the anterior superior iliac spine (ASIS) (Yüksel and Yüksel, 1995; Arslan, 2005). It has two branches – superficial and deep. The superficial branch pierces the deep fascia and proceeds in a latero-cranial direction to the deep fat, whereas the deep branch runs subfascially over a longer distance and supplies the deep inguinal lymph nodes, sartorius muscle and deep fascia (Zubler et al., 2021). The SCIA branches anastomose with branches of the SEA, deep circumflex iliac artery, superior gluteal and lateral femoral circumflex artery (Arslan, 2005; Tubbs et al., 2016).

Anatomical variations and discussion
Generally, the SCIA is more constant than the SEA. It could arise from the superficial or deep femoral artery or in a common stem with the SEA (Ogami et al., 2017; Zubler et al., 2021). Ogami et al. (2017) observed deep circumflex iliac artery and
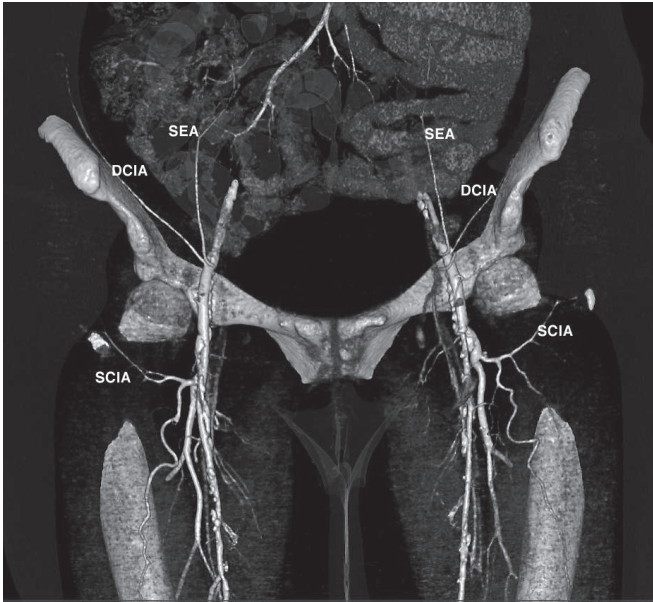
Figure 5 – Thin slice volume rendered computed tomography reconstruction of ilio-femoral vascular segment. Superficial epigastric artery (SEA), deep circumflex iliac artery (DCIA) and superficial circumflex iliac artery (SCIA) is annotated bilaterally.

SCIA in 130 femoral triangles derived from 65 formalin-fixed cadavers. Authors reported for double SCIA in 7.7% of cases. Bilateral double SCIA was identified in one cadaver. Ghassemi et al. (2013) reported for three types of variations of the SCIA. In type I, the artery had one or two branches and originated below the inguinal ligament. In type II, the artery originated from its deep counterpart. Type III variations was associated with absence of the SCIA, which was observed in 5.5% of specimens.

Superficial external pudendal artery
The SEPA arises from the femoral artery below the origin of SEA and SCIA. It continues medially, generally below the great saphenous vein and across the round ligament. Subsequently, the SEPA divides into two main branches. The superior branch supplies the symphysis pubis and the lower part of the AAW. The inferior branch supplies the skin of the labia majora. The branches of SEPA anastomose with branches of the internal pudendal artery (Gray et al., 2005).

Anatomical variations and discussion
La Falce et al. (2006) investigated the anatomy and variations of the SEPA in 50 inguinal regions of cadavers. Authors found that in the majority of cases the SEPA originated from the femoral artery – 98%. The incidence of SEPA originating from the deep femoral artery was 2%. A duplicated SEPA was found in 46% of specimens.

Superficial veins of the anterior abdominal wall

Superficial veins of the AAW are the following: superficial epigastric vein (SEV), superficial circumflex iliac vein (SCIV), superficial external pudendal vein (SEPV). These veins are shown in Figures 6 and 7.

Superficial epigastric vein

SEV drains into the great saphenous vein. It also drains in the portal vein through the paraumbilical veins. The SEV is located medial and superficial compared to the artery and forms multiple anastomoses at the superficial layer of the AAW. Venous connections between the SEV and thoracoepigastric vein form the cavo-caval anastomoses. Additionally, the anastomoses between the SEV/thoracoepigastric vein and paraumbilical veins form the portocaval anastomoses. The SEV also connects through anastomoses with the other superficial veins of the AAW (Arslan, 2005; Gray et al., 2005; Mahadevan, 2006; Fukaya et al., 2011).

Anatomical variations and discussion
In some atlases of anatomy, it was illustrated that the SEV drained into the femoral vein (Netter, 2014). It is debatable, as SEV draining in the femoral vein is rather an anatomical variation that a general draining pattern of the vein. Reardon et al. (2004) performed 22 cadaveric dissections and examined the anatomy of the SEV and SEA. Authors observed that the SEV drained into the saphenous bulb in 95.3% of cases.
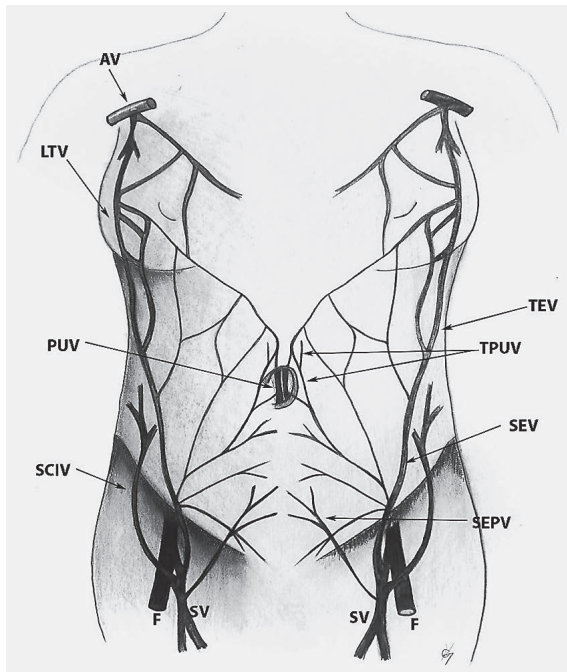
Figure 6 – Superficial veins of the AAW (anterior abdominal wall). AV – axillary vein; LTV – lateral thoracic vein; TEV – thoraco-epigastric vein; TPUV – tributaries of para-umbilical veins; PUV – para-umbilical veins; SCIV – superficial circumflex iliac vein; F – femoral vein; SV – saphenous vein; SEPV – superficial external pudendal vein; SEV – superficial epigastric vein.
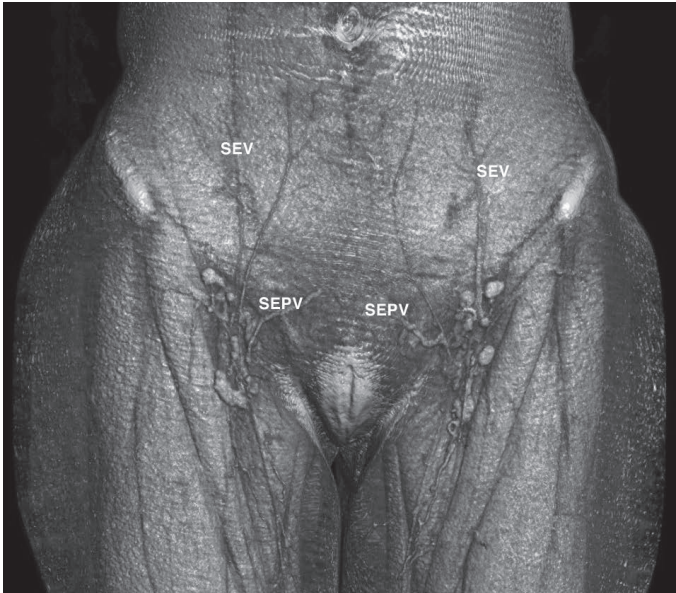
Figure 7 – Volume rendered image of computed tomography venography depicturing SEV and SEPV bilaterally (anterior view of the AAW – anterior abdominal wall). SEV – superficial epigastric vein; SEPV – superficial external pudendal vein.

The vein was absent in one case. The vein drained as an individual vein, as multiple veins, or both in 57, 38, and 4.7% of cases, respectively. Mühlberger et al. (2009) dissected 114 formalin fixed bodies with 217 great saphenous veins. Authors found that the SEV drained in the saphenous vein in 78.3% of cases. In the majority of cases, it entered the great saphenous vein 1.2 cm distally to its orifice. Contrary to these results, Rozen et al. (2009) observed that the SEV drained into the superficial
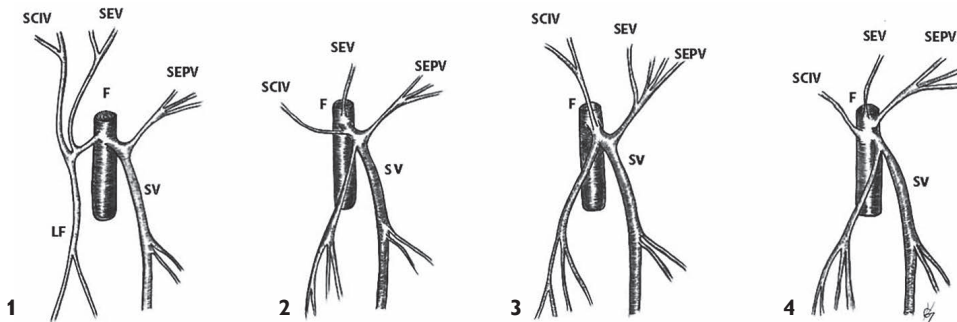
Figure 8 – Draining pattern variations of the SEV. SEPV – superficial external pudendal vein; SCIV – superficial circumflex iliac vein; SEV – superficial epigastric vein; SV – saphenous vein; LF – lateral femoral vein; F – femoral vein.
1 – SEV forms a common trunk with the lateral superficial femoral and superficial circumflex iliac vein. The drunk drain into the femoral vein. 2 – The SEV drains directly into the femoral vein. 3 – A common trunk between the SEV and superficial external pudendal vein, which drains into the saphenous vein. 4 – SEV, SEPV and SCIV drains separately into the saphenous vein.

Kostov S.; Dineva S.; Kornovski Y.; Slavchev S.; Ivanova Y.; Yordanov A.

femoral vein in 62.5% of among 200 examined sides. However, the term "superficial femoral vein" has been discarded. Terminologica anatomica did not recognized this term and replaced it with just femoral vein, as the vein is deep, not superficial (Monkhouse, 2001; Caggiati et al., 2002; Chua et al., 2017). Chun et al. (1992) investigated 249 lower limbs among Koreans and found that the SEV drained in the great saphenous vein directly or by a common trunk in 77.1% of cases. The most common draining pattern variations of the SEV are shown in Figure 8.

Superficial circumflex iliac vein

The SCIV runs parallel to the inguinal ligament following its arterial counterpart. In most cases it drains in the great saphenous vein. The SCIV collects the blood from the lateral lower part of the AAW (the area, which is located superior to the lateral part of the inguinal ligament) and the proximal region of the superficial thigh (Arslan, 2005; Gray et al., 2005; Netter, 2014). Its branches anastomose with the branches of the SEV, deep circumflex iliac vein, external pudendal vein and thoracoepigastric veins.

Anatomical variations and discussion
Mühlberger et al. (2009) examined 14 formalin fixed bodies with 217 great saphenous veins. Authors observed that the SCIV drains in the great saphenous vein in the 82.9% of cases. Glasser (1943) performed a dissection of 50 cadavers (100 lower extremities) and examined the venous variations in the fossa ovalis. Authors found that the incidence of SCIV, which drained into the femoral vein was approximately 1%. Glasser also found an incidence of 9% for the SCIV drained in a
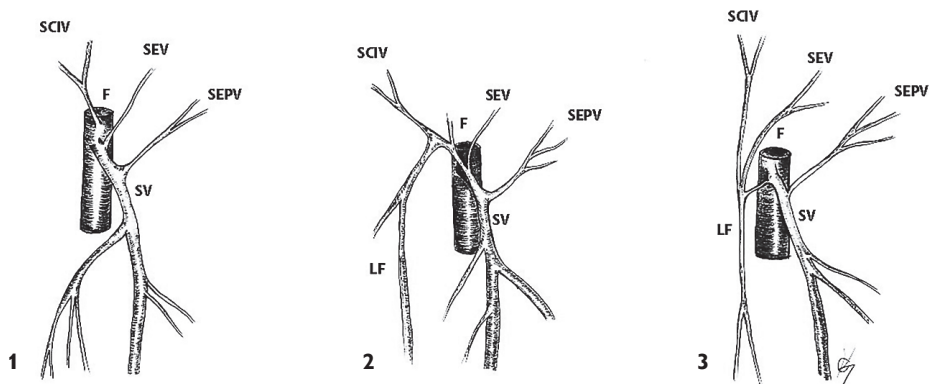
Figure 9 – Draining pattern variations of the SCIV. SEPV – superficial external pudendal vein; SCIV – superficial circumflex iliac vein; SEV – superficial epigastric vein; SV – saphenous vein; LF – lateral femoral vein; F – femoral vein.
1 – SCIV drains into the femoral vein. 2 – SCIV forms a common trunk with the lateral femoral vein. Both veins drain into the saphenous vein. 3 – SCIV, SEV and lateral femoral vein drain into the saphenous vein in a common trunk.

common trunk with lateral femoral and SCIV. A common trunk between the lateral femoral and SCIV, which drained in the great saphenous vein, was observed in 1% of cases. Actually, the term "lateral femoral vein" correspondence with the term "deep femoral vein" or "profunda femoris vein" according to Terminologica anatomica (Monkhouse, 2001; Caggiati et al., 2002). However, Glasser (1943) concluded that venous variations were not common since the venous patterns tend to be generally inconstant in the body. Penteado (1983) examined the anatomy of SCIV in 43 formalin-fixed cadavers. In only two cases the SCIV drained in the femoral vein, whereas in all other cases it entered in the great saphenous vein. In 36.3%, the SCIV and the SEV shared a common trunk and drained in the great saphenous vein. Authors also found that in 12.7% of cases the SCIV shared a common trunk with superficial accessory saphenous vein and a common trunk with the SEV and superficial accessory saphenous vein in 10.9% of cases. Rozen et al. (2011) observed a common trunk between SCIV and SEV in 21% of examined cases. Chun et al. (1992) found that the SCIV entered in the great saphenous vein either directly or in a common trunk in 83.1% of cases. Authors described 10 variant types, of which a common trunk between SCIV and lateral accessory saphenous vein was the most common – 13.3%. The most common draining pattern variations of the SCIV are shown in Figure 9.

Superficial external pudendal vein

The SEPV follows its arterial counterpart and in the majority of cases drains in the great saphenous vein. The SEPV is a continuation of the labial veins. It collects the blood from the medial lower part of the AAW and from the symphysis pubis. Its branches anastomose with the branches of deep external pudendal vein, SEV.
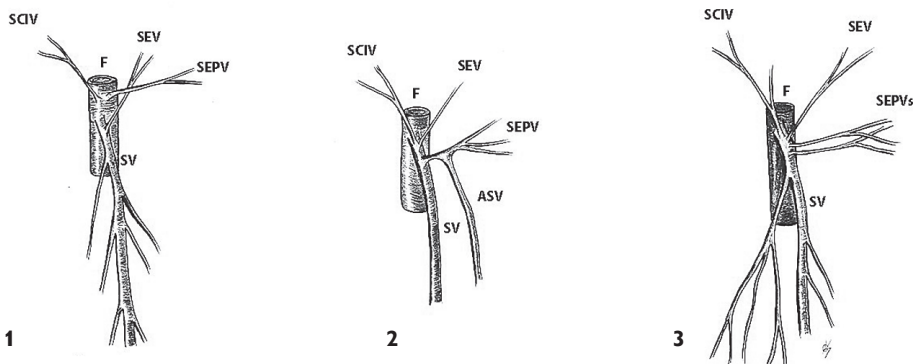
Figure 10 – Draining pattern variations of the SEPV are shown in Figure 8. SEPV – superficial external pudendal vein; SEPVs – superficial external pudendal veins; SCIV – superficial circumflex iliac vein; SEV – superficial epigastric vein; SV – saphenous vein; ASV – accessory saphenous vein; LF – lateral femoral vein; F – femoral vein. 1 – The SCIV and the SEPV drain separately into the femoral vein. 2 – An accessory saphenous vein forms a common stem with the SEPV. Both veins drain into the saphenous vein. 3 – Two SEPVs drain separately into the saphenous vein.

The bilateral superficial external pudendal veins form many anastomoses above the symphysis pubis (Gray et al., 2005; Netter, 2014).

Anatomical variations and discussion
Chun et al. (1992) found that SEPV drained in the great saphenous vein in 61.9% of cases. Glasser (1943) reported an incidence of 81% for this draining pattern. The incidence of SEPV draining in the femoral vein was 1%.

Chun et al. (1992) reported that the most frequent draining pattern variation was a common trunk between SEPV, medial accessory and SEV.

The incidence of a common trunk between SEPV and accessory saphenous vein, which drain in the great saphenous vein, is 6%. In 3% of cases, two separate SEPVs could be observed. A common trunk between SEPV and SEV is observed in 2% of the population (Glasser, 1943). Draining pattern variations of the SEPV are shown in Figure 10.

Deep arteries of the anterior abdominal wall
The deep arteries of the AAW are the following: the inferior epigastric artery (IEA), deep circumflex iliac artery (DCIA), internal thoracic artery (ITA) and superior epigastric artery (SUEA). Deep arteries of the AAW are shown in Figure 11.

Inferior epigastric artery
The IEA originates from the anteromedial aspect of the external iliac artery in the extraperitoneal connective tissue just above and the inguinal ligament (Figures 12
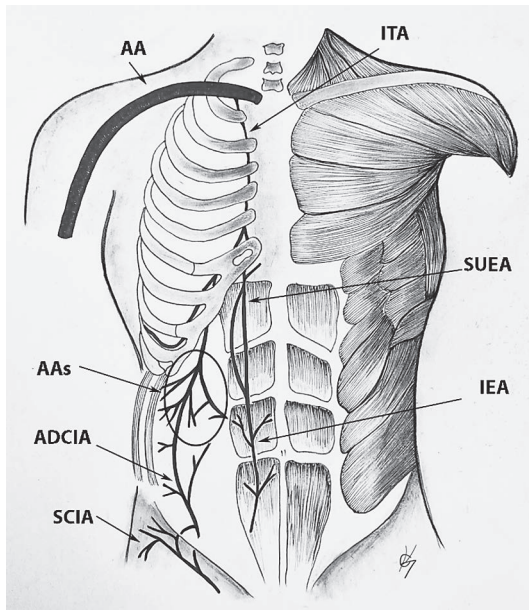
Figure 11 – Deep arteries of the AAW (anterior abdominal wall). The superficial circumflex iliac artery is also illustrated for better differentiation from the ascending branch of the deep circumflex iliac artery. AA – axillary artery; ITA – internal thoracic artery; SCIA – superficial circumflex iliac artery; ADCIA – ascending branch of the deep circumflex iliac artery; AAs – arterial anastomoses between the lower intercostal, subcostal and lumbar arteries; IEA – inferior epigastric artery; SUEA – superior epigastric artery.
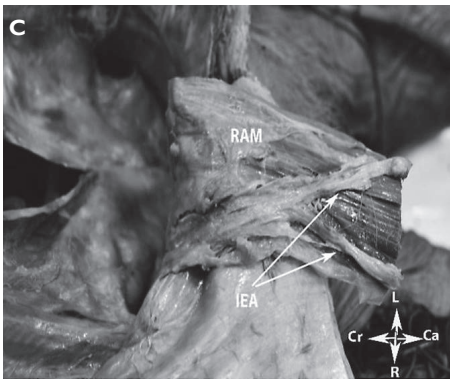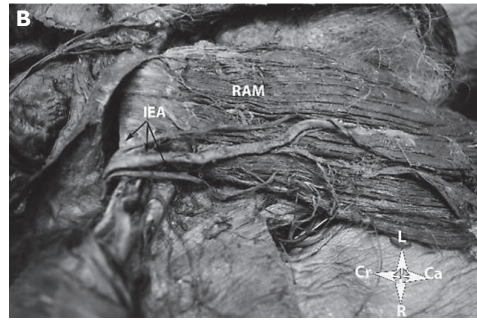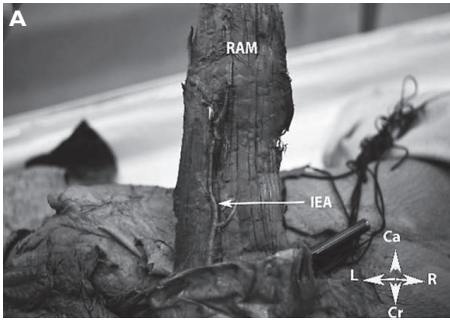
Figure 12 – Inferior epigastric artery (embalmed cadaver). A – The left rectus abdominis muscle is stretched cranially and the posterior surface of the muscle is observed. B – Two branches of the inferior epigastric artery – lateral and medial branches. The right rectus abdominis muscle is stretched caudally and the posterior surface of the muscle is observed. C – Three branches of the inferior epigastric artery (embalmed cadaver). The right rectus abdominis muscle is stretched caudally and the posterior surface of the muscle is observed. RAM – rectus abdominis muscle; IEA – inferior epigastric artery; Cr – cranial; Ca – caudal; L – left; R – right.
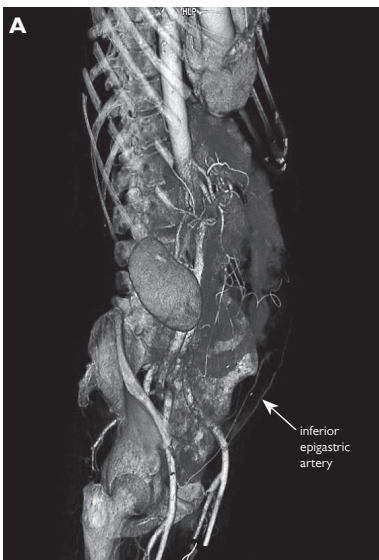
Figure 13 – Contrast enhanced computed tomography (CT) thick slice volume rendered (VR) coloured body reconstruction depicting inferior epigastric artery as annotated. A – lateral view of abdomen; B – anterior view of the anterior abdominal wall.

Kostov S.; Dineva S.; Kornovski Y.; Slavchev S.; Ivanova Y.; Yordanov A.

and 13). It then ascends on the AAW medial to the deep inguinal canal. The IEA passes posterior and medial to the round ligament. Moreover, the artery runs from lateral to medial, pierces the transversalis fascia at the level of the arcuate line and ascends between the lateral margin of the rectus abdominis muscle and the posterior rectal sheath. In some cases, it divides into two branches – lateral (dominant in 50% of cases) and medial (dominant in 7% of cases) (Gagnon and Blondeel, 2006) (Figure 12). In the lower part of the AAW, the IEA forms a fold of the parietal peritoneum known as lateral umbilical ligament. The latter is located lateral to the obliterated umbilical vessels (Anandhi et al., 2016; Joy et al., 2017; Higgins et al., 2021). The IEA participates in the formation of the Hesselbach's triangle (Baggish and Karram, 2006). Moreover, the IEA is the medial boundary of the Bogros space (Yang and Liu, 2016). The IEA gives branch to the round ligament, which is known as Sampson's artery (Sampson, 1917). The IEA gives three more branches – pubic, muscular and cutaneous (Netter, 2014).

The Sampson's artery anastomoses with the ascending branch of the uterine artery at the level of the round ligament. The pubic branch of the IEA anastomoses with a branch of the obturator artery. This anastomotic vessel is known as "Corona mortis" (Anandhi et al., 2016). The muscle branches anastomose with the ascending branch of the deep circumflex iliac artery and branches of the lumbar and intercostal arteries. Branches of the IEA anastomose with branches of the superior epigastric artery (Gray et al., 2005; Netter, 2014).

Anatomical variations and discussion
The IEA could arise from the obturator artery and femoral artery. It could also originate from the external iliac artery or internal iliac artery in a common trunk within the obturator artery (Gray et al., 2005; Tubbs et al., 2016) (Figure 14). Surgeons should know the approximate distance of the IEA from the important
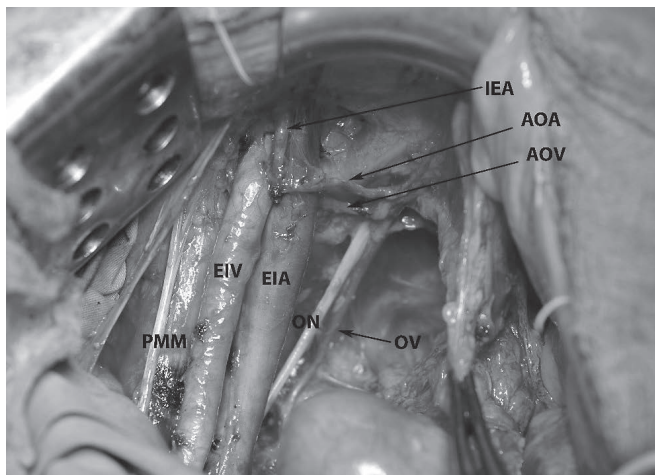
Figure 14 – A common trunk between the inferior epigastric artery and an aberrant obturator artery (open surgery – left pelvic sidewall). AOA – aberrant obturator artery; AOV – accessory obturator vein; IEA – inferior epigastric artery; ON – obturator nerve; OV – obturator vein; PMM – psoas major muscle; EIV – external iliac vein; EIA – external iliac artery.

Vascular Anatomy of the Anterior Abdominal Wall

anatomical landmarks of the AAW. Anandhi et al. (2016) examined the IEA in 50 cadaveric specimens. Authors reported that the distance of IEA from midline at the level of umbilicus was 3.6 cm on right side and 3.5 cm on the left side, respectively. The distance of IEA from the midline at the level between the umbilicus and the symphysis pubis was 3.5 on the right and 3.4 on the left. Rahn et al. (2010) examined the anatomy of IEA among 11 female cadavers. Authors found that at the level, which was 2 cm superior to symphysis pubis, the distance of the vessels from midline was 6.1 cm. Authors concluded that the IEA is located always lateral to the rectus muscle at the level above 2 cm from the symphysis pubis. Joy et al. (2017) estimated an average distance of the IEA from the midline being 4.45 ± 1.42 cm at mid-inguinal point level.

Hesselbach's triangle – Clinical significance and discussion
Hesselbach's triangle is located in the lower posterior aspect of the AAW. The German anatomist and surgeon Franz Hesselbach was the first, who described the triangle and its boundaries. It is limited medially by the lateral border of the rectus abdominis muscle, inferiorly by the inguinal ligament (also known as Poupart's ligament) and laterally by the inferior epigastric vessels (Hesselbach, 1806; Agarwal and Mukherjee, 2008; Misiakos et al., 2014). The triangle represents a potential anatomical area of weakness in the groin, where an inguinal hernia can occur. The triangle is also a part of the modern classification of inguinal hernias and separates the hernias into direct (the hernia protrudes through the triangle) and indirect (the hernia does not protrude through the triangle) (Hesselbach, 1806; Agarwal and Mukherjee, 2008; Misiakos et al., 2014).

Corona mortis – Clinical significance and discussion
Corona mortis is a heterogeneous term, which causes controversies in medical literature (Kostov et al., 2021). Some authors define corona mortis as any vessels, which passes over the superior pubic branch, regardless of whether it is a vascular anastomose or an obturator vessel related to the external iliac artery or vein (Rusu et al., 2009). The incidence according to this terminology was found to be 80% of the examined cadavers (Rusu et al., 2009) However, the majority of authors described corona mortis, as every anastomotic vessel, located behind the superior pubic ramus and on the posterior aspect of the lacunar ligament, between obturator vessels and external iliac system. Therefore, the vessels should participate in anastomoses to be stated as corona mortis (Sanna et al., 2018; Kostov et al., 2021). The anastomoses could be between external iliac/inferior epigastric vessels and obturator vessels. Other vessels, which originate from an external iliac artery or its branches, do not participate in anastomoses and pierced the obturator membrane are termed "aberrant" obturator vessels. The incidence of aberrant obturator artery originating from the inferior epigastric artery varies – 20–34% (Pick et al., 1942; Kostov et al., 2021). Sanna et al. (2018) performed a meta-analysis and estimated
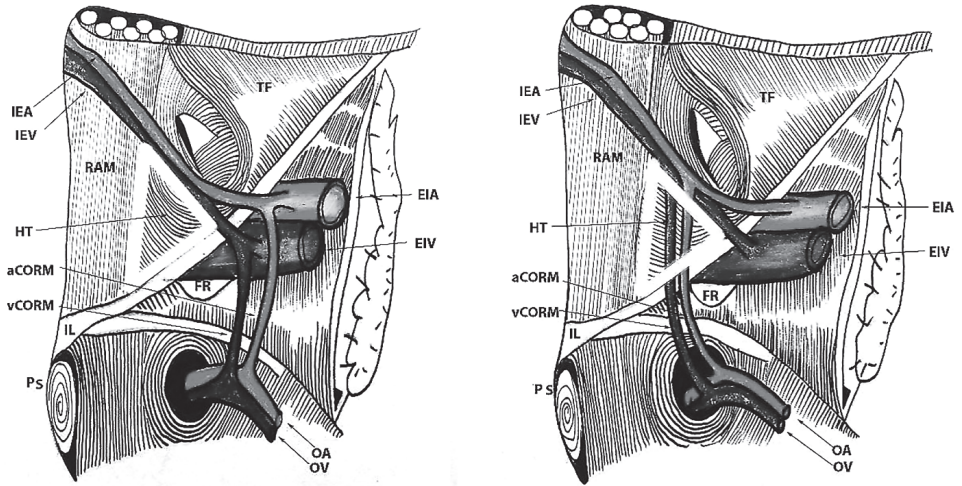
Figure 15 – The Hesselbach's triangle. A – Hesselbach triangle limits. Corona mortis passes lateral to the femoral ring and does not cross the Hesselbach's triangle. B – Corona mortis passes medial to the femoral ring (crosses the Hesselbach's triangle) and could be injured during inguinal hernia repair or urogynecological procedures.
IEA – inferior epigastric artery; IEV – inferior epigastric vein; RAM – rectus abdominis muscle; HT – Hesselbach's triangle in the yellow triangle; TF – transversalis fascia; PS – pubic symphysis; EIA – external iliac artery; EIV – external iliac vein; IL – inguinal ligament; FR – femoral ring; OA – obturator artery; OV – obturator vein; vCORM – venous corona mortis; aCORM – arterial corona mortis.
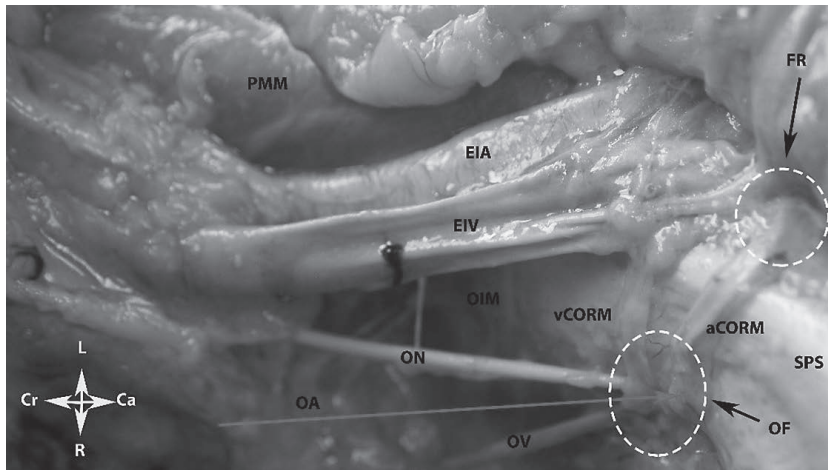
Figure 16 – Venous and arterial corona mortis (fresh cadaver – left sidewall). EIA – external iliac artery; EIV – external iliac vein; FR – femoral ring; OF – obturator foramen; PMM – psoas major muscle; OIM – obturator internus muscle; ON – obturator nerve; OA – obturator artery (injured during dissection); OV – obturator vein; SPS – superior pubis symphysis; aCORM – arterial corona mortis; vCORM – venous corona mortis; Cr – cranial; Ca – caudal; L – left; R – right.

Vascular Anatomy of the Anterior Abdominal Wall

that the real incidence of the corona mortis in hemi-pelvises was high (49.3%). Authors also reported that the rate of the venous corona mortis is higher compared to its arterial counterpart – 41.7% vs. 17.0%.

Surgeons should be familiar with the anatomy of corona mortis, as it could be injured during inguinal hernia repair, urogynecological procedures or pelvic lymphadenectomy. However, the risk of lacerations of corona mortis depends on its location regarding the femoral ring. Corona mortis lateral to the femoral ring could be damaged during pelvic lymphadenectomy. Corona mortis medial to the femoral ring might be injured during inguinal hernia repair (crosses the Hesselbach's triangle) or urogynecological procedures (Kostov et al., 2021).

The Hesselbach's triangle and its close relation with corona mortis is illustrated in Figure 15. Corona mortis is shown in Figure 16.

Bogros space – Clinical significance
The Bogros space (also known as retroinguinal space) is an extraperitoneal space, which is located lateral to the prevesical space (Retzius space). It is limited laterally by the iliac fascia, medially by the inferior epigastric vessels, anteriorly by the transversalis fascia and posteriorly by the parietal peritoneum. The Bogros space is divided into two compartments – medial (containing the femoral vessels) and lateral (provide passage of the iliopsoas muscle, allowing attachment to the femur, along with the femoral nerve). The space of Bogros is dissected during laparoscopic inguinal hernia repair in order to provide access to the iliac fossa and further easier placement of the lateral mesh (Yang and Liu, 2016; Lorenz et al., 2022).

Deep circumflex iliac artery
The DCIA arises from the lateral aspect of the external iliac artery just above the inguinal ligament. It has lateral and superior course until its branches reach the ASIS. The DCIA passes behind the inguinal ligament in a sheath, which is derived from the iliacus and transversalis fascia. It crosses the transversus abdominis muscle and proceeds between transversus and internal oblique muscle to anastomose with branches of the iliolumbar and superior gluteal artery. At the level of ASIS, a large branch of the DICA supplies both muscles and anastomoses with branches of gluteal and IEA artery (Gray et al., 2005; Netter, 2014).

Anatomical variations and discussion
The DCIA is a relatively constant artery, and its variations are extremely rare. Sarna et al. (2020) examined the anatomy of the DCIA in 52 embalmed cadavers. Authors found that the artery was bilateral and presented in all cases. Moreover, in all cases its origin was the external iliac artery.

There are many pelvic anastomoses in the pelvis, which are divided into horizontal and vertical. The internal iliac artery (IIA) is the main arterial vessel of the pelvis. IIA ligation is a lifesaving procedure in cases of severe bleeding during

surgical interventions in the pelvis. Just after ligation of the IIA, the following pathophysiological mechanisms are activated – terminating the blood pressure in small arteries distal to the ligation and transforming the arterial system into a venous one. After ligation, the pelvic blood supply is maintained through three major pelvic anastomoses – 4th lumbar with the iliolumbar arteries, middle sacral with lateral sacral arteries and superior rectal with middle or inferior rectal arteries. However, there are other small anastomoses, which provide the blood supply in the pelvis and prevent necrosis to the buttocks and gluteal maximus muscle. Some of these anastomoses are part of the arteries of the AAW. The DCIA anastomoses with branches of superior gluteal artery, 4th lumbar artery, IEA and iliolumbar artery. The SCIA anastomoses with the superior gluteal artery (Cocq, 1966; Burchell, 1968; Keith et al., 2008; Akinwande et al., 2015). Corona mortis is also a part of the anastomoses after IIA ligation. The other anastomoses are from the femoral artery – medial circumflex femoral artery (anastomoses with branches of inferior gluteal artery and obturator artery) and lateral circumflex femoral artery (anastomoses with superior gluteal artery) (Cocq, 1966; Burchell, 1968; Keith et al., 2008; Akinwande et al., 2015).

Deep veins of the anterior abdominal wall – Inferior epigastric, deep external pudendal and deep circumflex iliac veins
Usually, two inferior epigastric veins follow its arterial counterparts and drain in the external iliac vein just above the inguinal ligament. The deep circumflex iliac vein
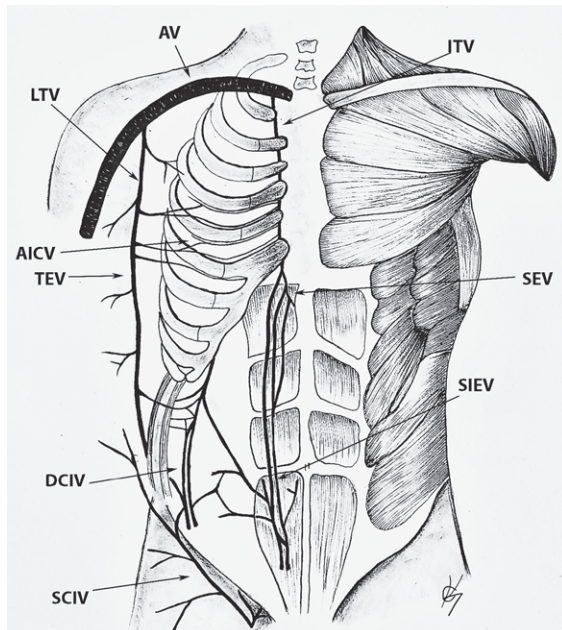
Figure 17 – Deep veins of the anterior abdominal wall. The superficial circumflex iliac vein is also shown for better differentiation from the deep circumflex iliac vein. AV – axillary vein; LTV – lateral thoracic vein; ITV – internal thoracic vein; AIVC – anterior intercostal vein; TEV – thoraco-epigastric veins; DCIV – deep circumflex iliac vein; SCIV – superficial circumflex iliac vein; IEV – inferior epigastric vein; SUEV – superior epigastric vein.

(DCIV) drains in the external iliac vein by passing anterior to the external iliac artery. It drains the blood from the lateral lower part of the AAW. In 17.5% of cases, the DCIV could pass posterior to the external iliac artery (Ghassemi et al., 2013). The deep external pudendal vein (DEPV) drains in the great saphenous vein and below the SEPV. It collects the blood from the vulvar region (Gray et al., 2005; Netter, 2014). The deep veins of the AAW are shown in Figure 17.

Less significant vessels of the AAW in abdominal surgery
The SUEA is less encountered in gynecological surgery. It arises from the internal thoracic artery and pierces the posterior layer of the rectus sheath. It proceeds in caudal direction to anastomose with the IEA at the level of the umbilicus (Figure 18). At the level of the xiphoid process, branches of SUEA anastomose with the contralateral counterpart (Gray et al., 2005; Netter, 2014). The superior epigastric vein (SUEV) accompanies the arterial counterpart and drains into the internal thoracic vein. It anastomoses with the IEV at the level of the umbilicus (cavo-caval anastomoses) (Figure 17).

The musculophrenic artery is the caudal branch of the ITA. It supplies the external, internal and transversus abdominis muscles. The artery anastomoses with the DCIA and the intercostal arteries.

The thoracoepigastric vein collects the blood from the lateral and lower part of the AAW. It drains into the lateral thoracic vein, which enters in the axillary vein. The thoracoepigastric vein communicates with the majority of veins (SUEV, SCIV, DCIV, IEV), but the most numerous anastomoses are with the SUEV and SCIV.

Branches of the posterior intercostal, subcostal and lumbar arteries anastomose with each other just above and slightly medial to the ASIS and between the
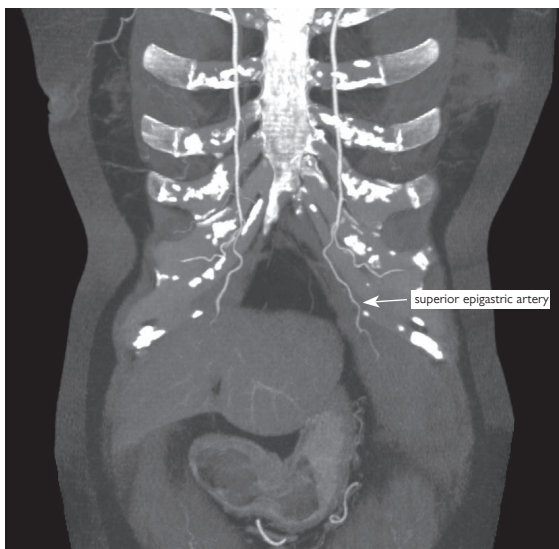
Figure 18 – Contrast enhanced computed tomography (CT) thick slice maximum intensity projection (MIP) reconstruction of anterior thoracic region depicting superior epigastric artery (SUEA).

transversalis abdominis and internal oblique muscles. Branches of these arteries also anastomose with branches of the SCIA and IEA. In the same region, there are anastomoses between the SCIV, DCIV, SEV, thoracoepigastric and subcostal vein (Gray et al., 2005; Netter, 2014).

Paraumbilical veins are formed at the level of the umbilicus. They enter at the falciforme ligament (teres ligament or round ligament of the liver contains the partly obliterated umbilical vein) and confine in a common trunk, which drains in the portal vein. The adult umbilical vein is deviated slightly to the right of the midline. Paraumbilical veins communicate with the IEV, SUEV and thoracoepigastric vein (Martin and Tudor, 1980; Arslan, 2005; Mahadevan, 2006).

Anatomical variations of these vessels are beyond the scope of this review, as their origin or draining pattern is away from the AAW.

Open surgery – Abdominal incisions
Maylard's incision
The Maylard's incision is a transverse incision, which is done approximately 3 to 8 cm superior to the symphysis pubis and 3 cm medial to the ASIS. The level of the incision depends on the type of surgery and BMI (body mass index) of the patient. The Maylard's incision should be avoided in a deep skin crease (Maylard, 1907; Burger et al., 2002; Baggish and Karram, 2006; Rock et al., 2008; Ortiz Molina et al., 2020). The transverse incision is carried down through the skin, subcutaneous fat, superficial fascia, and the aponeurosis of rectus abdominis muscle. Lateral limit is the external edge of the rectus muscles or the greater or lesser part of the aponeurosis of the oblique abdominis muscle (Baggish and Karram, 2006; Ortiz Molina et al., 2020). Consequently, the inferior epigastric vessels are identified, isolated, doubly clamped, cut and ligated. Both rectus abdominis muscles are cut between the two fingers of the surgeon, which are inserted from medial to lateral to the muscles. The underling transversalis fascia and parietal peritoneum are incised transversely along the length of the incision. During closure, an approximation of the rectus abdominis muscles is not necessary (Baggish and Karram, 2006; Ortiz Molina et al., 2020). This type of incision is suitable for radical hysterectomy, pelvic lymphadenectomy and pelvic exenteration as it provides excellent access to the pelvic retroperitoneum. It is associated with low postoperative complications (less hernia formation, better cosmetic results) compared to midline incision, especially in obese patients (Baggish and Karram, 2006; Rock et al., 2008; Ortiz Molina et al., 2020). Ortiz Molina et al. (2020) concluded that if midline laparotomy is not indicated (previous midline incision, upper abdominal surgery), the Maylard's incision is the preferable incision technique for optimal pelvic exposure.

Vascular anatomy of the AAW – Surgical consideration and discussion
As mentioned above, they inferior epigastric vessels are located lateral and posterior to the rectus abdominis muscles. Surgeons should identify vessels in the lateral aspect

of the muscles. It is preferable to ligate IEA instead of using bipolar coagulation, as these are the largest vessels in the AAW. Surgeons should be aware that in some case the IEA divides into two or three arterial branches – lateral and medial (Gagnon and Blondeell, 2006). Additionally, it should be reminded that two veins accompany the arterial counterpart. The Maylard's incision and ligation of IEA must be avoided in patients with aortoiliac occlusive disease, as in such cases the collaterals between the IEA and internal thoracic artery provide blood flow to the lower extremities. Ligation of the IEA could be associated with severe leg ischemia in these particular cases (Yurdakul et al., 2006; Tada et al., 2022).

In the majority of cases, the SEA is cut and ligated. However, if it is possible, the SEA should be preserved. This artery could have a great clinical importance in plastic surgery of the AAW (abdominoplasty) in the future (Almeida et al., 2016). Moreover, the SEA flap is often used in plastic surgery, especially for breast reconstruction, as the lower abdominal skin and subcutaneous fat are preferable materials (Gagnon and Blondeell, 2006).

Pfannensteil incision
The incision is similar to the Maylard's incision. The differences are – the incision is generally performed 2–3 cm above the symphysis pubis with a convexity downward in order to preserve the blood vessels and nerves; the rectus abdominis muscles are not cut; the transversalis fascia and the parietal peritoneum are opened vertically in the midline. The Pfannensteil incision is generally 10–15 cm long, but it could be extended laterally (Burger et al., 2002; Baggish and Karram, 2006; Rock et al., 2008). In cases of lower incision, the pyramidalis muscle should be separated. As mentioned above the pyramidalis muscles are absent in about 20% of the population (range between 10 and 70%) (Lovering and Anderson, 2008). The parietal peritoneum should be incised at the upper end of the incision and after catheterization of the bladder in order to avoid its injury (Baggish and Karram, 2006; Rock et al., 2008).

Surgical considerations and discussion
Similar to the Maylard's incision, it is advisable to preserve the SEA. The incidence of hematomas at the AAW after Pfannensteil incision varies between 1.6 and 8% (van Coeverden de Groot et al., 1983; Hemsell et al., 1993; Vercellini et al., 1996; Lavoie et al., 2014). Vercellini et al. (1996) reported an incidence of 6.1% of subfascial hematomas in 131 patients who underwent Pfannensteil incision. Authors also compared postoperative hematomas after the Küstner (53 patients) and Pfannenstiel (131 patients) incision. They observed a significantly higher rate of postoperative hematomas in patients with Pfannensteil compared to Küstner incision (6.1% versus 1.9%). Lavoie et al. (2014) reported a case of 73-year-old woman with adipose tissue necrosis as a result of postoperative subcutaneous hematoma. The patient had endometrial cancer and authors performed a total abdominal hysterectomy with

Pfannensteil incision. These studies showed that although this type of incision was preferable in obstetrics and gynecology (for patient with nonmalignant conditions), it could be often associated with postoperative hematomas. Therefore, surgeons should be aware of pathways and draining pattern of the superficial epigastric, inferior epigastric and superficial external pudendal vessels. Although, the rectus abdominis muscles are not transected in this type of incision, the IEA could also be injured. The deep and superficial circumflex iliac arteries are at low risk of injury, as they are located lateral at the AAW. However, in cases of lateral extension of the Pfannensteil incision, these vessels together with their branches and anastomoses could be injured. Generally, the subfascial hematomas are due to inadequate hemostasis of the inferior epigastric vessels, whereas suprafascial hematomas are observed after laceration of the superficial epigastric and superficial external pudendal vessels. The risk of hematomas and postoperative wound complications is increased in cases of obesity, diabetes, hypertension, or previous laparotomies (Lavoie et al., 2014). The division of the pyramidalis muscles should be gentle and precious, as there are many arterial and venous anastomoses in the suprapubic region (Gray et al., 2005; Netter, 2014). Nerves of the AAW are not the topic of the present article, but it should be noted that lateral extension of the incision is associated with increased risk of ilioinguinal and iliohypogastric nerves injury (Rock et al., 2008).

Küstner incision
The Küstner incision is similar to the Pfannensteil incision. Firstly, a transverse incision of the skin, subcutaneous fat and superficial fascia is performed. The procedure is followed by an excessive superior and inferior dissection of the subcutaneous fat from the aponeurosis of the anterior muscle abdominis. Consequently, the anterior aponeurosis of the rectus abdominis, transversalis fascia and the parietal peritoneum are incised in the midline along the linea alba (Baggish and Karram, 2006; Rock et al., 2008). Surgical considerations do not differ from the Pfannensteil incision.

Cherney incision
The Cherney incision is similar to the Maylard's incision. The main difference is that incision is located lower compared to the Maylard's and the rectus abdominis muscles are separated transversely from their attachment into the symphysis pubis. The inferior epigastric vessels are cut and ligated, but it could be spared compared to Maylard's incision. The incised rectus muscles could be elevated upward in order to provide better exposure (Baggish and Karram, 2006; Lee et al., 2008; Rock et al., 2008). During closure of the abdominal incision, the rectus muscles are approximated to the symphysis pubis. The Cherney incision provides access to the Retzius space, maximizes exposure to the pelvic sidewall and retroperitoneum in patient with high BMI. Lee et al. (2008) compared modified Cherney incision

and vertical midline incision for management of early stage cancer of the uterine cervix. Authors observed no clinical differences between both groups and equal number of removed lymph nodes among both groups. Authors concluded that the Cherney incision is preferable in young patients, who underwent surgery for cervical cancer.

Surgical considerations and discussion
During separation of the rectus abdominis muscles and dissection of the Retzius space, surgeons should be aware of the presence of the following vessels and their anastomoses (Gray et al., 2005; Netter, 2014; Kostov et al., 2020):

- SEA/SEV – anastomose with the SEPA/SEPV;
- SEPA/SEPV – the SEPV anastomoses with the collateral venous counterpart and forms a rich suprapubic collateral connection. These vessels also anastomose with superficial epigastric vessels; the SEPA/SEIV anastomose with the Sampson artery just above the round ligament;
- anastomoses between the retropubic branches of both obturator arteries;
- anastomoses between the suprapubic branches of both inferior epigastric arteries;
- anastomoses between the retropubic and suprapubic branches of the obturator artery and the IEA;
- arterial branches of the internal pudendal artery;
- dorsal vein of the clitoris and its anastomoses with the majority of veins in the suprapubic region.

Midline incision
The midline incision is commonly used in abdominal surgery. It is also useful for emergency procedures, as it provides the most rapid entry and the lowest amount of incisional bleeding. Moreover, the midline incision gives the best exposure to the abdominal cavity. Additionally, this type of incision spares the nerves. It is obvious that the incision has many advantages. However, its disadvantages are that dehiscence and hernias are more frequent (Burger et al., 2002; Baggish and Karram, 2006; Rock et al., 2008). The midline incision starts at the level of the symphysis pubis to the level of the umbilicus. Its long is different and depends on the surgical procedure. Extension of the midline incision could be made superiorly by passing around the umbilicus and exceeding to the level of the xiphoid process. The curve of the incision around the umbilicus should be performed on the left side of the midline in order to spare the falciforme ligament and to avoid bleeding from the umbilical veins (Burger et al., 2002; Baggish and Karram, 2006; Rock et al., 2008). The following structure of the AAW are incised vertically – skin, subcutaneous fat, superficial fascia, aponeurosis of rectus abdominis muscle, linea alba, transversalis fascial, preperitoneal fat and parietal peritoneum. The incision provides minimal blood loss due to the avascular plane in the linea alba (Burger et al., 2002).

Kostov S.; Dineva S.; Kornovski Y.; Slavchev S.; Ivanova Y.; Yordanov A.

Surgical consideration and discussion
Dissection should be meticulous near the suprapubic region due to the presence of many vessels and their anastomoses, which have been clearly described above.

Paramedian incision
The paramedian incision is an alternative to the midline incision and could be separated into lateral and medial. The most commonly used is the lateral, where a lateral vertical incision is performed on the lateral aspect of the rectus muscle (approximately 3 cm lateral to the midline). The anterior rectus sheath is incised and separated from the muscle. The latter is retracted laterally, and inferior epigastric vessels are preserved. The posterior rectal sheath, the transversalis fascia and the parietal peritoneum are incised in vertical direction. The extension of the paramedian incision in cranial direction is limited by the costal margin. This incision provides access to the left or right pelvic sidewall depending on the incision side. It is also used for extraperitoneal or transperitoneal pelvic lymphadenectomy (Köse et al., 2017). It is associated with lower hernia rates compare to midline incision (Rock et al., 2008).

Surgical considerations and discussion
Gentle and meticulous dissection between the aponeurosis and the rectus abdominis muscle will prevent injury to the inferior epigastric vessels. Peripheral branches of these vessels will be encountered during dissection and should be precisely dissected and ligated. The chance of injury of the iliohypogastric and ilioinguinal nerve is higher compared to midline incision. Mandelkow and Loeweneck (1988) reported that injury of the iliohypogastric nerve will be avoided if the incision was performed at least 5 cm cranial to the inguinal ligament. Avsar et al. (2002) examined 12 adult cadavers and tried to determine the distances of ilioinguinal and iliohypogastric nerves to McBurney's and paramedian incisions. Authors concluded that the paramedian incision was safer compared to McBurney's regardless nerve injury. Avsar et al. (2002) also reported that the incidence injury (if both incisions are performed) of at least one of the two nerves on the right was 75% and 41.66% on the left. Authors concluded that by measuring the distance of both nerves according to both incisions. The incidence of total nerves being in the dangerous region was 43.18%.

Surgical procedures at the anterior abdominal wall
Abdominal paracentesis
The remaining question is the placement location of the ascitic drains in the AAW in cases of absence of the ultrasound guidance. The British Society of Gastroenterology (2021) recommended that the point of puncture should be located no less than 8 cm from the midline and 5 cm superior to the symphysis pubis. Authors concluded that this point of puncture would prevent injury to

the inferior epigastric vessels, spleen or liver (Aithal et al., 2021). However, Siau et al. (2021) disagreed and reported that the use of absolute measurement was controversial as it varied and depended on obesity, age, amount of ascites or distortion due to chronic ascites. Authors offered the contralateral McBurney's point guided by abdominal percussion and patient in a supine position. They concluded that the contralateral (left) McBurney's point was preferable as the AAW was thinner and the sigma was more mobile than the caecum. Sakai et al. (2005) measured the thickness of the AAW by ultrasound in 52 patients with cirrhosis and ascites. Authors reported that the left lower quadrant was the preferable point of puncture, as the AAW was significantly thinner and the deep of ascites greater in that particular region.

Safety zones of the anterior abdominal wall for intraoperative draining placement
These zones are similar to the placement of second trocars during laparoscopy. There are only few reports, which described vascular injuries to the AAW during drainage placement. Ng et al. (2016) reported for vessel injury of the AAW caused by drain insertion after anterior lumbar spine fusion. Authors concluded that the danger zone for vessel injury is located just superior to the level of the umbilicus and roughly from 4 cm to 8 cm lateral from the midline.

Surgical consideration and discussion
That particular area is rich of anastomotic branches of the lumbar, intercostal, subcostal and the ascending branch of the DCIA. The advisable point of drain insertion should be located below the umbilicus and at least 8 cm lateral from the midline (Sakai et al., 2005; Ng et al., 2016; Siau et al., 2021).

Laparoscopic surgery
Primary trocar placement and vascular injury of the AAW are rare as they are located in an avascular plane – either at the umbilicus or cranial and caudal to it (at linea alba) (Watrowski et al., 2021). However, in cases of previous abdominal surgery, there is an increased risk of injuries to the gastrointestinal tracts. Therefore, new access points (Palmer's point, Jain's pont, Lee-Huang point) for primary trocar placement should be considered (Palmer, 1974; Jain et al., 2016). The Jain point is located at the level of the umbilicus just between abdominal regions 5 and 6, in a straight line, which is drawn vertically upward from a point 2.5 cm medial to ASIS (Jain et al., 2016). The Palmer's point is located 3 cm below the left subcostal margin in the mid-clavicular line (Palmer, 1974). Additionally, the Palmer's point is also used in cases of large ovarian tumours or uterine fibroids (Granata et al., 2010). The Jain point is the preferable point of entry in cases of previous splenic or gastric surgery, where the Palmer's point has to be excluded. Moreover, by using these two points of entry, there is no risk of injury of major retroperitoneal vessels. Jain et al. (2016) used the Jain point as a laparoscopic entry site in 623 patients. Authors reported no
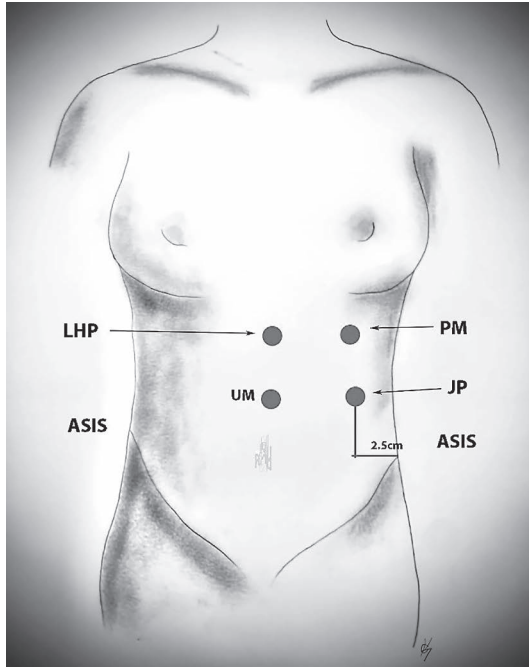
Figure 19 – Different laparoscopic primary trocar entry points. UM – umbilicus; ASIS – anterior superior iliac spine; PM – Palmer's point; JP – Jain point; LHP – Lee Huang point.

cases of injuries to superficial or deep vessels of anterior abdominal wall. Therefore, the Jain point could be also used for intraoperative draining placement, if draining the abdomen is necessary in cases of surgery at the upper abdomen.

The Lee-Huang point is located in the middle upper abdomen (abdominal region 2) between the xiphoid process and the umbilicus. It is used for patient with high risk of subumbilicus adhesions due to previous surgery. It is also preferable point of laparoscopic primary entry in cases of gynecological malignancies or large abdominal masses. Contraindication for Lee-Huang point is previous surgery at the supra-umbilical region (Lee et al., 2001; Thepsuwan et al., 2013). The three primary points of laparoscopic trocar entry are shown in Figure 19.

Vascular injury of the anterior abdominal wall in secondary trocar placement
Injury of the SEA/SEV, SCIA/SCIV of the AAW could be avoided by transilluminating the AAW before secondary trocar placement. Similarly, to the superficial vessels of the AAW, injury of IEA/IEV could be avoided by identification of these vessels by direct laparoscopic vision. The inferior epigastric vessels are located at the lateral umbilical ligament, which is slightly lateral to the medial umbilical ligament (obliterated umbilical arteries). However, in the majority of cases the superficial and deep vessels of the AAW are hardly visible by laparoscopy, especially in obese patients or in cases with previous abdominal incision (Watrowski et al., 2021). Moreover, although the abdominal wall vessels injuries are usually

preventable, one third of trocar-related complications are observed during secondary trocar insertion (de Rosnay et al., 2011). Therefore, many articles, either anatomical or surgical, tried to establish the safety zone of the second trocar placement in the AAW (Rahn et al., 2010; Mohammadhosseini and Shirani, 2011).

Injury of the inferior epigastric vessels occurs in approximately 2% of laparoscopic procedures at the abdomen. The laceration of these vessels could lead to severe haemorrhage (requiring hemotransfusion), hematoma or abscess formation (Hurd et al., 1994; Saber et al., 2004).

Hurd et al. (1994) investigated the location of the IEA, DIEAD and SCIA in 21 women by using CT (computed tomography) images. Authors concluded that the ideal location of secondary trocars insertion was at least 5 cm above the symphysis pubis (SP) and 8 cm from the midline. There were two alternative locations – the first was 3 cm above the SP and 4 cm from midline, and the second was at the level of the umbilicus and 8 cm from midline (Shawki, 2004).

Saber et al. (2004) investigated the location of the inferior epigastric vessels among 100 patients by using CT scan. Authors concluded that these vessels are located in the area between 4 and 8 cm from the midline, regardless of the level of the AAW. Saber et al. (2004) also observed that in obese patients (BMI ≥ 26.3) the inferior epigastric vessels are located more laterally from the midline.

Baggish and Karram (2006) reported that the distance from the linea alba to the inferior epigastric vessels (superior to the upper margin of the SP) was 6–7 cm.

Anandhi et al. (2016) examined the anatomy of the inferior epigastric vessels in 50 specimens. Authors concluded that the danger zone was located between 3 cm and 8 cm from the midline.

Shawki (2004) examined the IEA, SEA and SCIA among 30 women who underwent diagnostic laparoscopy. The author examined the distance of the IEA, SEA and SCIA from the midline and either 3 cm or 5 cm above the SP. Shawki (2004) concluded that lateral secondary trocar placement 3 cm above the SP was related with increased risk of vessels injury, as the distance between laterally located SCIA and IEA/SEA was usually less than 1 cm. Contrary, lateral trocar insertion 5 cm above the SP was a safer zone as the distance between the more laterally located SCIA and IEA/SEA was more than 4 cm.

However, other studies reported different findings. Joy et al. (2017) examined the location of 60 inferior epigastric arteries among 30 adult cadavers. Authors observed that the safe zone was located 5.5 cm from the linea alba. Rahn et al. (2010) investigated the anatomy of IEA in 11 female cadavers. Authors found that IEA and the ilioinguinal and iliohypogastric nerves would be sacrificed if the secondary trocars were inserted above the ASIS and 6 cm from the midline. Moreover, Balzer et al. (1999) investigated the anatomy of the IEA and the ascending branch of the DCIA in 21 human cadavers. Authors reported that half of the recommended trocar sites placements in the medical literature were within the range of the IEA and the DCIA. They concluded that the safe zone should be located at the line alba or 5 cm from

the lateral aspect of the rectus abdominis muscle. Epstein et al. (2004) examined the anatomy of the IEA among 30 fresh cadavers. Authors defined two safety zone in the AAW – 1) the linea alba, 2) more than two-thirds of the distance along a horizontal line, which was located between the midline and the ASIS.

Logically, the danger zone (3–8 cm from the midline) for the superior epigastric vessels is the same as the inferior counterparts, as they lie in the same axis. Bhatti et al. (2008) investigated the anatomy of the superior epigastric vessels and estimated that the danger zone was located 4–7.5 cm from the midline at the level between the xiphoid process and the umbilicus and 3.9–4.8 cm from the midline at the level of the xiphoid process.

Anatomical variations

In should be noted that the IEA could have two or more branches. Epstein et al. (2004) found that a large median branch of the IEA was presented in 60% of cases. In more than two third of cases the IEA had at least one branch > 1 mm diameter that raised from the lateral aspect of the rectus sheath. Joy et al. (2017) reported for an average of 3.3 branches per IEA. Authors found a large medial branch of 20% of cases.

Bowness et al. (2019) observed the anatomy of the IEA in 100 patients by a CT scan. Authors noticed that the IEA generally lied within the rectus abdominis muscle, despite that most studies reported that the IEA lies within the posterior aponeurosis of the rectus sheath. In some cases, the IEA could be absent (Tregaskiss et al., 2007; Bowness et al., 2019).

Unfortunately, there is a huge variety of the morphology, course and orientation of the perforator arterial branches of the AAW (El-Mrakby and Milner, 2002). Tregaskiss et al. (2007) examined arterial supply of the AAW among 10 fresh cadavers. Authors found that the perforators of the superior epigastric artery (SEA) were constant compared to the IEA, which varied noticeably. Tregaskiss et al. (2007) estimated an average number of seven perforators in each hemiabdomen. In their research, the SEA was absent in half of cases. The branches of the IEA were less extensive when the SEA was noticed in the specimens. El-Mrakby and Milner (2002) performed a microdissection of the IEA in 20 cadavers. Authors found that perforators of the lateral branch of the IEA were more prevalent and constant compared to medial ones. The average number of perforators, which was dissected in each specimen were 5.4. These two studies showed that the perforator branches of the IEA did not follow any particular pattern. Therefore, knowledge of their anatomical location of the AAW is impossible. Moreover, in the lateral AAW and just above the ASIS there are many anastomoses between the deep/superficial circumflex, superficial epigastric, lumbar, intercostal and subcostal arteries. Possible injuries of such anastomoses or perforators are unavoidable, as they could have different course in the AAW. Fortunately, injuries of such small vessels are not associated with severe bleeding or huge hematomas.

It could be concluded that the lateral secondary trocar placement should be inserted 5 cm above the SP and 8 cm lateral to the midline due to the possibility of anatomical variations, especially of the IEA (two or three branches). The safety zone of the medial secondary trocar insertion is located between the linea alba and 3 cm laterally (Epstein et al., 2004; Rahn et al., 2010; Joy et al., 2017).

Conclusion

Detailed knowledge of the human anatomy is an integral part of many surgical procedures. The anatomy of the AAW is complex as it is a layered structure, which is rich in vessels and their anastomoses. Nevertheless, anatomical variations of the vessels of the AAW are often observed. Intraoperative and postoperative complications associated with entry and closure of the AAW could compromise the best surgical procedure. Therefore, sound knowledge of the vascular anatomy of the AAW is fundamental and a prerequisite to having a favourable quality of patient care.

References

Agarwal, A. K., Mukherjee, R. (2008) Franz Kaspar Hasselbach (1759–1816). *Indian J. Surg.* **70(2)**, 96–98.

Aithal, G. P., Palaniyappan, N., China, L., Härmälä, S., Macken, L., Ryan, J. M., Wilkes, E. A., Moore, K., Leithead, J. A., Hayes, P. C., O'Brien, A. J., Verma, S. (2021) Guidelines on the management of ascites in cirrhosis. *Gut* **70(1)**, 9–29.

Akinwande, O., Ahmad, A., Ahmad, S., Coldwell, D. (2015) Review of pelvic collateral pathways in aorto-iliac occlusive disease: Demonstration by CT angiography. *Acta Radiol.* **56(4)**, 419–427.

Almeida, C. L. A., Vieira, L. F. D. F., Leite, L. A. S., Oliveira, J. A. V., Ataide, R. F., Oliveira, E. J. B., Brandt, C. T. (2016) Importance of superficial circumflex iliac artery preservation to prevent abdominal wall necrosis in patients who underwent mini-abdominoplasty: An surgical-anatomic descriptive and prospective study. *Rev. Bras. Cir. Plást.* **31(2)**, 178–185.

Anandhi, V., Rajeswari, K., Jebakani, C. F. (2016) A study of the origin and course of the inferior epigastric artery and its significance in laparoscopic surgery. *Int. J. Anat. Res.* **4(3)**, 2692–2697.

Arslan, O. E. (2005) Anatomy of the abdominal wall. In: *Aesthetic Surgery of the Abdominal Wall*, eds. Shiffman, M. A., Mirrafati, S., pp. 1–28, Springer, Berlin, Heidelberg.

Avsar, F. M., Sahin, M., Arikan, B. U., Avsar, A. F., Demirci, S., Elhan, A. (2002) The possibility of nervus ilioinguinalis and nervus iliohypogastricus injury in lower abdominal incisions and effects on hernia formation. *J. Surg. Res.* **107(2)**, 179–185.

Baggish, M. S., Karram, M. M. (2006) *Atlas of Pelvic Anatomy and Gynecologic Surgery*, 2nd Edition. Elsevier, Philadelphia.

Balzer, K. M., Witte, H., Recknagel, S., Kozianka, J., Waleczek, H. (1999) Anatomic guidelines for the prevention of abdominal wall hematoma induced by trocar placement. *Surg. Radiol. Anat.* **21(2)**, 87–89.

Bhatti, A. F., Iqbal, S., Lee, T. C. (2008) Variation in surface marking of superior epigastric vessels. A guide to safe laparoscopic port insertion. *Surgeon* **6(1)**, 50–52.

Bohman, V. R., Gilstrap, L. C. III., Ramin, S. M., Little, B. B., Santos-Ramos, R., Goldaber, K. G., Dax, J., Leveno, K. J. (1994) Subcutaneous tissue: To suture or not to suture at cesarean section. *Infect. Dis. Obstet. Gynecol*. **1**, 259–265.

Bowness, J., Seeley, J., Varsou, O., McKinnie, A., Zealley, I., McLeod, G., Grant, C. (2019) Arterial anatomy of the anterior abdominal wall: Evidence-based safe sites for instrumentation based on radiological analysis of 100 patients. *Clin. Anat*. **33(3)**, 350–354.

Burchell, R. C. (1968) Physiology of internal iliac artery ligation. *J. Obstet. Gynaecol. Br. Commonw*. **75**, 642.

Burger, J. W., van 't Riet, M., Jeekel, J. (2002) Abdominal incisions: Techniques and postoperative complications. *Scand. J. Surg*. **91(4)**, 315–321.

Caggiati, A., Bergan, J. J., Gloviczki, P., Jantet, G., Wendell-Smith, C. P., Partsch, H.; International Interdisciplinary Consensus Committee on Venous Anatomical Terminology (2002) Nomenclature of the veins of the lower limbs: An international interdisciplinary consensus statement. *J. Vasc. Surg*. **36(2)**, 416–422.

Chua, C. C., Hong, F. S., Ho, W. K. (2017) The superficial femoral vein – Time to change this misnomer. *J. Med. Imaging Radiat. Oncol*. **61(4)**, 500–502.

Chun, M. H., Han, S. H., Chung, J. W., Cho, S. S., Ko, J. S., Chung, I. H., Chung, G. B., Lee, M. S., Kang, H. S., Park, S. S. (1992) Anatomical observation on draining patterns of saphenous tributaries in Korean adults. *J. Korean Med. Sci*. **7(1)**, 25.

Cocq, F. L. (1966) Internal iliac artery ligation. *Am. J. Obstet. Gynecol*. **95(3)**, 320–325.

de Rosnay, P., Chandiraman, M., Usman, S., Owen, E. (2011) Injury of epigastric vessels at laparoscopy: Diagnosis and management. *Gynecol. Surg*. **8**, 353–356.

El-Mrakby, H. H., Milner, R. H. (2002) The vascular anatomy of the lower anterior abdominal wall: A microdissection study on the deep inferior epigastric vessels and the perforator branches. *Plast. Reconstr. Surg*. **109(2)**, 539–543.

Epstein, J., Arora, A., Ellis, H. (2004) Surface anatomy of the inferior epigastric artery in relation to laparoscopic injury. *Clin. Anat*. **17(5)**, 400–408.

Farthing, A. (2018) Clinical anatomy of the pelvis and reproductive tract. In: *Dewhurst's Textbook of Obstetrics and Gynaecology*, 9th Edition. Edmonds, K., Lees, C., Bourne, T., pp. 473–484, John Wiley and Sons, Hoboken.

Fathi, M., Hatamipour, E., Fathi, H. R., Abbasi, A. (2008) The anatomy of superficial inferior epigastric artery flap. *Acta Cir. Bras*. **23(5)**, 429–434.

Fukaya, E., Kuwatsuru, R., Iimura, H., Ihara, K., Sakurai, H. (2011) Imaging of the superficial inferior epigastric vascular anatomy and preoperative planning for the SIEA flap using MDCTA. *J. Plast. Reconstr. Aesthet. Surg*. **64(1)**, 63–68.

Gagnon, A., Blondeell, P. (2006) Deep and superficial inferior epigastric artery perforator flaps. *Cirugía Plástica Ibero-Latinoamericana* **32**, 243–258.

Ghassemi, A., Furkert, R., Prescher, A., Riediger, D., Knobe, M., O'dey, D., Gerressen, M. (2013) Variants of the supplying vessels of the vascularized iliac bone graft and their relationship to important surgical landmarks. *Clin. Anat*. **26(4)**, 509–521.

Glasser, S. T. (1943) An anatomic study of venous variations at the fossa ovalis. *Arch. Surg*. **46(2)**, 289.

Granata, M., Tsimpanakos, I., Moeity, F., Magos, A. (2010) Are we underutilizing Palmer's point entry in gynecologic laparoscopy? *Fertil. Steril*. **94(7)**, 2716–2719.

Gray, H., Standring, S., Ellis, H., Berkovitz, B. K. B. (2005) *Gray's Anatomy: The Anatomical Basis of Clinical Practice*, 39th Edition. Elsevier Churchill Livingstone, Edinburgh.

Hemsell, D. L., Hemsell, P. G., Nobles, B., Johnson, E. R., Little, B. B., Heard, M. (1993) Abdominal wound problems after hysterectomy with electrocautery vs. scalpel subcutaneous incision. *Infect. Dis. Obstet. Gynecol.* **1(1)**, 27–31.

Hesselbach, F. K. (1806) *Anatomisch-chirurgische Abhandlung über den Urspurng der Leistenbrüche*. Baumgärtner, Würzburg.

Higgins, R. V., Naumann, R. W., Hall, J., Randall, L. M. (2021) Abdominal Incisions and Sutures in Gynecologic Oncological Surgery. Medscape. Available at: https://emedicine.medscape.com/article/271349-overview

Hodgson, N. C., Malthaner, R. A., Ostbye, T. (2000) The search for an ideal method of abdominal fascial closure: A meta-analysis. *Ann. Surg.* **231**, 436–442.

Hurd, W. W., Bude, R. O., DeLancey, J. O., Newman, J. S. (1994) The location of abdominal wall blood vessels in relationship to abdominal landmarks apparent at laparoscopy. *Am. J. Obstet. Gynecol.* **171(3)**, 642–646.

Jain, N., Sareen, S., Kanawa, S., Jain, V., Gupta, S., Mann, S. (2016) Jain point: A new safe portal for laparoscopic entry in previous surgery cases. *J. Hum. Reprod. Sci.* **9(1)**, 9–17.

Joshi, R., Duong, H. (2022) *Anatomy, Abdomen and Pelvis, Scarpa Fascia*. StatPearls [Internet].

Joy, P., Prithishkumar, I. J., Isaac, B. (2017) Clinical anatomy of the inferior epigastric artery with special relevance to invasive procedures of the anterior abdominal wall. *J. Minim. Access. Surg.* **13**, 18–21.

Keith, L. G., Lynch, C. B. (2008) *Surgical Management of Intractable Pelvic Hemorrhage*. Glob. Libr. Women's Med.

Köse, M. F., Kiseli, M., Kimyon, G., Öcalan, R., Yenen, M. C., Tulunay, G., Turan, A. T., Üreyen, I., Boran, N. (2017) Extraperitoneal lymph node dissection in locally advanced cervical cancer; the prognostic factors associated with survival. *J. Turk. Ger. Gynecol. Assoc.* **18(2)**, 77–84.

Kostov, S., Slavchev, S., Dzhenkov, D., Mitev, D., Yordanov, A. (2020) Avascular spaces of the female pelvis – Clinical applications in obstetrics and gynecology. *J. Clin. Med.* **9(5)**, 1460.

Kostov, S., Slavchev, S., Dzhenkov, D., Stoyanov, G., Dimitrov, N., Yordanov, A. D. (2021) Corona mortis, aberrant obturator vessels, accessory obturator vessels: Clinical applications in gynaecology. *Folia Morphol. (Warsz.)* **80(4)**, 776–785.

La Falce, O. L., Ambrosio, J. D., Souza, R. R. (2006) The anatomy of the superficial external pudendal artery: A quantitative study. *Clinics (Sao Paulo)* **61(5)**, 441–444.

Lavoie, M. C., Plante, M., Lemieux, M. C., Roberge, C., Renaud, M. C., Grégoire, J., Roy, M., Sebastianelli, A. (2014) Extensive adipose tissue necrosis following Pfannenstiel incision for endometrial cancer. *J. Obstet. Gynaecol. Can.* **36(3)**, 253–257.

Lee, C.-L., Huang, K.-G., Jain, S., Wang, C.-J., Yen, C.-F., Soong, Y.-K. (2001) A new portal for gynecologic laparoscopy. *J. Am. Assoc. Gynecol. Laparosc.* **8(1)**, 147–150.

Lee, S. H., Yim, G. W., Lee, D. W., Kim, S. W., Kim, S., Kim, J. W., Kim, Y. T. (2008) Comparison of modified Cherney incision and vertical midline incision for management of early stage cervical cancer. *J. Gynecol. Oncol.* **19(4)**, 246–250.

Lorenz, A., Augustin, C., Konschake, M., Gehwolf, P., Henninger, B., Augustin, F., Öfner, D. (2022) The preperitoneal space in hernia repair. *Front. Surg.* **9**, 869731.

Lovering, R. M., Anderson, L. D. (2008) Architecture and fiber type of the pyramidalis muscle. *Anat. Sci. Int.* **83(4)**, 294–297.

MacKay, M. D., Mudreac, A., Varacallo, M. (2022) *Anatomy, Abdomen and Pelvis, Camper Fascia*. StatPearls [Internet].

Mahadevan, V. (2006) Anatomy of the anterior abdominal wall and groin. *Surgery (Oxford)* **24(7)**, 221–223.

Mandelkow, H., Loeweneck, H. (1988) The iliohypogastric and ilioinguinal nerves. *Surg. Radiol. Anat.* **10(2)**, 145–149.

Martin, B. F., Tudor, R. G. (1980) The umbilical and paraumbilical veins of man. *J. Anat.* **130(2)**, 305–322.

Maylard, A. E. (1907) Direction of abdominal incision. *Br. Med. J.* **2**, 895–901.

Mian, A., Bertino, F., Shipley, E., Shoja, M. M., Tubbs, R. S., Loukas, M. (2014) Petrus Camper: A history and overview of the clinical importance of Camper's fascia in surgical anatomy. *Clin. Anat.* **27(4)**, 537–544.

Misiakos, E. P., Bagias, G., Zavras, N., Tzanetis, P., Patapis, P., Machairas, A. (2014) Strangulated inguinal hernia. In: *Inguinal Hernia*. Canonico, S., IntechOpen, London.

Mohammadhosseini, B., Shirani, S. (2011) Intra-abdominal and abdominal wall haematoma from 5 mm port insertion site in laparoscopic cholecystectomy. *Wideochir. Inne Tech. Maloinwazyjne* **6(3)**, 164–166.

Monkhouse, W. S. (2001) Terminologia Anatomica. International Anatomical Terminology. *J. Anat.* **199(Pt 6)**, 741–742.

Mühlberger, D., Morandini, L., Brenner, E. (2009) Venous valves and major superficial tributary veins near the saphenofemoral junction. *J. Vasc. Surg.* **49(6)**, 1562–1569.

Netter, F. H. (2014) *Atlas of Human Anatomy*, 6th Edition. Saunders/Elsevier, Philadelphia.

Ng, W. K., Lui, T. H., Ngai, W. K. (2016) Abdominal wall vascular injury by drain insertion after anterior lumbar spinal fusion. *Journal of Orthopaedics, Trauma and Rehabilitation* **20**, 46–47.

Ogami, K., Murata, H., Sakai, A., Sato, S., Saiki, K., Okamoto, K., Manabe, Y., Hara, T., Tsurumoto, T. (2017) Deep and superficial circumflex iliac arteries and their relationship to the ultrasound-guided femoral nerve block procedure: A cadaver study. *Clin. Anat.* **30(3)**, 413–420.

Ortiz Molina, E., Díaz de la Noval, B., Rodríguez Suárez, M. J., Hernández Pailos, R., García Sánchez, F., García González, J. (2020) Maylard's incision: How to make an easy incision for complex pelvic abdominal surgery. *Int. J. Gynecol. Cancer* **30(1)**, 154–155.

Palmer, R. (1974) Safety in laparoscopy. *J. Reprod. Med.* **13(1)**, 1–5.

Penteado, C. V. (1983) Venous drainage of the groin flap. *Plast. Reconstr. Surg.* **71(5)**, 678–682.

Pick, J., Anson, B., Ashley, F. (1942) The origin of the obturator artery. A study of 640 body-halves. *Am. J. Anat.* **70(2)**, 317–343.

Rahn, D. D., Phelan, J. N., Roshanravan, S. M., White, A. B., Corton, M. M. (2010) Anterior abdominal wall nerve and vessel anatomy: Clinical implications for gynecologic surgery. *Am. J. Obstet. Gynecol.* **202(3)**, 234.e1–234.e5.

Reardon, C., O'Ceallaigh, S., O'Sullivan, S. (2004) An anatomical study of the superficial inferior epigastric vessels in humans. *Br. J. Plast. Surg.* **57(6)**, 515–519.

Rock, J. A., Jones, H. W., Te Linde, R. W. (2008) *Te Linde's Operative Gynecology*, 10th Edition. Lippincott Williams and Wilkins, Philadelphia.

Rozen, W. M., Pan, W. R., Le Roux, C. M., Taylor, G. I., Ashton, M. (2009) The venous anatomy of the anterior abdominal wall: An anatomical and clinical study. *Plast. Reconstr. Surg.* **124(3)**, 848–853.

Rozen, W. M., Chubb, D., Grinsell, D., Ashton, M. W. (2010) The variability of the superficial inferior epigastric artery (SIEA) and its angiosome: A clinical anatomical study. *Microsurgery* **30(5)**, 386–391.

Rozen, W. M., Chubb, D., Whitaker, I. S., Ashton, M. W. (2011) The importance of the superficial venous anatomy of the abdominal wall in planning a superficial inferior epigastric artery (SIEA) flap: Case report and clinical study. *Microsurgery* **31(6)**, 454–457.

Rusu, M. C., Cergan, R., Motoc, A. G. M., Folescu, R., Pop, E. (2009) Anatomical considerations on the corona mortis. *Surg. Radiol. Anat.* **32(1)**, 17–24.

Saber, A. A., Meslemani, A. M., Davis, R., Pimentel, R. (2004) Safety zones for anterior abdominal wall entry during laparoscopy: A CT scan mapping of epigastric vessels. *Ann. Surg.* **239(2)**, 182–185.

Sakai, H., Sheer, T. A., Mendler, M. H., Runyon, B. A. (2005) Choosing the location for non-image guided abdominal paracentesis. *Liver Int.* **25(5)**, 984–986.

Sampson, J. A. (1917) The variations in the blood supply of the ovary and their possible operative importance. *Surg. Gynecol. Obstet*. **24**, 339–350.

Sanna, B., Henry, B. M., Vikse, J., Skinningsrud, B., Pękala, J. R., Walocha, J. A., Cirocchi, R., Tomaszewski, K. A. (2018) The prevalence and morphology of the corona mortis (Crown of death): A meta-analysis with implications in abdominal wall and pelvic surgery. *Injury* **49(2)**, 302–308.

Sarna, K., Amuti, T., Butt, F., Kamau, M., Muriithi, A. (2020) Variations of the anatomy and bony landmarks of deep circumflex iliac artery in a select Kenyan population. *Craniomaxillofac. Trauma Reconstr*. **13(4)**, 300–304.

Shawki, O. (2004) Laparoscopy and the anterior abdominal wall: A guide to vascular mapping for safe entry. *Gynecol. Surg*. **1**, 27–30.

Siau, K., Robson, N., Bollipo, S.; Global Online Alliance for Liver Studies (GOAL) (2021) Where should ascitic drains be placed? Revisiting anatomical landmarks for paracentesis. *Gut* **70(11)**, 2216–2217.

Stern, H. S., Nahai, F. (1992) The versatile superficial inferior epigastric artery free flap. *Br. J. Plast. Surg*. **45(4)**, 270–274.

Tada, K., Murai, A., Nakamura, Y., Suganuma, S., Tsuchiya, H. (2022) Deep inferior epigastric artery as a collateral pathway to the lower extremities: A case report. *JPRAS Open* **32**, 13–17.

Taylor, G. I., Daniel, R. K. (1975) The anatomy of several free flap donor sites. *Plast. Reconstr. Surg*. **56(3)**, 243–253.

Thepsuwan, J., Huang, K.-G., Wilamarta, M., Adlan, A.-S., Manvelyan, V., Lee, C.-L. (2013) Principles of safe abdominal entry in laparoscopic gynecologic surgery. *Gynecol. Minim. Invasive Ther*. **2(4)**, 105–109.

Tregaskiss, A. P., Goodwin, A. N., Acland, R. D. (2007) The cutaneous arteries of the anterior abdominal wall: A three-dimensional study. *Plast. Reconstr. Surg*. **120(2)**, 442–450.

Tubbs, R. S., Shoja, M. M., Loukas, M. (2016) *Bergman's Comprehensive Encyclopedia of Human Anatomic Variation*. John Wiley and Sons, Hoboken.

van Coeverden de Groot, H. A., Jeeva, M. A., Gunston, K. D. (1983) Morbidity after total abdominal hysterectomy. *S. Afr. Med. J*. **63(14)**, 515–516.

Vercellini, P., Cortesi, I., Oldani, S., Bologna, E., Perotti, D., Crosignani, P. G. (1996) Comparison of postoperative complications after Küstner and Pfannenstiel transverse suprapubic incisions. *Arch. Gynecol. Obstet*. **258(4)**, 201–206.

Watrowski, R., Kostov, S., Alkatout, I. (2021) Complications in laparoscopic and robotic-assisted surgery: Definitions, classifications, incidence and risk factors – An up-to-date review. *Wideochir. Inne Tech. Maloinwazyjne* **16(3)**, 501–525.

Whitmore, I. (1999) Terminologia anatomica: New terminology for the new anatomist. *Anat. Rec*. **257(2)**, 50–53.

Yang, X. F., Liu, J. L. (2016) Anatomy essentials for laparoscopic inguinal hernia repair. *Ann. Transl. Med*. **4(19)**, 372.

Yüksel, M., Yüksel, E. (1995) A rare origination of the first two branches of the femoral artery. *Marmara Medical Journal* **8(3)**, 155–156.

Yurdakul, M., Tola, M., Özdemir, E., Bayazit, M., Cumhur, T. (2006) Internal thoracic artery-inferior epigastric artery as a collateral pathway in aortoiliac occlusive disease. *J. Vasc. Surg*. **43(4)**, 707–713.

Zubler, C., Haberthür, D., Hlushchuk, R., Djonov, V., Constantinescu, M. A., Olariu, R. (2021) The anatomical reliability of the superficial circumflex iliac artery perforator (SCIP) flap. *Ann. Anat*. **234**, 151624.

Kostov S.; Dineva S.; Kornovski Y.; Slavchev S.; Ivanova Y.; Yordanov A.

The Effects of Nasocomial SARS-CoV-2 Infection after Elective Gastrointestinal Oncologic Procedures: Single Center 30-day Follow-up Results

Serdar Şenol[1], Mustafa Kuşak[2]

[1]Department of Gastroenterological Surgery, Samsun Training and Research Hospital, Samsun, Turkey;
[2]Department of General Surgery, Samsun Training and Research Hospital, Samsun, Turkey

Abstract: Although there is extensive debate for the best treatment strategies, limited studies, which reflect the effects of postoperative severe acute respiratory syndrome coronavirus 2 (SARS-CoV-2) infection on mortality and hospital stay after elective gastrointestinal oncologic procedures were published. In order to contribute to the existing literature, a single-center, retrospective, cross-sectional study, including 301 patients who underwent elective gastrointestinal oncological procedures was planned. Patients' data on sex, age, diagnosis, types of procedures, hospital stay, mortality, and SARS-CoV-2 preoperative screening tests were recorded. Four of them were postponed due to positive preoperative screening for SARS-CoV-2. 395 procedures were performed due to cancer originating from colon (105), rectum (91), stomach (74), periampullar region (16), distal pancreas (4), esophagus (3), retroperitoneum (2), ovary (2), endometrium (1), spleen (1) and small bowel (2). Laparoscopy was the approach of choice for 44 patients (14.7% vs. 85.3%). In the postoperative period, two patients were infected with SARS-CoV-2 and one of them died in the intensive care unit (n=1/2, 50% mortality). Two patients died due to surgical complications unrelated to SARS-CoV-2 (n=2/299, 0.67% mortality) (p<0.01). The mean hospital stay was longer in patients with SARS-CoV-2

Mailing Address: Serdar Şenol, MD., Department of Gastroenterological Surgery, Samsun Training and Research Hospital, Kadıköy Mahallesi, Barış Blv. No. 199, 55090 Ilkadim, Samsun, Turkey; Phone: +90 036 231 115 00; e-mail: serdarardaduru@gmail.com

infection (21.5 ± 9.1 – 8.2 ± 5.2 days, respectively, p<0.01). 298 patients were safely discharged (99%). During the pandemic elective gastrointestinal oncologic procedures may be safely performed; however, preoperative testing, precautions to minimize contamination should be performed strictly to reduce in-hospital infection rates, since the mortality rate due to SARS-CoV-2 in this setting is particularly high and hospital stay is also significantly increased.

Introduction

The World Health Organization declared SARS-CoV-2 infection as a pandemic on March 11, 2020. On the same day, the Turkish Ministry of Health reported the first case in Turkey (Turkish Ministry of Health, 2021). The initial wave of the COVID-19 pandemic had a global impact on the provision of cancer care. The need to divert resources to the pandemic response forced many countries to cancel elective operations (Richards et al., 2020). This has a manifest in postponement of and alterations to standard therapy, cessation of screening programmes (Tan and Lau, 2020). As in the World (Carrano et al., 2020; Iacobucci, 2020) all health services in our country have undergone radical changes that have led to the suspension of many elective surgeries. Patients with underlying malignancies and advanced ages are at higher risk of getting more serious illness when infected with SARS-CoV-2 (Dai et al., 2020). Therewithal, not receiving regular treatment for cancer increases the risk of cancer-related morbidity, complications, and mortality (Yang et al., 2020). Due to the surgery's pro-inflammatory nature and its associated immunosuppressive response patients undergoing surgery have a greater risk of becoming infected with COVID-19 (Besnier et al., 2020; Huang et al., 2020). According to the international collaborative group COVIDSurg's available data on complications in patients undergoing surgery during this pandemic the 30-day mortality rate was 23.8% (COVIDSurg Collaborative, 2020). Other series have also shown high mortality rates between 20 and 25% (Doglietto et al., 2020; Lei et al., 2020; Luong-Nguyen et al., 2020).

Although there is extensive debate for the best treatment strategies, limited data on elective gastrointestinal oncologic procedures' results have been published. We aimed to present the perioperative surgical approach and 30 days follow-up outcomes of patients who underwent elective gastrointestinal oncological procedures to reflect the effect of postoperative SARS-CoV-2 infection on mortality and hospital stay and contribute to the existing literature.

Material and Methods

This study was conducted in accordance with the 1983 Helsinki Declaration, approved by the Turkish Ministry of Health Science Committee and the hospital's ethical committee for clinical studies (GOKA/2021/19/7). Written informed consent was obtained from all patients concerning the risks associated with the relevant surgeries, as well as COVID-19 infection.

   This was a retrospective, cross-sectional and single-center study. Data from patients who underwent gastrointestinal oncological procedures were retrospectively reviewed from the surgical database collected from a single tertiary hospital.

   All adult patients of both sexes, who underwent elective surgery between April 2020 and November 2021 were included in this study. Patients undergoing emergency surgery for cancer-related gastrointestinal system complications, such as obstruction, bleeding, and perforation, and patients with unresectable metastatic disease were excluded.

   Every patient scheduled for surgery screened for SARS-CoV-2 infection with polymerase chain reaction (PCR) tests using nasopharyngeal swab and/or chest computed tomography (CT). Patients with at least one positive result (chest CT or nasal swab) had their surgery postponed and were treated according to their symptoms and severity of the disease. Patients with negative result underwent surgery. Postoperative SARS-CoV-2 test was not routinely performed unless acute infection was suspected.

   Patient data on sex, age, indication of surgery, diagnosis, types of procedures, hospital stay, mortality, and SARS-CoV-2 screen test results were recorded. Hospital stay was defined as the time elapsed from hospitalization to discharge. After the surgical procedure, patients were clinically monitored during the entire postoperative hospital stay, and if SARS-CoV-2 infection was suspected, chest CT was performed, and nasal swab PCR were collected. Many precautions have been taken to minimize contamination between staff and patients during the hospital stay, such as mandatory use of surgical masks by both patients and staff, minimizing hospital visits and rapid transport of infected patients to COVID-19 services or intensive care units.

   Continuous variables are presented as means and standard deviation. Statistical analysis was performed with Student's *t*-test to compare hospital stay, and chi-square test was used to compare mortality between patients with and without SARS-CoV-2 infection.

Results
During the study period, 301 surgeries were planned. Surgical procedures were performed due to cancer originating from colon (105, 34.8%), rectum (91, 30.2%), stomach (74, 24.6%), periampullar region (16, 5.3%; head of pancreas 12, 4%; duodenum 1, 0.3%; ampulla 3, 1%), distal pancreas (4, 1.3%), esophagus (3, 1%), retroperitoneum (2, 0.7%), ovary (2, 0.7%), endometrium (1, 0.3%), spleen (1, 0.3%) and small bowel (2, 0.7%). The mean age of the patients was 64 ± 12 years. The number of male and female patients was 200 and 101, respectively. According to the American Society of Anesthesiology (ASA) Physical Status Classification, the proportional sequence of the patients was as follows: ASA-3 53.4% (161), ASA-2 39.3% (118), ASA-4 5.6% (17), ASA-1 1.7% (5).
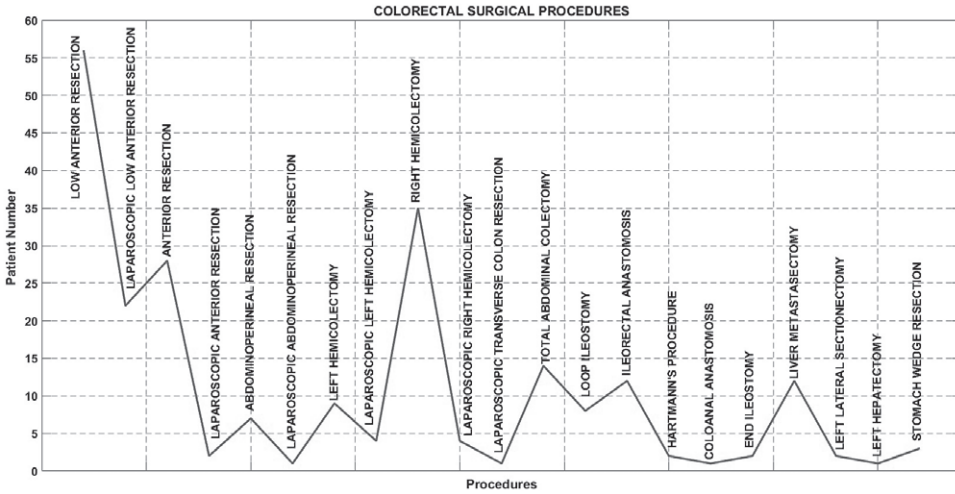
Figure 1 – Colorectal surgical procedures.
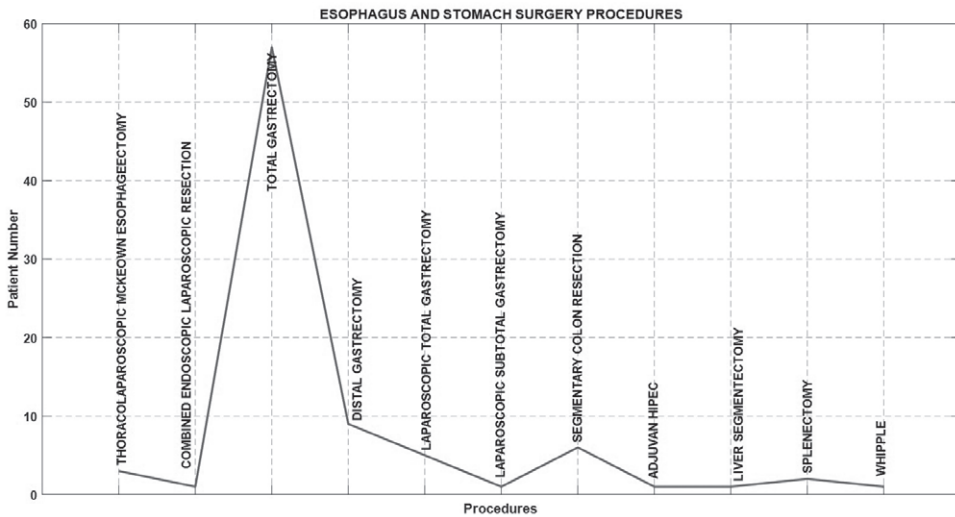
Figure 2 – Esophageal and gastric surgical procedures.

The total number of surgical procedures performed at our hospital within this period was 395. The surgical procedures classified as colorectal, esophageal/gastric, cytoreductive and other surgical procedures. Figures 1–4 show them.

Preoperative screening for SARS-CoV-2 infection was performed in 301 patients and was positive in 4 (1.3%). All four patients were asymptomatic and had their surgeries postponed. There were no patients who had chest CT findings suggestive
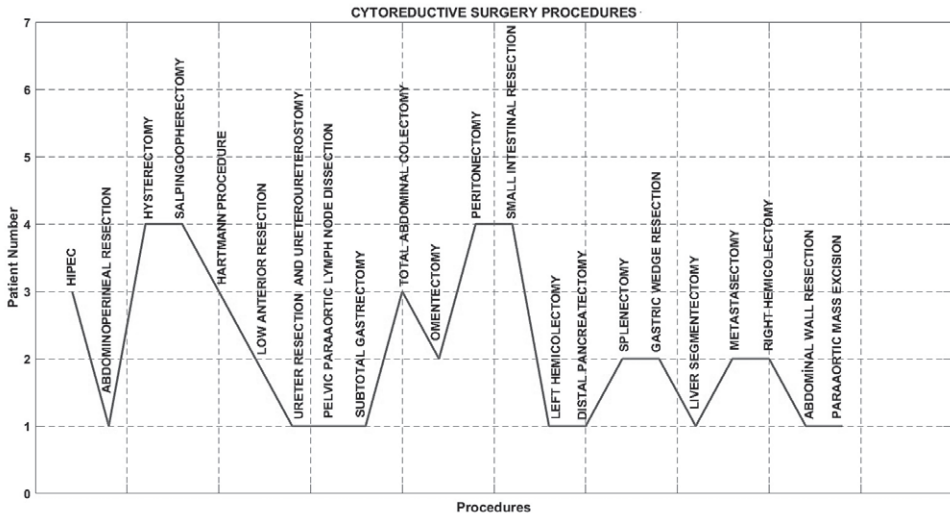
Figure 3 – Cytoreductive surgery procedures.
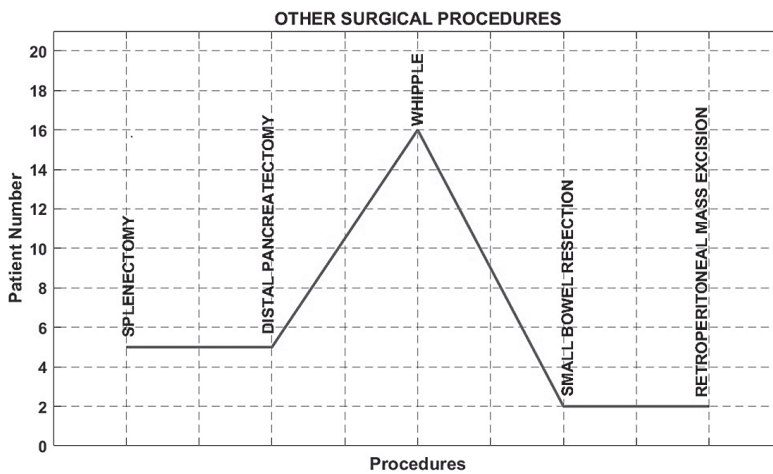
Figure 4 – Other surgical procedures.

of SARS-CoV-2 infection, and/or who had both tests positive. These patients were taken to isolation rooms. Their treatment was completed, and surgery was performed after the SARS-CoV-2 test results became negative.

During the postoperative period, 2 (0.67%) patients developed respiratory symptoms and tested positive for SARS-CoV-2 infection, of which 1 died in the intensive care unit, with a mortality rate of 50% (n=1/2). The fatality due to COVID-19 was described as follows: a 68-year-old man who underwent open

total gastrectomy and D2 lymph node dissection for gastric cancer and had a past medical history of diabetes and smoking. The cause of death was attributed to COVID-19-related complications.

Of the patients without SARS-CoV-2 infection, two patients died in the postoperative period, with a mortality rate of 0.67% (n=2/299): a 72-year-old man who had a past medical history of diabetes, chronic renal failure underwent open total gastrectomy and D2 lymph node dissection. The patient had a sudden onset of abdominal pain on the eighth postoperative day, was re-operated for small bowel perforation. He died as a result of multiple organ failure on the fourteenth postoperative day. The other was a 75-year-old man who had a past medical history of hypertension, coronary artery disease underwent total gastrectomy and D2 lymph node dissection. The patient had postoperative ileus. On the tenth postoperative day, he underwent re-laparatomy and bridectomy. During the intensive care follow-up, respiratory failure developed due to acute respiratory distress. The mortality rate was significantly higher in patients infected with SARS-CoV-2 (p<0.01). The mean hospital stay was also significantly longer in patients who developed the infection during the postoperative period (21.5 ± 9.1 days versus 8.2 ± 5.2 days; p<0.01). According to the national patient registration system, no COVID-19 positivity was observed during the follow-up period.

Discussion
At the beginning of the COVID-19 pandemic, postponing surgeries and cancelling medical appointments seemed to be the most reasonable option (Grubic et al., 2020; Iacobucci, 2020). However, they were proven to be inadequate as the pandemic has not subsided and we have severely struggled with Omicron variant of SARS-CoV-2, as a new challenge for the global public health (Thakur and Ratho, 2022) while this paper is written.

Despite the strict visitor policies and protective measures, during the postoperative period, 2 (0.67%) patients developed respiratory symptoms and tested positive for SARS-CoV-2 infection. This suggested the possibilities of in-hospital contamination and preoperative screening test performed during the window period of acute infection.

Due to the theoretical risk of aerosolization, at the beginning of the pandemic we avoided the laparoscopic approach. But the lack of strong evidence against the benefits of minimally invasive surgery (Mintz et al., 2020; Ribeiro et al., 2020) we abandoned this practice. However, due to the decrease in the number of operating rooms, intensive care and service beds, performing complex surgical procedures and the continuation of elective surgeries for benign diseases, except for the first wave of the pandemic, prevented laparoscopic procedures from being performed as often as we wanted (14.7% vs. 85.3%).

The mortality rate of COVID-19 in the postoperative period was considered high. One of two patients (50%) who developed symptomatic infection died after

prolonged hospital stay in the intensive care unit. Studies on COVID-19 mortality in the postoperative period for elective gastrointestinal oncological surgical procedures are limited but the general mortality of this infection in patients with cancer is up to 25% (COVIDSurg Collaborative, 2020; Doglietto et al., 2020; Lei et al., 2020; Luong-Nguyen et al., 2020; Yang et al., 2020). It is likely that the mortality rate due to COVID-19 in our series is overestimated because patients were not routinely tested in the postoperative period, just those with a suggestive clinical scenario, which likely led to a selection bias. As shown in different studies (Liang et al., 2020; Yanez et al., 2020; Zhang et al., 2020), we attribute the high mortality found in our study to the disease severity and the profile of patients that attended our hospital, which is a tertiary institution that treats patients with advanced tumours, aged over 65 years, male gender, frequently have other associated chronic disease, as demonstrated by the ASA classification, in which 161 patients (53.4%) were classified as ASA-3. The profile of surgical procedures was also extremely complex as shown Figures 1–4. Despite these, 99% of patients were safely discharged after elective gastrointestinal surgical procedures during the pandemic.

As a limitation, this study reflects a single-center experience; therefore, we are aware that our outcomes should be compared with comprehensive studies to make an exact comment on gastrointestinal surgical procedures due to cancer during pandemics.

Conclusion

Our results suggest that during the pandemic elective gastrointestinal oncological procedures may be safely performed, but preoperative testing and precautions to minimize contamination are paramount, since the mortality due to SARS-CoV-2 infection in the postoperative period is particularly high and hospital stay is also significantly increased.

References

Besnier, E., Tuech, J. J., Schwarz, L. (2020) We asked the experts: Covid-19 outbreak: Is there still a place for scheduled surgery? "Reflection from pathophysiological data". *World J. Surg.* **44**, 1695–1698.

Carrano, F. M., Foppa, C., Carvello, M., Spinelli, A. (2020) With adequate precautions colorectal cancer surgery can be safely continued during COVID-19 pandemic. *Br. J. Surg.* **107(10)**, e417.

COVIDSurg Collaborative (2020) Mortality and pulmonary complications in patients undergoing surgery with perioperative SARS-CoV-2 infection: An international cohort study. *Lancet* **396**, 27–38.

Dai, M., Liu, D., Liu, M., Zhou, F., Li, G., Chen, Z., Zhang, Z., You, H., Wu, M., Zheng, O., Xiong, Y., Xiong, H., Wang, C., Chen, C., Xiong, F., Zhang, Y., Peng, Y., Ge, S., Zhen, B., Yu, T., Wang, L., Wang, H., Liu, Y., Chen, Y., Mei, J., Gao, X., Li, Z., Gan, L., He, C., Li, Z., Shi, Y., Qi, Y., Yang, J., Tenen, D. G., Chai, L., Mucci, L. A., Santillana, M., Cai, H. (2020) Patients with cancer appear more vulnerable to SARS-CoV-2: A multicenter study during the COVID-19 outbreak. *Cancer Discov.* **10(6)**, 783–791.

Doglietto, F., Vezzoli, M., Gheza, F., Lussardi, G. L., Domenicucci, M., Vecchiarelli, L., Zanin, L., Saraceno, G., Signorini, L., Panciani, P. P., Castelli, F., Maroldi, R., Rasulo, F. A., Benvenuti, M. R., Portolani, N., Bonardelli, S., Milano, G., Casiraghi, A., Calza, S., Fontanella, M. M. (2020) Factors associated with surgical

mortality and complications among patients with and without coronavirus disease 2019 (COVID-19) in Italy. *JAMA Surg*. **155(8)**, 691–702.

Grubic, A. D., Ayazi, S., Zebarjadi, J., Tahmasbi, H., Ayazi, K., Jobe, B. A. (2020) COVID-19 outbreak and surgical practice: The rationale for suspending non-urgent surgeries and role of testing modalities. *World J. Gastrointest. Surg*. **12(6)**, 259–268.

Huang, C., Wang, Y., Li, X., Ren, L., Zhao, J., Hu, Y., Zhang, L., Fan, G., Xu, J., Gu, X., Cheng, Z., Yu, T., Xia, J., Wei, Y., Wu, W., Xie, X., Yin, W., Li, H., Liu, M., Xiao, Y., Gao, H., Guo, L., Xie, J., Wang, G., Jiang, R., Gao, Z., Jin, Q., Wang, J., Cao, B. (2020) Clinical features of patients infected with 2019 novel coronavirus in Wuhan, China. *Lancet* **395**, 497–506.

Iacobucci, G. (2020) Covid-19: All non-urgent elective surgery is suspended for at least three months in England. *BMJ* **368**, m1106.

Lei, S., Jiang, F., Su, W., Lei, S., Jiang, F., Su, W., Chen, C., Chen, J., Mei, W., Zhan, L. Y., Jia, Y., Zhang, L., Liu, D., Xia, Z. Y., Xia, Z. (2020) Clinical characteristics and outcomes of patients undergoing surgeries during the incubation period of COVID-19 infection. *EClinicalMedicine* **21**, 100331.

Liang, W., Guan, W., Chen, R., Wang, W., Li, J., Xu, K., Li, C., Ai, Q., Lu, W., Liang, H., Li, S., He, J. (2020) Cancer patients in SARS-CoV-2 infection: A nationwide analysis in China. *Lancet Oncol*. **21**, 335–337.

Luong-Nguyen, M., Hermand, M., Abdalla, S., Cabrit, N., Hobeika, C., Brouquet, A., Goéré, D., Sauvanet, A. (2020) Nosocomial infection with SARS-Cov-2 within departments of digestive surgery. *J. Visc. Surg*. **157**, S13–S18.

Mintz, Y., Arezzo, A., Boni, L., Baldari, L., Cassinotti, E., Brodie, R., Uranues, S., Zheng, M. H., Fingerhut, A. (2020) The risk of COVID-19 transmission by laparoscopic smoke may be lower than for laparotomy: A narrative review. *Surg. Endosc*. **34(8)**, 3298–3305.

Ribeiro, S. C., Lauletta, A. L. F., Franco, B. C., Bezerra, R. L. A., Vanni, D. G. B. S., Baracat, E. C. (2020) Laparoscopic surgery and coronavirus disease: What do we know now? *Clinics (Sao Paulo)* **75**, e2083.

Richards, M., Anderson, M., Carter, P., Ebert, B. L., Mossialos, E. (2020) The impact of the COVID-19 pandemic on cancer care. *Nat. Cancer* **1**, 563–565.

Tan, K. K., Lau, J. (2020) Cessation of cancer screening: An unseen cost of the COVID-19 pandemic? *Eur. J. Surg. Oncol*. **46**, 2154–2155.

Thakur, V., Ratho, R. K. (2022) OMICRON (B.1.1.529): A new SARS-CoV-2 variant of concern mounting worldwide fear. *J. Med. Virol*. **99(5)**, 1821–1824.

Turkish Ministry of Health (2021) Current situation in Turkey. Access date: November 22. Available at: https://covid19.saglik.gov.tr

Yanez, N. D., Weiss, N. S., Romand, J. A., Treggiari, M. M. (2020) COVID-19 mortality risk for older men and women. *BMC Public Health* **20(1)**, 1742.

Yang, K., Sheng, Y., Huang, C., Jin, Y., Xiong, N., Jiang, K., Lu, H., Liu, J., Yang, J., Dong, Y., Pan, D., Shu, C., Li, J., Wei, J., Huang, Y., Peng, L., Wu, M., Zhang, R., Wu, B., Li, Y., Cai, L., Li, G., Zhang, T., Wu, G. (2020) Clinical characteristics, outcomes, and risk factors for mortality in patients with cancer and COVID-19 in Hubei, China: A multicentre, retrospective, cohort study. *Lancet Oncol*. **21(7)**, 904–913.

Zhang, L., Zhu, F., Xie, L., Wang, C., Wang, J., Chen, R., Jia, P., Guan, H. Q., Peng, L., Chen, Y., Peng, P., Zhang, P., Chu, Q., Shen, Q., Wang, Y., Xu, S. Y., Zhao, S. Y., Zhou, M. (2020) Clinical characteristics of COVID-19-infected cancer patients: A retrospective case study in three hospitals within Wuhan, China. *Ann. Oncol*. **31(7)**, 894–901.

Maxillary Sinus Volume and Its Effect on Treated Impacted Canines

Martin Horáček[1], Taťjana Dostálová[1], Petra Urbanová[2], Hana Eliášová[1], Miloš Špidlen[3], Petra Hliňáková[1]

[1]Department of Stomatology, Second Faculty of Medicine, Charles University and University Hospital Motol, Prague, Czech Republic;
[2]Department of Anthropology, Faculty of Science, Masaryk University, Brno, Czech Republic;
[3]Institute of Oral Dentistry and Oral Sciences, Palacký University, Olomouc, Czech Republic

Abstract: The goal of study was to explore the role of 3D CBCT (cone beam computer tomography) in detecting impacted canines and their movement to evaluate the influence of orthodontic therapy parameters on treatment options, and to monitor quality of healing process based on shape and size of sinus maxillae volume. It is known that the volume of maxillary sinus plays an important role in patients with impacted teeth. The prospective study consisted of 26 individuals. For each individual, pre-treatment and post-treatment CBCT data were acquired. Changes of size, and position of impacted canine in 3D CBCT image before and after therapy were prepared using 3D reconstruction. Volumetric measurements of the maxillary sinuses were performed before and after orthodontic therapy of impacted canines, using InVivo6 software. The main effects MANOVA performed on linear measurements showed metric differences between pre-op and post-op images. A paired *t*-test showed no statistically significant differences between pre-op and post-op values of the sinus volume. Changes of size and position of impacted canine in 3D image before and after therapy were precise and reproducible, using 3D reconstruction in three planes – horizontal, midsagittal, and coronal. The linear measurements showed metric differences between pre-op and post-op images.

Mailing Address: Prof. Taťjana Dostálová, MD., DSc., MBA, Department of Stomatology, Second Faculty of Medicine, Charles University and University Hospital Motol, V Úvalu 84, 150 06 Prague 5, Czech Republic; Phone: +420 224 433 101; Fax: +420 224 433 120; e-mail: tatjana.dostalova@fnmotol.cz

Introduction

The maxillary canine is one of the most important teeth of the dental arch, essential for functional and stable occlusion and playing an important role in aesthetics (Servais et al., 2018). These teeth are the most frequently impacted teeth after the third molars (Alqerban et al., 2014) with an incidence ranging from 0.9 to 2.2%. Patients requiring orthodontic treatment related to an impacted maxillary canine account for 1% to 5% of the total orthodontic therapy (Celikoglu et al., 2010). Radiographic examinations represented by conventional two-dimensional (2D) radiographs (panoramic, periapical, occlusal, and lateral cephalograms) have been used in orthodontic practice for many years. However, their diagnostic value for localizing an impacted maxillary canine has been questioned because 2D image deformation (Eliasova et al., 2021) makes it difficult to accurately localize the canine and visualize root abnormalities.

The prevalence of impacted maxillary canines has been reported to range from 1.7 to 4.7% (Lövgren et al., 2019). They occur more frequently in females than in males and impaction is more frequently observed in the maxilla than in the mandible and affects both sides of the dental arch simultaneously in approximately one quarter of all cases (Mazurová et al., 2015). The maxillary canine is the second most common impacted tooth after the third molar, with a prevalence of 1–3%, depending on population studies (Mazurová et al., 2015; Eslami et al., 2017). The maxillary impacted canine is more often located palatally (85%) than labially (15%) (Grisar et al., 2019). Root dilaceration is reported to be present in up to 59.5% of the cases (da Silva Santos et al., 2014). Depending on the position of the impacted tooth, we distinguish between complete impaction when the affected tooth is covered by both hard and soft tissues and partial impaction, when the impacted tooth is covered by soft tissue only. Exact etiological factor has not been specified. The cause is probably multifactorial, with genetics playing the largest role (Becker and Chaushu, 2015).

The maxillary canines play a key role in facial aesthetics, development of the dental arch, and occlusion. Despite a relatively simple diagnosis supported by clinical and radiological examination, it is not uncommon to find an impacted canine in an adult patient. Treatment of this anomaly later in life carries some risks of complications and failure.

Various diagnostic methods are used to localize the impacted teeth. The techniques allow for the practitioner to predict the orthodontic treatment, surgical therapy, including also autotransplantation or possible canine extraction followed by implant insertion (Eslami et al., 2017). The diagnostic process begins with a clinical examination and palpation of the alveolar bone and is followed by radiographic evaluation. However, classic 2-dimensional (2D) conventional radiographs, mainly orthopantomograms (OPG), have two disadvantages – the information limit resulting from anatomic superimposition and geometric distortion of the imagery with poor visibility, and misrepresentation of structures surrounding maxillary impacted canines (Eliasova et al., 2021). Reliance on 2-dimensional imaging restricts the ability of

clinicians to predict the length of treatment (Schubert and Baumert, 2009). Contrary to conventional radiography, cone beam computed tomography (CBCT) produces three-dimensional (3D) volumetric data in the axial, coronal, and sagittal planes. Eslami et al. (2017) in a systematic review confirmed that CBCT was more accurate than conventional radiographs in localizing impacted maxillary canines.

It is known that the volume of the maxillary sinus plays an important role in patients with impacted teeth (Schubert and Baumert, 2009). The maxillary sinus is a bilateral air-filled cavity located in the maxillary complex (Tassoker et al., 2020). The maxillary sinuses are surrounded by the ethmoid bone, nasal concha, palate, and lacrimal bone. The floor is formed by the alveolar processes of the maxilla. The roots of the premolar and molar and canine are separated from the maxillary sinus by a compact bone. For patients with impacted canines, anatomical shape and size and other pathological findings have been shown to affect the volume of the maxillary sinus and change its pneumatization (Emirzeoglu et al., 2007; Tassoker et al., 2020). Genetic and environmental etiologic factors were confirmed for maxillary canine impaction and the alveolar bone area was also increased on the impacted side compared than the non-impacted side (Oz et al., 2017).

The aim of the study was three-fold:
1) to explore the role of 3D CBCT in detecting impacted canines and their movement during the prospective study
2) to evaluate the influence of orthodontic therapy parameters on treatment options
3) to monitor the quality of healing process based on shape and size of sinus maxillae volume versus impacted and non-impacted canines.

Material and Methods
Subjects
The sample under study was composed of 26 individuals (21 females, 5 males).

For each individual, pre-treatment (pre-op) and post-treatment (post-op) CBCT data were acquired. The maxillary canine impaction was all the times unilateral. The mean age of patients prior to treatment was 13.5 years (females: 13.3 years, males: 14.4 years). When the treatment was concluded, it was 15.7 years (females: 15.3 years, males: 17.1 years). The timespan between pre- and post-treatment imagery ranged from seven months to 4.3 years.

The prospective study was conducted according to the recommendations of the American Dental Association (ADA). In accordance with the Declaration of Helsinki patients were requested to provide informed consent to the clinical examination and regular follow-ups by means of the informed consent form. The anonymity of the data obtained was strictly respected. Ethical approval for the study was obtained from the Ethics Committee. The exclusion criterion for one patient was as follows: the person was indicated for surgical removal of impacted canine due to resorption of root and treatment continued with the implant insertion.
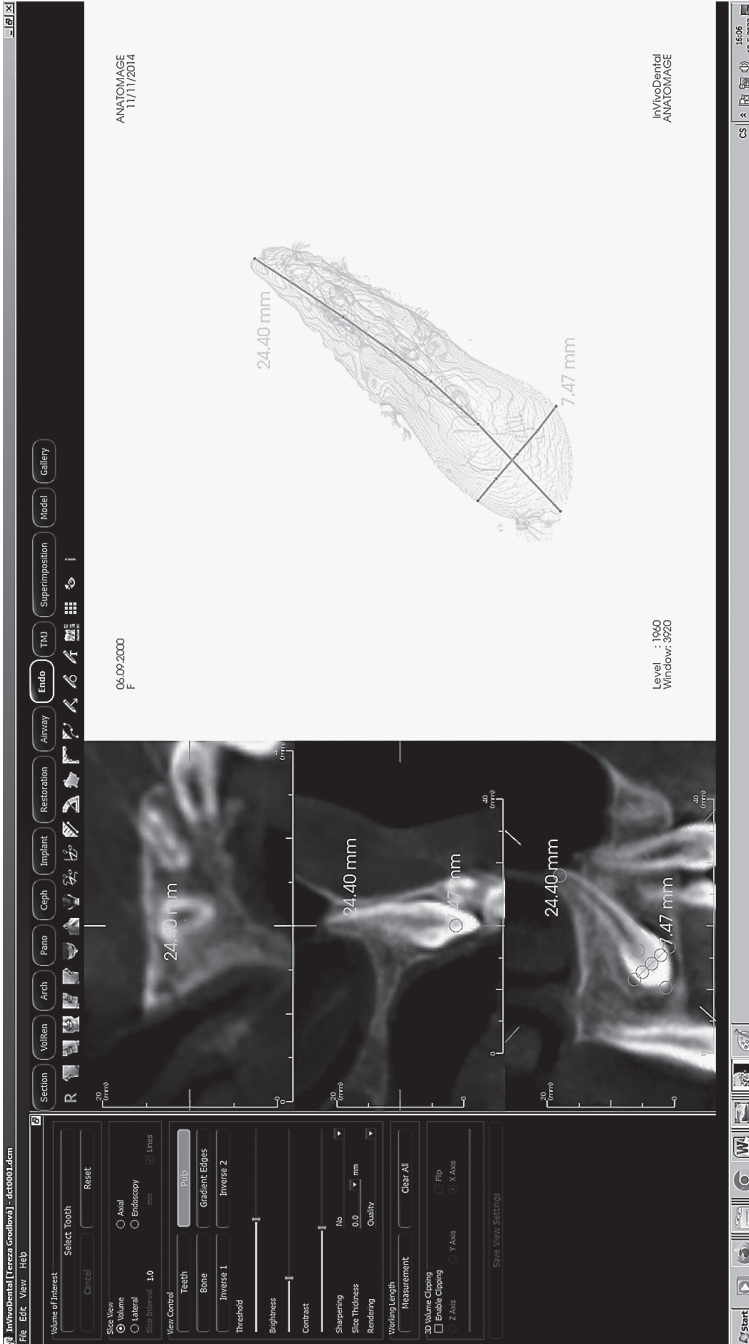
Figure 1 – The impacted canine before therapy with its 3D reconstruction in three planes: horizontal (points A-B); midsagittal; and coronal plane going through the canine cusp tip (C point).
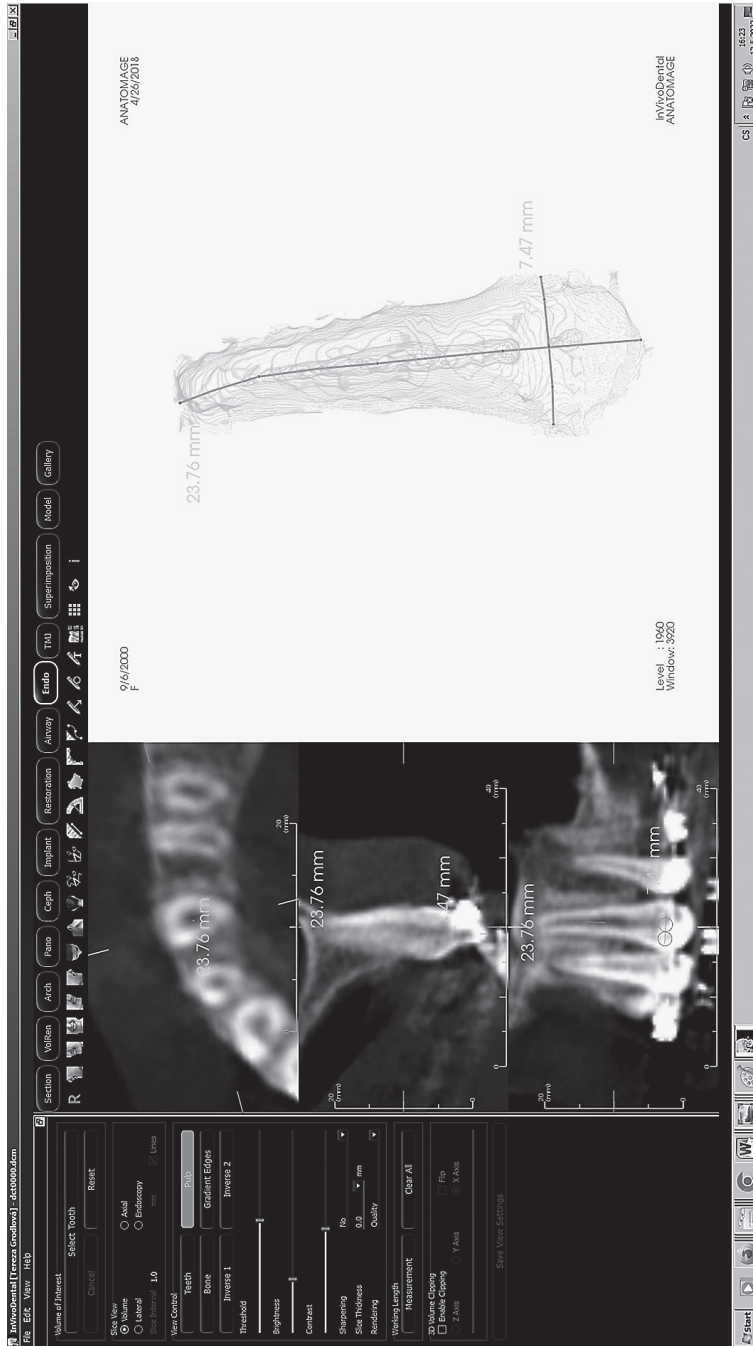
Figure 2 – The canine after therapy and its 3D reconstruction.

Treatment arrangement
For the radiological diagnosis, the Cone Beam Computed Tomography, KaVo Dental GmbH, Biberach, Germany (CBCT) was used to determine the position, number, shape, and size of impacted canines before and after therapy (Figure 1) with 17 cm × 23 cm FOV (field of view), 0.3 mm voxel size at 120 kV, 5 mA, according to manufacturer's directions. All CBCT examinations were indicated for surgical and orthodontic treatment; none of the examinations was performed solely for the purpose of this study.

Changes of shape, size, and position of impacted canine in 3D image before and after therapy were prepared using a 3D reconstruction and ENDO program (InVivo6 – Dental Anatomage Europe/Santa Clara, USA) (Figures 1 and 2).

Maxillary sinuses volumetric measurements
Volumetric measurements of the maxillary sinuses were performed before and after orthodontic therapy of impacted canines using also the InVivo6 software. Images were oriented in three spatial planes. The axial slice was adjusted to represent the Frankfort horizontal plane; the sagittal cross-section was used as the midsagittal plane; and the coronal slice was going through the furcation of the upper first molar roots. The volumes of right and left sinuses were measured individually step by step by Volume Render program (Figures 3 and 4).

For the pre-op sinuses, side differences were revealed for the pooled individuals as well as separately for patients with impacted and normal canines. The impacted canines, however, were associated with the sinus asymmetry merely at a 10% level of significance. For the post-op sinuses, all asymmetry comparisons (all together, impacted, normal canines) were shown statistically significant. In all cases the left-sided sinuses were larger than the right-sided.

Exploring impaction of canine teeth
Four linear measurements of the crania and canines were taken using the InVivo6 program. The measurements included: 1) the interlandmark distance between the right and left frontomalare orbitale points (A-B), 2) the shortest perpendicular distance between the line running through the right and left frontomalare orbitale points (A-B) and the canine cusp tip (right, left) (point C) (vector A-B), 3) the canine length measured from the canine cups tip to the apex, and 4) the canine width taken at the widest part of the crown. Furthermore, the volume of the maxillary sinus was taken, again, using measuring functionalities available in the InVivo6 program. Asymmetry in bilateral measurements was expressed in terms of right-to-left differences. In all cases, the measurements were acquired on volumetric visualizations.

Each 3D image – all distances, vectors and volumes were measured repeatedly twice after one month calculating intra-operator error. The differences between repeated measurements (intra-operator error) were tested in the pair-wise manner
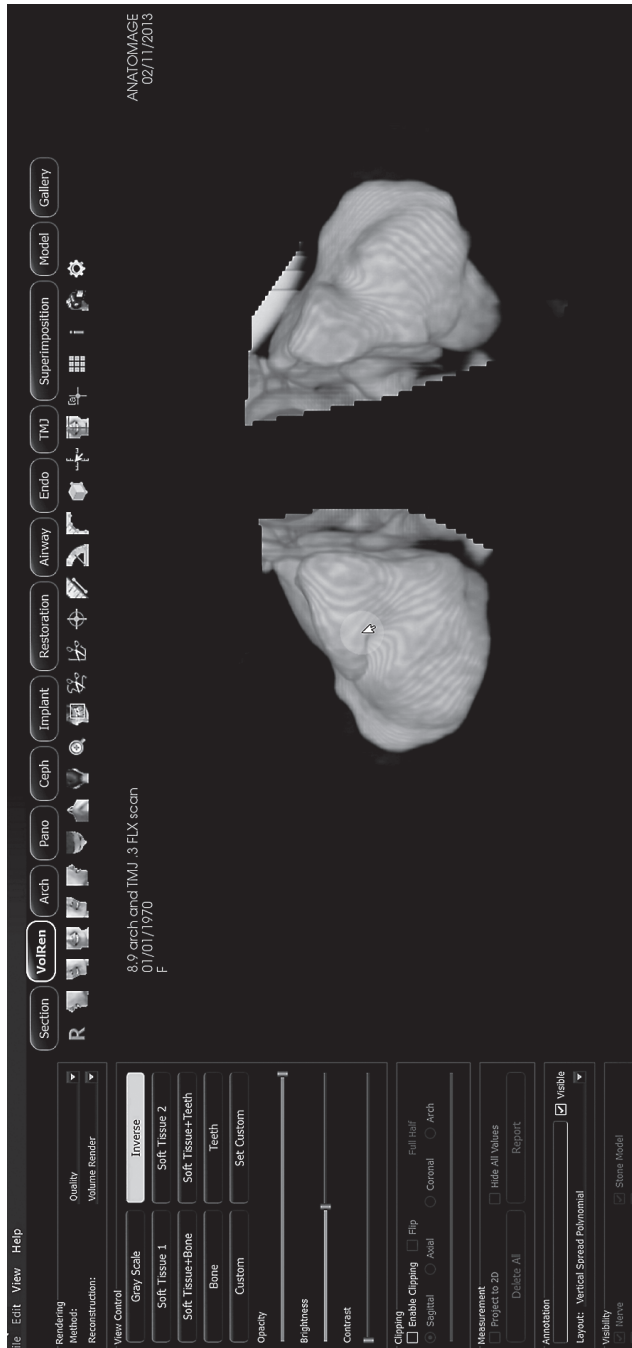
Figure 3 – Segmentation process during three-dimensional reconstruction of maxillary sinuses.
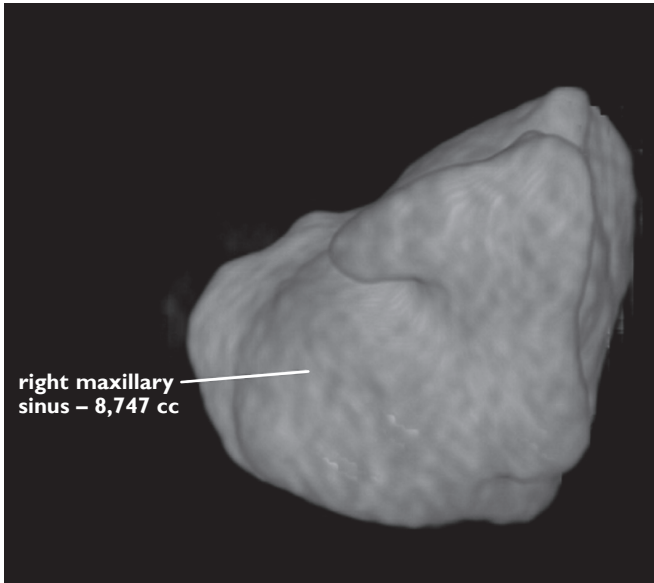
Figure 4 – Volumetric measurement of right maxillary sinus – 8747 mm³ was automatically calculated in Volume Render program.

by the Repeated Measures ANOVA. Prior to testing, assumptions were verified by a Levene's test. Side-related differences were tested by paired *t*-tests. While relationships between measurements and continuous parameters (age, duration of treatment) were tested by Pearson's correlation coefficient, differences by categorical variables (impacted/normal tooth, pre-op/post-op image) were explored by a *t*-test and a multivariate analysis of variance. Statistical tests were performed at a 5% level of significance, if not stated otherwise.

Results

The results were inserted to the following Tables 1 and 2. The Repeated Measures ANOVA showed no statistically significant differences between two sets of measurements for any of the linear nor volumetric measurements.

   All measurements, except for the crown width, correlated positively with age (R ranging from 0.2 to 0.46). Logically, the strongest relationship was shown for the A-B distance. A-B line as well as the tooth length also showed positive relationships with the duration of treatment (R ranging from 0.22 to 0.42) (Table 3). The volume of the maxillary sinus correlated positively with the A-B line and with the perpendicular distance from the line to the canine cusps tip (vector A-B) (Table 4). When tested separately for groups (pre/post-op, side, normal/impacted canines), the positive correlations varied largely among groups with no specific pattern.

   The presence of normal and impacted canines was distributed evenly on the right and left side sides. No side-related prevalence was observed for impacted canines (chi-square, P-value = 0.575) (Tables 5 and 6).

Table 1 – Descriptive statistics was prepared for repeated measurements

Measure-ment	Repeat measure-ment	Valid NM	Mean	Median	Mini-mum	Maxi-mum	SD
A-B	1	104	93.064	92.910	78.530	102.620	5.204
	2	103	92.914	93.500	77.640	103.390	5.495
Length – canine	1	103	22.214	22.180	16.580	29.770	2.365
	2	103	22.127	21.640	16.670	29.920	2.381
Width – canine	1	103	7.619	7.470	6.080	11.300	0.897
	2	103	7.589	7.440	5.840	11.930	0.937
Distance A-B	1	103	65.942	66.310	51.350	77.930	6.024
	2	103	65.918	66.190	51.650	77.280	5.958
Right sinus – volume	1	50	9.973	9.703	5.868	18.712	2.541
	2	50	9.974	9.768	5.882	18.723	2.536
Left sinus – volume	1	52	11.713	11.722	3.465	18.806	2.790
	2	52	11.769	11.735	3.481	18.724	2.821

NM – number of measurements; SD – standard deviation

Table 2 – Descriptive statistics of the sinus volume grouped by pre/post treatment and types of canines

	Stage	Normal/impacted	NI	Means	Median	SD	Min	Max
Right sinus	pre-op	R	14	9.084	9.122	1.606	6.507	12.273
	pre-op	N	11	10.758	9.958	3.216	5.868	18.359
	post-op	R	14	9.645	9.859	1.852	7.073	13.294
	post-op	N	11	10.736	9.791	3.305	6.091	18.712
Left sinus	pre-op	N	10	10.401	11.050	2.646	3.465	12.440
	pre-op	R	16	11.362	11.185	2.942	5.360	16.476
	post-op	N	10	12.792	13.094	1.283	9.559	13.961
	post-op	R	16	12.209	11.620	3.209	5.512	18.806

R – retained; N – normal; NI – number of individuals; SD – standard deviation

The main MANOVA effects performed on linear measurements showed metric differences between measurements of normal and impacted teeth as well as between pre-op and post-op images. Post-hoc tests specified that of the measurements studied, differences between impacted and normal teeth and pre-op and post-op images were significant in canine position expressed in terms of vector A-B distance.

In addition to MANOVA, side differences of the measurements were tested by an unpaired and paired t-test. The unpair variant revealed statistically significant

Table 3 – Pearson's correlation coefficient between the measurements and continuous variables

Measurement	Age	TS
A-B	0.404	0.224
Length	0.226	0.386
Width	0.116	0.133
Vector A-B	0.391	0.085
Maxillary sinus	0.202	0.032

TS – time span between to two repeated measurements

Table 4 – Pearson's correlation coefficient between the measurements and volume of the maxillary sinus

Measurement	Maxillary sinus
A-B	0.425
Length	−0.066
Width	0.011
Vector A-B	0.331

Table 5 – Among-group variation in the linear measurements

Normal/impacted	Left-sided		Right-sided		Total
	NI	%	NI	%	
Normal	10	45.45	12	54.55	22
Impacted	16	53.33	14	46.67	30
Total	26	50.00	26	50.00	52

NI – number of individuals

Table 6 – Main effects MANOVA

	Test	Value	F test	Effect	Error	P-value
Intercept	Wilks	0.002	9839.549	4	96	0.000
Normal/impacted	Wilks	0.620	14.679	4	96	0.000
Body side	Wilks	0.953	1.180	4	96	0.325
Pre/post-treatment	Wilks	0.830	4.927	4	96	0.001

Table 7 – Linear regression analysis

		SS	Degrees	MS	F test	P-value
Right sinus	age	4906.551	1	4906.551	628.041	0.00
	error	382.811	49	7.812		
Left sinus	age	7095.668	1	7095.668	831.822	0.00
	error	435.044	51	8.530		

SS – sum of squares; MS – mean sum of squares

Horáček M.; Dostálová T.; Urbanová P.; Eliášová H.; Špidlen M.; Hliňáková P.

Table 8 – Paired _t_-test testing differences in regression residuals between pre-treatment and post-treatment sinuses

Subset	Sinus residuals		Mean	SD	NI	Diff.	SD	t-test	P-value
Pooled	right	pre-op	0.689	2.578	25	0.984	1.129	4.358	0.000
		post-op	−0.295	2.952					
	left	pre-op	0.285	2.981	26	0.173	1.725	0.511	0.614
		post-op	0.112	2.901					
Impacted	right	pre-op	0.026	1.396	14	1.134	1.112	3.816	0.002
		post-op	−1.107	2.145					
	left	pre-op	0.451	2.905	16	0.572	1.189	1.925	0.073
		post-op	−0.121	3.532					
Normal	right	pre-op	1.532	3.468	11	0.793	1.174	2.239	0.049
		post-op	0.740	3.583					
	left	pre-op	0.019	3.240	10	−0.466	2.273	−0.648	0.533
		post-op	0.485	1.526					

SD – standard deviation; NI – number of individuals

differences in the canine width, with the left teeth being, on average, wider than the right ones (t = 2.249, P-value = 0.027). The same results were revealed by the paired _t_-test (t = 2.411, P-value = 0.0196). When treated by groups, normal canines showed side-related differences in canine length, and vector A-B distance, where the left-sided measurements were larger in both cases. In contrast, the left and right impacted canines differed in width, where the right-sided teeth were narrower, and in vector A-B distance, where the right-sided teeth were positioned in an upper position than the left-sided canines.

No side-related differences were revealed for the pre-op group, while in the post-op teeth the sides varied in the canine width, where the left-sided teeth were wider than those on the right side.

Maxillary sinus
A paired _t_-test showed no statistically significant differences between pre-op and post-op values of the sinus volume when the individuals with impacted and normal canines were pooled. When tested separately, patients with impacted canines exhibited enlarged sinuses once the treatment was concluded. The results were valid for both sides. For the left sinuses, however, the enlargement occurred also in patients with normal canines. To test whether the enlargement was affected by the underwent treatment as opposed to be merely the factor of age-related sinus growth, a linear regression analysis was first conducted with the individual's age as the independent variable and the sinus volume as the dependent variable (for right and left sinuses separately) (Tables 7 and 8). Then, regression residuals were tested for the differences between pre-op and post-op volumes by a paired _t_-test.

The analysis has confirmed that, indeed, there were differences between the pre-op and post-op volumes of the maxillary sinus once the volume was controlled for age variations (Table 8). On the right side, post-op sinuses of the individuals with impacted canines showed smaller volume than expected by the age model. The same results were shown on the left side, but these differences were not statistically significant at a 5% level of significance (albeit significant at a 10% level). For the sinuses associated with normal canines, the pre-op and post-op residuals were, on average, all of positive values. This means that the regression generally underestimated their real volume, i.e. the retarded growth was not present. Yet, there were still differences between the pre-op and post-op sinuses on the right side.

According to a *t*-test, the right-to-left differences were revealed between the pre-op and post-op sinuses at a 10% level of significance, where the post-op ones exhibited greater asymmetry than the pre-op ones (t = 1.868, P-value = 0.069). When the canine groups were considered, the median R-L differences for post-op sinuses were larger than for the pre-op sinuses, but none of the tests returned as statistically significant.

When performed on age-controlled residuals, however, no asymmetry was revealed for any of the comparisons.

Discussion
Our study has confirmed that the 3D CBCT reconstruction with the special program ENDO based on three planes, i.e. the horizontal plane (A-B), the midsagittal plane, and the coronal plane going through (vector A-B), allowed us to produce precise 3D images which were reproducible in time for linear or volumetric measurements. These results were important for orthodontic and maxillofacial plans of therapy. Real 3D measurements only in three planes explain methodologic diversity and possible different complexity levels of the subjects between the studies in the Eslami systematic review (Eslami et al., 2017) and can help us in the decision-making process.

All our measurements, except for the crown width, correlated positively with age (R ranging from 0.2 to 0.46). Logically, the strongest relationship was shown for the A-B distance. A-B line as well as the tooth length also showed positive relationship with the duration of treatment (R ranging from 0.22 to 0.42). This was to be expected as all patients were subadults at the beginning of the study and these increments in craniofacial measurements reflect growth changes. We also witnessed the differences between measurements before and after treatment as a result of the age-related growth. For the maxillary sinus, however, the opposite trend was present for the post-op sinuses with impacted canines once the age-dependency was controlled. This suggests that the impaction affected the size of the maxillary sinus.

As stated above, the process of resorption teeth can be difficult to diagnose with conventional two-dimensional (2D) dental radiographs, especially if the canine is located in the direct palatal or buccal position relative to the roots of adjacent teeth

(Celikoglu et al., 2010). CBCT provided improved detection rates (63%) of root resorption associated with impacted canines. The measurements using "Three-Dimensional Leeds Orthodontic Root Resorption Target Scale" can evaluate the subjective nature of CBCT images (Ericson and Kurol, 1988). Resorption of incisors alongside ectopic maxillary canines have been studied with computed tomography (CT). The vast majority (93%) of ectopic canines were found to be in contact with the roots of the adjacent lateral incisor and a significant number (19%) were in contact with the central incisor. In contrast, only 49% of normally positioned canines contacted the lateral incisor. Almost half (48%) of ectopically erupting maxillary canines had resorption of the maxillary incisors, with 38% and 9% found on the lateral and central incisors, respectively (Ericson and Kurol, 2000). More recent studies using CBCT similarly found that impacted maxillary canines had some degree of resorption on the incisors with 62% and 10% of these found on the lateral and central incisors respectively (Aktuna Belgin et al., 2019).

Our statistic measurements based on the specific 3D software program ENDO which compare all 3 planes: the horizontal plane (points A-B); the midsagittal plane; the coronal plane going through the canine cusp tip (C point) showed metric differences between measurements of normal and impacted teeth, and pre-op and post-op images were significant in canine position expressed in terms of vector A-B distance.

Of the four paranasal sinuses, the maxillary sinus is known to be the largest and the first to develop (Emirzeoglu et al., 2007). An interesting fact is that its shape and size have no significant effect on the low, high, and normal face growth groups (Ericson and Kurol, 2000). These results are especially important for maxillofacial surgery planning. The results by Aktuna Belgin et al. (2019) showed that the volume of the maxillary sinus decreased with increasing age. It was also found that the sinus volume was statistically significantly higher in males than in females in the age group of 18–24 years (Walker et al., 2005).

Our study has confirmed that there was no statistically significant difference in volume between the right and left maxillary sinus and that the maxillary sinus volume in males was significantly higher than that of females (Jawad et al., 2016; Okşayan et al., 2017). According to a t-test, the post-op sinuses exhibited greater asymmetry than the pre-op ones.

Conclusion
The role of 3D CBCT in detecting impacted canines and their movement during the prospective study is the basis of orthodontic therapy. Changes of shape, size, and position of impacted canines in 3D image before and after therapy were very precise and reproducible using 3D reconstruction and program ENDO (InVivo Dental Anatomage) in all three planes – horizontal, midsagittal and coronal.

The influence of 3D orthodontic therapy parameters on treatment options are the following:

The linear measurements showed metric differences between the measurements of normal and impacted teeth as well as between pre-op and post-op images. All measurements, except for the crown width, correlated positively with age. The A-B line as well as the tooth length also showed positive relationships with the duration of treatment. Healthy and impacted canines were distributed evenly on the right and left sides, showing thus no prevalence of the body side.

In our prospective study, monitoring the healing process quality based on the shape and size of sinus maxillae volume and also on impacted and non-impacted canines had no direct influence on face growth, but was important for 3D surgery treatment plan.

References

Aktuna Belgin, C., Colak, M., Adiguzel, O., Akkus, Z., Orhan, K. (2019) Three-dimensional evaluation of maxillary sinus volume in different age and sex groups using CBCT. *Eur. Arch. Otorhinolaryngol.* **276(5)**, 1493–1499.

Alqerban, A., Willems, G., Bernaerts, C., Vangastel, J., Politis, C., Jacobs, R. (2014) Orthodontic treatment planning for impacted maxillary canines using conventional records versus 3D CBCT. *Eur. J. Orthod.* **36(6)**, 698–707.

Becker, A., Chaushu, S. (2015) Etiology of maxillary canine impaction: a review. *Am. J. Orthod. Dentofacial Orthop.* **148(4)**, 557–567.

Celikoglu, M., Kamak, H., Oktay, H. (2010) Investigation of transmigrated and impacted maxillary and mandibular canine teeth in an orthodontic patient population. *J. Oral Maxillofac. Surg.* **68(5)**, 1001–1006.

da Silva Santos, L. M., Bastos, L. C., Oliveira-Santos, C., da Silva, S. J., Neves, F. S., Campos, P. S. (2014) Cone-beam computed tomography findings of impacted upper canines. *Imaging Sci. Dent.* **44(4)**, 287–292.

Eliasova, H., Dostalova, T., Prochazka, A., Sediva, E., Horacek, M., Urbanova, P., Hlinakova, P. (2021) Comparison of 2D OPG image versus orthopantomogram from 3D CBCT from the forensic point of view. *Leg. Med. (Tokyo)* **48**, 101802.

Emirzeoglu, M., Sahin, B., Bilgic, S., Celebi, M., Uzun, A. (2007) Volumetric evaluation of the paranasal sinuses in normal subjects using computer tomography images: A stereological study. *Auris Nasus Larynx* **34(2)**, 191–195.

Ericson, S., Kurol, J. (1988) Resorption of maxillary lateral incisors caused by ectopic eruption of the canines. A clinical and radiographic analysis of predisposing factors. *Am. J. Orthod. Dentofacial Orthop.* **94(6)**, 503–513.

Ericson, S., Kurol, P. J. (2000) Resorption of incisors after ectopic eruption of maxillary canines: a CT study. *Angle Orthod.* **70(6)**, 415–423.

Eslami, E., Barkhordar, H., Abramovitch, K., Kim, J., Masoud, M. I. (2017) Cone-beam computed tomography vs conventional radiography in visualization of maxillary impacted-canine localization: A systematic review of comparative studies. *Am. J. Orthod. Dentofacial Orthop.* **151(2)**, 248–258.

Grisar, K., Piccart, F., Al-Rimawi, A. S., Basso, I., Politis, C., Jacobs, R. (2019) Three-dimensional position of impacted maxillary canines: Prevalence, associated pathology and introduction to a new classification system. *Clin. Exp. Dent. Res.* **5(1)**, 19–25.

Jawad, Z., Carmichael, F., Houghton, N., Bates, C. (2016) A review of cone beam computed tomography for the diagnosis of root resorption associated with impacted canines, introducing an innovative root resorption scale. *Oral Surg. Oral Med. Oral Pathol. Oral Radiol.* **122(6)**, 765–771.

Lövgren, M. L., Dahl, O., Uribe, P., Ransjö, M., Westerlund, A. (2019) Prevalence of impacted maxillary canines – An epidemiological study in a region with systematically implemented interceptive treatment. *Eur. J. Orthod.* **41(5)**, 454–459.

Mazurová, K., Dubovská, I., Fudalej, P. (2015) Retence špičáků (Impacted canines). *Prakt. Zub. Lék.* **63(3)**, 34–37. (in Czech)

Okşayan, R., Sökücü, O., Yeşildal, S. (2017) Evaluation of maxillary sinus volume and dimensions in different vertical face growth patterns: A study of cone-beam computed tomography. *Acta Odontol. Scand.* **75(5)**, 345–349.

Oz, A. Z., Oz, A. A., El, H., Palomo, J. M. (2017) Maxillary sinus volume in patients with impacted canines. *Angle Orthod.* **87(1)**, 25–32.

Schubert, M., Baumert, U. (2009) Alignment of impacted maxillary canines: Critical analysis of eruption path and treatment time. *J. Orofac. Orthop.* **70(3)**, 200–212.

Servais, J. A., Gaalaas, L., Lunos, S., Beiraghi, S., Larson, B. E., Leon-Salazar, V. (2018) Alternative cone-beam computed tomography method for the analysis of bone density around impacted maxillary canines. *Am. J. Orthod. Dentofacial Orthop.* **154(3)**, 442–449.

Tassoker, M., Magat, G., Lale, B., Gulec, M., Ozcan, S., Orhan, K. (2020) Is the maxillary sinus volume affected by concha bullosa, nasal septal deviation, and impacted teeth? A CBCT study. *Eur. Arch. Otorhinolaryngol.* **277(1)**, 227–233.

Walker, L., Enciso, R., Mah, J. (2005) Three-dimensional localization of maxillary canines with cone-beam computed tomography. *Am. J. Orthod. Dentofacial Orthop.* **128(4)**, 418–423.

Sperm DNA Fragmentation Index in Abortion or *in Vitro* Fertilization Failure in Presence of Normal Semen Analysis

Hamed Akhavizadegan[1], Nazila Yamini[2], Amir Masoud Musavi[3], Maryam Moradi[2], Farnaz Khatami[3]

[1]Department of Urology, Tehran University of Medical Sciences, Tehran, Iran;
[2]Arash Infertility Center, Tehran University of Medical Sciences, Tehran, Iran;
[3]School of Medicine, Tehran University of Medical Sciences, Tehran, Iran

Abstract: Role of male factor in recurrent abortion and *in vitro* fertilization failure has not been fully defined yet and there is much controversy about evaluating male patients with normal semen analysis. One of the factors that might help establish the male role is DNA fragmentation index. However, strong correlation between this factor and quality of semen, has caused many clinicians to believe that it does not help in abortion and implantation failure. We aim to assess this factor in our patients. In a prospective observational study, we assessed age, duration of infertility, undesired fertility related events (assisted reproductive techniques attempts and abortions), semen parameters and DNA fragmentation index in patients with multiple abortions or *in vitro* fertilization failures and analysed the results by statistical software SPSS version 24. DNA fragmentation index was remarkably correlated with age, duration of infertility and semen parameters. Among all groups in our study, patients with abnormal semen analysis had statistically significant higher level of DNA fragmentation. Ten percent of patients with normal or slightly abnormal semen analysis had abnormally high SDFI (sperm DNA fragmentation index). Checking DNA fragmentation index is recommended in all couples with fertilization problems even in the presence of normal semen analysis. It might be more reasonable to assess it in aged men, long duration of infertility or candidates with remarkable semen abnormality.

Mailing Address: Assoc. Prof. Hamed Akhavizadegan, MD., Department of Urology, Tehran University of Medical Sciences, Infertility Ward, Arash Women Hospital, Tehranpars, Baghdardnia Street, No. 115, 1653915981, Tehran, Iran; Phone: +98 912 533 53 22; Fax: +98 216 312 15 38; e-mail: h-akhavizadegan@tums.ac.ir

Introduction

Infertility is a common problem for both the urologists and gynecologists. Although its treatment has been revolutionized by assisted reproductive techniques (ART), recurrent spontaneous abortion (RSA) and recurrent implantation failure (RIF) are still mysterious problems which are difficult to treat (ESHRE Guideline Group on RPL et al., 2018).

Role of male factor which contributes to 50% of infertility cases has not been established completely in these two conditions. Since sperm DNA fragmentation index (SDFI) was introduced, it has been used as an adjuvant assessment in RSA and RIF; however, we still have a long way to provide a comprehensive guideline for how and when to use it (Shaulov et al., 2020).

In this study we are presenting our findings regarding SDFI in patients with assisted reproductive techniques failure and abortion.

Material and Methods

In an observational prospective study, the information of couples who were referred to our infertility center because of RIF or RSA and had been assessed by history, physical examination, semen analysis, sperm DNA fragmentation index and karyotype, were collected. Inclusion criteria were normal karyotype, absence of azoospermia and at least three events of abortion and *in vitro* fertilization failure, or their combinations.

The patients were educated how to provide a standard semen sample.

Sperm count and motility were assessed by computer assisted semen analysis (CASA) (St. Petersburg 190000, Russia) and all specimens were controlled and corrected by an experienced andrology laboratory technician according to WHO (World Health Organization) 2010 criteria. Morphology report was based on a prepared separate sample after staining.

Simultaneously another part of semen was used for SDFI which was evaluated by Sperm Chromatin Dispersion (SCD) test using Sperm DNA Fragmentation Assay (SDFA) kit (Dianzystazma.cat 02 Tehran, Iran).

The information was collected by an anonymous information sheet from patients' files and was analysed by SPSS version 24. Inform consent was obtained from patients to use their information anonymously and the project was approved in Ethics Committee of Tehran University of Medical Sciences.

Results

During years 2017 to 2020, 172 couples were referred to our Andrology Clinic in order to be assessed for different combinations of infertility, ART failure and abortion.

Mean age of male candidate was 37.19 ± 6.5134 (minimum 23 and maximum 60). There was a positive relationship between age and SDFI (P-value = 0.035). Mean duration of infertility was 6.855 ± 5.0521 years with minimum of 12 months and

Table 1 – Number of patients and number of IVF failure or abortion

	1	2	3 and more	Total
IVF	13.37% (23)	16.86% (29)	22.09% (38)	(90)
Abortion	16.86% (29)	13.37% (23)	17.44% (30)	(82)
				100% (172)

IVF – *in vitro* fertilization

Table 2 – Mean of SDFI in patients related to cause and number of events

Number of events	1	2	3 or more	Average
IVF	25.95 ± 14.519	25.33 ± 13.924	28.79 ± 15.189	26.94
Abortion	22.41 ± 10.393	25.55 ± 16.772	22.68 ± 12.288	23.38

SDFI – sperm DNA fragmentation index; IVF – *in vitro* fertilization

maximum of 27 years. There was a strong positive correlation between duration of infertility and SDFI (P-value < 0.000).

Number and percentage of patients with *in vitro* fertilization (IVF) failure and abortion are demonstrated in Table 1.

There was not any meaningful relationship between SDFI and number of IVF failure or abortion. Mean of SDFI in separate groups are shown in Table 2.

Mean sperm count in this study was 21.32 ± 11.91 million/ml with maximum 56 and minimum 0.5 million per milliliter. 26.2% of patients had less than 15 million sperm/ml (oligospermia) and 73.8% of them had more than 15 million/ml (normozoospermia). There was a significant inverse relationship between SDFI and sperm count (P-value < 0.000).

Mean A + B motility in our patients was 28.13 ± 19.19% with minimum 0 and maximum 66%.

45.7% of patients had motility more than 32% (normal motility) and 55.3% of them had motility less than 32%. SDFI and motility had strong inverse relationship (P-value < 0.000).

Mean normal morphology was 3.25 ± 1.676 (minimum 0 and maximum 7%). 44.5% of patients had normal morphology less than 4% (teratospermia) and 55.5% of them had morphology more than 4%.

Morphology and SDFI had significant inverse relationship (P-value < 0.01).

Results of SDFI analysis in patients with normal or slightly abnormal semen analysis (47.7%) are shown in Table 3.

55 (32%) patients had normal semen analysis and 27 (15.7%) had abnormality only in one of three major factors of semen analysis (count, motility and morphology) which their SDFI levels are shown in Table 3.

Akhavizadegan H.; Yamini N.; Musavi A. M.; Moradi M.; Khatami F.

Table 3 – SDFI in normal or slightly abnormal semen analysis in patients with multiple IVF failures or abortions

SDFI	<25	25–30	>30	Total
Completely normal semen analysis	63.41% (52)	1.2% (1)	2.4% (2)	67.0% (55)
Semen analysis with only one major factor abnormality	25.60% (21)	3.6% (3)	3.6% (3)	32.8% (27)
				100% (82)

SDFI – sperm DNA fragmentation index; IVF – *in vitro* fertilization

Discussion

RSA defined as 3 or more abortions and RIF with three or more IVF cycles failure have prevalence of 1% and 10% in fertility clinic respectively (ESHRE Guideline Group on RPL et al., 2018). Unfortunately, semen analysis parameters cannot predict them and defining the role of male partner in RIF and RSA becomes much sophisticated (Shaulov et al., 2020). Possible influencing factors such as paternal age, semen oxidative level and the genetic material of sperm (karyotype, chromatin structure and SDFI) have been reviewed in several studies without consistent result (Tan et al., 2019).

The significant relationship between age and duration of infertility with SDFI in our study indicates that patients of older age and longer duration of infertility should be screened for abnormal SDFI and may predict more profound problem. In several studies in addition to this finding the age of 40-years was suggested as a cut-off of SDFI checking (Humm and Sakkas, 2013; Gunes et al., 2016; Pino et al., 2020). According to our study even in younger males with long duration of these problems checking SDFI can be helpful.

In several studies, SDFI has been inversely related to spermiogram major parameters. Many physicians therefore believe that in these cases, SDFI does not provide clinicians with more information than semen analysis (Wiweko and Utami, 2017; Santi et al., 2018; McQueen et al., 2019). According to our survey, the decreased count, motility and sperm normal morphology are associated with higher SDFI. However, our findings (Table 3) indicate that failure to check the SDFI in the presence of normal or near-normal semen analysis results in the loss of 10% of patients with abnormal SDFI.

There are conflicting opinions in literature about the relationship of SDFI with RSA and RIF. In our study, the average amount of SDFI was very close to normal cut-off in overall and only in 3 and more IVF failures were reported to be slightly higher. The normal mean SDFI in our patients and similar studies can be explained by the multifactorial nature of fertility (Cho et al., 2017; Petersen et al., 2018; Yifu et al., 2020). The conflicting results regarding the association between SDFI and the

mentioned fertility problems can result from the simultaneous contribution of male, female conditions and also the laboratory factors in these cases are undeniable.

Deciding on the value of SDFI in RSA and RIF is difficult because SDFI has a proven relationship with the spermiogram, and both are inextricably linked to these two situations. Most likely, at least half of this lack of connection is related to the female factor and unknown causes.

Limitations

One of the factors that cause inconsistency in literature might be technique-related hence SDFI in one semen can be reported differently by various methods. We included all males without considering female factor. Taking into account the female factor adds to the accuracy of the study.

Another limitation was the time delay between last failure and semen evaluation, because most of couple were referred to us and were not our patients. Most importantly our study was retrospective with its own drawbacks.

Conclusion

Until a link is found between SDFI and fertility undesired events (RIF and RSA), SDFI measurement is recommended in these cases, even in the presence of a normal spermiogram, although an abnormal result might be found only in paternal aging, prolonged infertility, obvious spermiogram abnormalities and only in 10% of patients with normal semen analysis.

References

Cho, C. L., Agarwal, A., Majzoub, A., Esteves, S. C. (2017) Future direction in sperm DNA fragmentation testing. *Transl. Androl. Urol.* **6**, S525–S526 (Suppl. 4).

ESHRE Guideline Group on RPL; Bender Atik, R., Christiansen, O. B., Elson, J., Kolte, A. M., Lewis, S., Middeldorp, S., Nelen, W., Peramo, B., Quenby, S., Vermeulen, N., Goddijn, M. (2018) ESHRE guideline: Recurrent pregnancy loss. *Hum. Reprod. Open* **2018(2)**, hoy004.

Gunes, S., Hekim, G. N., Arslan, M. A., Asci, R. (2016) Effects of aging on the male reproductive system. *J. Assist. Reprod. Genet.* **33(4)**, 441–454.

Humm, K. C., Sakkas, D. (2013) Role of increased male age in IVF and egg donation: Is sperm DNA fragmentation responsible? *Fertil. Steril.* **99(1)**, 30–36.

McQueen, D. B., Zhang, J., Robins, J. C. (2019) Sperm DNA fragmentation and recurrent pregnancy loss: A systematic review and meta-analysis. *Fertil. Steril.* **112(1)**, 54–60.e3.

Petersen, C. G., Mauri, A. L., Vagnini, L. D., Renzi, A., Petersen, B., Mattila, M., Comar, V., Ricci, J., Dieamant, F., Oliveira, J. B. A., Baruffi, R. L. R., Franco, J. G. Jr. (2018) The effects of male age on sperm DNA damage: An evaluation of 2,178 semen samples. *JBRA Assist. Reprod.* **22(4)**, 323–330.

Pino, V., Sanz, A., Valdés, N., Crosby, J., Mackenna, A. (2020) The effects of aging on semen parameters and sperm DNA fragmentation. *JBRA Assist. Reprod.* **24(1)**, 82–86.

Santi, D., Spaggiari, G., Simoni, M. (2018) Sperm DNA fragmentation index as a promising predictive tool for male infertility diagnosis and treatment management – meta-analyses. *Reprod. Biomed. Online* **37(3)**, 315–326.

Akhavizadegan H.; Yamini N.; Musavi A. M.; Moradi M.; Khatami F.

Shaulov, T., Sierra, S., Sylvestre, C. (2020) Recurrent implantation failure in IVF: A Canadian Fertility and Andrology Society Clinical Practice Guideline. *Reprod. Biomed. Online* **41(5)**, 819–833.

Tan, J., Taskin, O., Albert, A., Bedaiwy, M. A. (2019) Association between sperm DNA fragmentation and idiopathic recurrent pregnancy loss: A systematic review and meta-analysis. *Reprod. Biomed. Online* **38(6)**, 951–960.

Wiweko, B., Utami, P. (2017) Predictive value of sperm deoxyribonucleic acid (DNA) fragmentation index in male infertility. *Basic Clin. Androl.* **27**, 1.

Yifu, P., Lei, Y., Shaoming, L., Yujin, G., Xingwang, Z. (2020) Sperm DNA fragmentation index with unexplained recurrent spontaneous abortion: A systematic review and meta-analysis. *J. Gynecol. Obstet. Hum. Reprod.* **49**, 101740.

Side Effects of Antihypertensives Induced by Switching to Different Generic Medications: Case Reports

Apichai Wattanapisit[1,2], Penpun Lertwatanachai[1,2], Thittita Pongsawat[2], Sanhapan Wattanapisit[3], Jaruporn Thongruch[2]

[1]School of Medicine, Walailak University, Nakhon Si Thammarat, Thailand;
[2]Walailak University Hospital, Nakhon Si Thammarat, Thailand;
[3]Thasala Hospital, Nakhon Si Thammarat, Thailand

Abstract: Generic medication is a product that contains the same active substance and pharmaceutical characteristics as brand-name medications. Generic medications are cost-effective and comparable to brand-name medications in terms of clinical endpoints. However, the use of generic medications instead of brand-name medications is a debatable issue among patients and healthcare providers. Two patients with essential hypertension experienced side effects after switching to different generic antihypertensives (one generic medication to another generic medication). Adverse drug reactions, including, hypersensitivity, side effects, and intolerance, should be identified through present and past medical history and clinical characteristics. The adverse drug reactions in both patients were more likely to be side effects of the medications after switching to different generic antihypertensives produced by different companies (patient 1: enalapril and patient 2: amlodipine). The side effects were possibly caused by the different inactive ingredients or excipients. These two case reports emphasise the importance of monitoring adverse drug reactions throughout the course of treatment and communicating with patients prior to switching to a new generic medication.

Mailing Address: Apichai Wattanapisit, MD., School of Medicine, Walailak University, Floor 8, Building C, Walailak University Hospital, 222, Thaiburi, Thasala, Nakhon Si Thammarat, 80160, Thailand; Phone: +66 75 47 7401; Fax: +66 75 67 2807; e-mail: apichai.wa@wu.ac.th

Introduction

Generic medication is defined as a product that contains the same active substance (with a difference of ± 5%) and has the same pharmaceutical characteristics as brand-name counterparts and exhibits bioequivalence (with a difference of ± 20%) (Gallelli et al., 2016; Desai et al., 2019). A major benefit of generic medications is that they are usually much cheaper than corresponding brand-name medications. In a study that included more than 2.2 million matched pairs of patients in the USA, generic medications were comparable to brand-name medications in terms of clinical endpoints (Desai et al., 2019). Notably however, serious adverse drug reactions (ADRs) due to switching from brand-name medications to generic medications have been reported (Gallelli et al., 2016). The prescription and use of generic medications instead of brand-name medications is a debatable issue among patients and healthcare providers. Many healthcare providers are concerned about the efficacy and safety of generic medications produced by different companies. Herein we describe the cases of two patients with primary hypertension treated at a family medicine clinic who had non-severe side effects after switching to different generic hypertensive medications. The treatments were adjusted to resolve the side effects.

Case reports

Patient 1
Patient 1 was a 62-year-old man with a history of primary hypertension, dyslipidaemia, and benign prostate hyperplasia. His medications were amlodipine 10 mg daily, simvastatin 20 mg daily, and doxazosin 2 mg daily. In July 2020, enalapril 5 mg (a generic medication) was added due to uncontrolled blood pressure. He was diagnosed with rotator cuff syndrome and carpal tunnel syndrome in December 2020, and treated with meloxicam, tolperisone, and gabapentin.

In January 2021, his blood pressure was under control and other examinations were unremarkable. Ten days later he developed dysuria and was diagnosed with a urinary tract infection (UTI). The initial treatment for the UTI was oral ciprofloxacin for 7 days followed by intravenous ceftriaxone. Renal caliculi were subsequently diagnosed via ultrasonography.

Two days after the intravenous antibiotic he presented at the family medicine clinic due to a dry cough. He noted that the cough had developed since he took a "new medication". At the previous family medicine clinic visit, he had received 5 mg enalapril as a generic formulation produced by a different company. The cough developed prior to the treatment for the UTI.

The family physician advised him to discontinue enalapril and prescribed 50 mg oral losartan as a replacement. A follow-up appointment was scheduled for 3 weeks' time, to assess any side effects of the antihypertensive medication. The patient reported no abnormal symptoms after discontinuing the second generic enalapril.

Patient 2

Patient 2 was a 40-year-old woman with primary hypertension. Her blood pressure had reached the treatment goal via administration of amlodipine 5 mg daily (generic medication produced by company A), and it had been maintained at that level for almost 2 years (since December 2018). After a family medicine clinic visit in September 2020, she noticed that a new antihypertensive medication (5 mg amlodipine, product of company B) had been prescribed. The patient had experienced a cramp in her right arm. She decided to stop her current medication and bought her previous medication (5 mg amlodipine, product of company A) from a pharmacy. The cramp in her arm recovered. Thereafter, she continued with the medication bought from the pharmacy.

At the next visit in February 2021, she informed her physician about the change in medications and the side effect. The physician revealed that both medications were generic medications (5 mg amlodipine) from different companies. The patient discussed the suspected side effect with her physician. The physician did not confirm that the arm cramp was a side effect of the medication and reassured the patient that she could take the currently prescribed amlodipine (product of company B). The physician also advised the patient to discontinue the medication if there were any abnormal symptoms or evidence of ADRs.

After that consultation, the patient tried the product from company B again. She again experienced a cramp in her right arm and stopped the medication as the suggestion of her physician. She resumed taking her initial form of amlodipine (product of company A), and no recurrence of the arm cramp had been reported.

Discussion

The two above-described patients noticed side effects after switching to different generic antihypertensives. A term "side effect" is a subset of an umbrella term, "adverse drug reaction (ADR)" which is a harmful reaction to a drug. The three main types of ADRs are allergy or hypersensitivity (immunological mechanism), side effects (pharmacological mechanism), and intolerance or sensitivity (pharmacological mechanism and susceptibility to a medication) (Smith, 2013). For example, enalapril can possibly cause various features of ADRs such as skin rash (allergy), dry cough (side effect), and hypotension (intolerance) (Smith, 2013). Another ADR classification system by World Health Organization (WHO) defines six types of reactions: type A (dose-related or "augmented"), type B (non-dose-related or "bizarre"), type C (dose-related and time-related or "chronic"), type D (time-related or "delayed"), type E (withdrawal or "end of use"), and type F (unexpected failure of therapy or "failure") (Edwards and Aronson, 2000).

In the current cases, the side effects were reported after switching one generic medication (patient 1: enalapril and patient 2: amlodipine) to another generic medication. These two cases raise a question as to why the patients experienced the

ADRs after the long-term use of medications. Type 4 hypersensitivity (cell mediated or delayed type), of which rash, angioedema, and anaphylaxis are common clinical features, should be differentiated. However, the ADRs described in both patients were more likely to be side effects of the medications than allergic reactions. Dry cough is a common side effect of enalapril, whereas muscle cramp is a less common side effect of amlodipine (Gibson, 1989; Yajnik et al., 1995). The ADRs in these two cases were defined as type A (dose-related or "augmented") according to the WHO classification, which related to the pharmacological actions of the drugs and predictable (Edwards and Aronson, 2000).

With respect to why the side effects occurred, one possible reason is that the two different generic medications produced by different companies contained some different ingredients. Oral forms of medication generally contain both active pharmaceutical ingredients and a mixture of inactive ingredients called excipients (Reker et al., 2019). Excipients are combined with the active pharmaceutical ingredient to control drug stability, preservation, tonicity, and delivery (Ionova and Wilson, 2020). Different excipients can cause a variety of ADRs via different mechanisms (Ionova and Wilson, 2020; Pottel et al., 2020). The side effects in the two current patients were possibly caused by the different excipients in the medications produced by different companies.

Medication side effects are a factor associated with poor treatment adherence in patients with chronic illnesses (Lemay et al., 2018). Managing side effects of medications in patients with chronic medical conditions is a challenge among primary care physicians (Sellappans et al., 2015). Within primary care settings, a recent systematic review and meta-analysis reported that the prevalence of ADRs was 8.32% (7.82–8.83%), and nearly a quarter (22.96%; 7.82–38.09%) of those ADRs were preventable (Insani et al., 2021).

Conclusion
The above-described case reports emphasise some lessons for physicians and healthcare providers. One is that ADRs associated with medications for chronic conditions should be monitored throughout the course of treatment. Another is that classifying ADRs into specific mechanisms (allergy, side effect, and intolerance) can help to identify the associated causes, which may be either active pharmaceutical ingredients or inactive ingredients (excipients). Lastly, there is a need to communicate with patients prior to switching to a new generic medication because its excipients may cause ADRs.

References
Desai, R. J., Sarpatwari, A., Dejene, S., Khan, N. F., Lii, J., Rogers, J. R., Dutcher, S. K., Raofi, S., Bohn, J., Connolly, J. G., Fischer, M. A., Kesselheim, A. S., Gagne, J. J. (2019) Comparative effectiveness of generic and brand-name medication use: A database study of US health insurance claims. *PLoS Med.* **16(3)**, e1002763.

Edwards, I. R., Aronson, J. K. (2000) Adverse drug reactions: Definitions, diagnosis, and management. *Lancet* **356(9237)**, 1255–1259.

Gallelli, L., Gallelli, G., Codamo, G., Argentieri, A., Michniewicz, A., Siniscalchi, A., Stefanelli, R., Cione, E., Caroleo, M. C., Longo, P., De Sarro, G. (2016) Recognizing severe adverse drug reactions: Two case reports after switching therapies to the same generic company. *Curr. Drug Saf.* **11(1)**, 104–108.

Gibson, G. R. (1989) Enalapril-induced cough. *Arch. Intern. Med.* **149(12)**, 2701–2703.

Insani, W. N., Whittlesea, C., Alwafi, H., Man, K. K. C., Chapman, S., Wei, L. (2021) Prevalence of adverse drug reactions in the primary care setting: A systematic review and meta-analysis. *PLoS One* **16(5)**, e0252161.

Ionova, Y., Wilson, L. (2020) Biologic excipients: Importance of clinical awareness of inactive ingredients. *PLoS One* **15(6)**, e0235076.

Lemay, J., Waheedi, M., Al-Sharqawi, S., Bayoud, T. (2018) Medication adherence in chronic illness: Do beliefs about medications play a role? *Patient Prefer. Adherence* **12**, 1687–1698.

Pottel, J., Armstrong, D., Zou, L., Fekete, A., Huang, X.-P., Torosyan, H., Bednarczyk, D., Whitebread, S., Bhhatarai, B., Liang, G., Jin, H., Ghaemi, S. N., Slocum, S., Lukacs, K. V., Irwin, J. J., Berg, E. L., Giacomini, K. M., Roth, B. L., Shoichet, B. K., Urban, L. (2020) The activities of drug inactive ingredients on biological targets. *Science* **369(6502)**, 403–413.

Reker, D., Blum, S. M., Steiger, C., Anger, K. E., Sommer, J. M., Fanikos, J., Traverso, G. (2019) "Inactive" ingredients in oral medications. *Sci. Transl. Med.* **11(483)**, eaau6753.

Sellappans, R., Lai, P. S., Ng, C. J. (2015) Challenges faced by primary care physicians when prescribing for patients with chronic diseases in a teaching hospital in Malaysia: A qualitative study. *BMJ Open* **5(8)**, e007817.

Smith, W. (2013) Adverse drug reactions – Allergy? Side-effect? Intolerance? *Aust. Fam. Physician* **42(1–2)**, 12–16.

Yajnik, V. H., Vatsaraj, D. J., Acharya, H. K., Yajnik, N. V. (1995) Evaluation of amlodipine in mild to moderate hypertension – A clinical report. *J. Assoc. Physicians India* **43(1)**, 34–35.

Torsion of the Falciform Ligament Diagnosed by Imaging Tests – Case Report of an Unusual Disease

Bruna Suda Rodrigues[1], Daniela Osti Bortolozzo[2], Maura Harumi Ito[1], Thaís Nogueira Dantas Gastaldi[3], Márcio Luís Duarte[4,5], Élcio Roberto Duarte[1]

[1]Department of Ultrasonography, Irmandade da Santa Casa de Misericórdia de Santos, Santos (SP), Brazil;

[2]Department of Internal Medicine, Hospital Frei Galvão, Santos (SP), Brazil;

[3]Department of Radiology, Ápice Telerradiologia, São José do Rio Preto (SP), Brazil;

[4]Universidade de Ribeirão Preto – Campus Guarujá, Guarujá (SP), Brazil;

[5]Department of Radiology, Centro Radiológico e Especialidades Médicas São Gabriel, Praia Grande (SP), Brazil

Abstract: The falciform ligament is a peritoneal double layer that anatomically divides the right and left hepatic lobes. Abnormality of the falciform ligament is rare – less than 20 cases of torsion of the falciform ligament have been reported to date in adults. The pathophysiology of these entities is similar to intra-abdominal focal fat infarction. The clinical of the patient with torsion of the falciform ligament is abdominal pain of sudden onset and focal location. Laboratory tests can lead to diagnostic confusion with cholecystitis. Ultrasonography is usually the initial evaluation test, but the gold standard diagnosis is computed tomography. We report the case of a 30-year-old female patient reporting sudden abdominal pain that radiates to the dorsal region associated with nausea and vomiting diagnosed with torsion of the falciform ligament with ultrasonography and confirmed with computed tomography. She was treated conservatively without the need for surgical treatment, being discharged after one week hospitalization.

Mailing Address: Dr. Márcio Luís Duarte, Centro Radiológico e Especialidades Médicas São Gabriel – Radiology Department, Rua Mihailo Lukich Michel, 94, Boqueirão, Praia Grande (SP), 11701-370, Brazil; Phone: (13) 33 57 45 00; e-mail: marcioluisduarte@gmail.com

Introduction

The falciform ligament is a peritoneal double layer that anatomically divides the right and left hepatic lobes (Uyttenhove et al., 2013; Indiran et al., 2018). Structurally, it extends from the upper border of the liver to the lower border of the diaphragm surrounded by a considerable amount of extraperitoneal fat (O'Connor et al., 2022).

Abnormality of the falciform ligament is rare. Less than 20 cases of torsion of the falciform ligament have been reported to date in adults (Indiran et al., 2018). Other recognized abnormalities of the falciform ligament include:

- Ligament cysts
- Tumours
- Abnormal vascularity due to portal hypertension
- Iatrogenic internal hernia through the ligament
- Gangrene related to necrotizing pancreatitis along with twisting of a fatty appendage.

Herein, we report the case of a 30-year-old female patient reporting sudden abdominal pain that radiates to the dorsal region associated with nausea and vomiting.

Case report

A 30-year-old female with pain that radiates to the back with vomiting for one day. She denies fever and reports an episode of diarrhea. She reports having had a cesarean section three months ago and is breastfeeding. On physical examination, she has a distended, flaccid, and painful abdomen on palpation in the upper hemiabdomen, with negative Giordano, Murphy, and sudden decompression tests. She denies other illnesses and the use of medications.
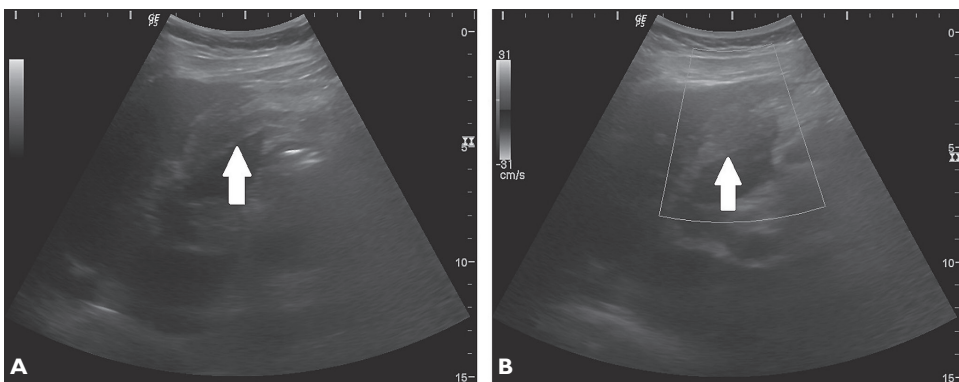
Figure 1 – Ultrasonography demonstrated a heterogeneous image, predominantly echogenic, elongated in A, without vascularization on the Doppler study between hepatic segments IV and II/III in B, compatible with torsion of the falciform ligament (white arrow).
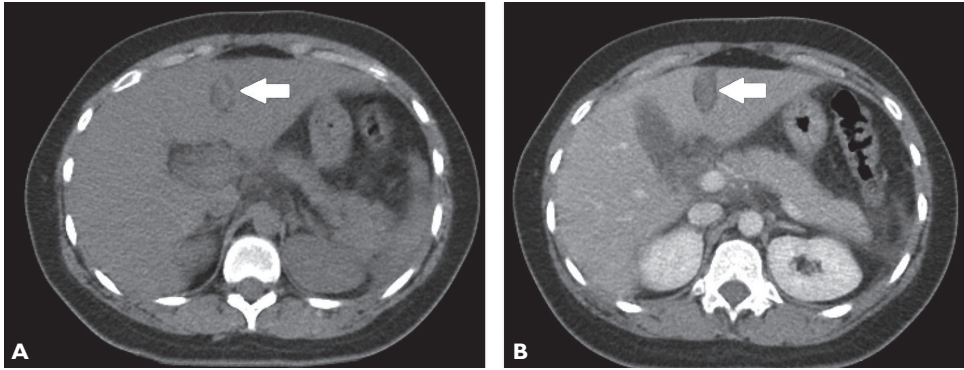
Figure 2 – Axial section of computed tomography scan without contrast in A and with contrast in the portal phase in B shows border sign and fatty mass along the falciform ligament, without contrast enhancement, compatible with torsion of the falciform ligament (white arrow).

The hemogram demonstrates leukocytosis ($29,930/mm^3$) with a shift to the left (myelocytes $299/mm^3$ and metamyelocytes $599/mm^3$). An increase in CRP (C-reactive protein) (62.08 mg/l) is also observed. Abdominal radiography is normal. Ultrasonography demonstrates a heterogeneous image, predominantly echogenic, elongated, and without vascularization in the Doppler study between hepatic segments IV and II/III, which may correspond to torsion of the falciform ligament (Figure 1). Computed tomography followed, which confirmed the ultrasound finding (Figure 2).

The patient was treated with dipyrone (1 gram every 6 hours) and ondansetron (8 mg every 12 hours) during a one-week hospitalization, without the need for surgical treatment, being discharged without symptoms and medication at home.

Discussion

The pathophysiology of these entities is similar to intra-abdominal focal fat infarction, and it can occur in several anatomical regions such as the greater omentum, epiploic appendix, and fatty appendix of the falciform ligament (O'Connor et al., 2022). The clinical of the patient with torsion of the falciform ligament is abdominal pain of sudden onset and focal location. Laboratory tests can lead to diagnostic confusion with cholecystitis. Differential diagnoses consist of ligament cysts, tumours, hernias, and acute necrohemorrhagic pancreatitis (O'Connor et al., 2022).

Therefore, due to their epigastric location and similar pain associated with non-specific laboratory tests, they can be mistakenly confused with other gastroduodenal pathologies, cholecystitis, and acute pancreatitis (Uyttenhove et al., 2013; Indiran et al., 2018; Horak et al., 2019; O'Connor et al., 2022). Thus, a thorough investigation through exams, especially imaging tests as ultrasound and computed tomography, is necessary for early and accurate diagnosis (Uyttenhove et al., 2013).

Ultrasonography, which is usually the initial evaluation test due to its low cost, demonstrates a hyperechoic, oval, non-compressible image, surrounded by a peripheral hypoechoic halo, located in the region of greatest pain intensity. This finding makes the diagnosis suspect but does not differentiate the different etiologies, usually requiring a more detailed imaging exam (Maccallum et al., 2015; Bangeas et al., 2020; O'Connor et al., 2022).

The gold standard diagnosis is performed by computed tomography as in the case described. Computed tomography demonstrates the border sign with inflammatory tissue around the falciform planes and an image of a fatty appearance along the falciform ligament, without contrast enhancement, consistent with torsion of the falciform ligament (Maccallum et al., 2015; Bangeas et al., 2020; O'Connor et al., 2022).

It is necessary to integrate the anomalies of the falciform ligament, from the subtle characteristics that can be clinically expressed, to the performance of imaging tests – ultrasound and/or computed tomography. The faster the diagnosis is made, the more feasible it is to treat the patient conservatively with analgesics and rest, as in the case described. However, there is the possibility of laparotomy or exploratory laparoscopy in more severe cases of pain that is refractory to conservative treatment or whose pain returns intensely after a few hours of improvement (Maccallum et al., 2015; Horak et al., 2019; Bangeas et al., 2020).

Conclusion

Torsion of the falciform ligament is a diagnosis that, although rare, should be listed among the differential diagnoses of abdominal pain. Its diagnosis is treacherous since its symptoms and changes in laboratory tests are similar to those of cholecystitis and pancreatitis, which are diseases with a much higher incidence. Thus, imaging tests are essential in analysing their differential diagnoses and the torsion of the falciform ligament itself.

References

Bangeas, P., Bitzika, S., Loufopoulos, P., Drevelegkas, K., Papadopoulos, V. N. (2020) Infarcted ligamentum teres hepatis lipoma mimicking acute abdomen in a female patient: A case report and mini-review of the literature. *J. Surg. Case Rep*. **2020(10)**, rjaa391.

Horak, R. D., Mega, J. D., Tanton, P. J., Criman, E. T., Tabak, B. D., Rooks, V. J. (2019) Fatty-falciform ligament appendage torsion (F-FLAT): Diagnosis and management in a pediatric patient. *Radiol. Case Rep*. **15(3)**, 181–185.

Indiran, V., Dixit, R., Maduraimuthu, P. (2018) Unusual cause of epigastric pain: Intra-abdominal focal fat infarction involving appendage of falciform ligament – Case report and review of literature. *GE Port. J. Gastroenterol*. **25(4)**, 179–183.

Maccallum, C., Eaton, S., Chubb, D., Franzi, S. (2015) Torsion of fatty appendage of falciform ligament: Acute abdomen in a child. *Case Rep. Radiol*. **2015**, 293491.

O'Connor, A., Sabri, S., Solkar, M., Ramzan, A., Solkar, M. (2022) Falciform ligament torsion as a rare aetiology of the acute abdomen. *J. Surg. Case Rep*. **2022(1)**, rjab150.

Uyttenhove, F., Leroy, C., Nzamushe Lepan Mabla, J. R., Ernst, O. (2013) Torsion of a fatty fringe of the falciform ligament, a rare cause of right hypochondrial pain. *Diagn. Interv. Imaging* **94(6)**, 637–639.

Cord Herniation through the Site of Undiagnosed Thoracic Dermoid Tumour during Spinal Anaesthesia; Report of a Case and Describing Ways to Avoid

Mansour Parvaresh, Eshagh Bahrami, Sayedali Ahmadi, Arash Fattahi, Ali Farid

Department of Neurosurgery, Faculty of Medicine, Iran University of Medical Sciences, Tehran, Iran

Abstract: Spinal anaesthesia (SA) is one of the most prevalent types of anaesthetic procedures. There are very few reports of cord herniation through the site of spinal canal stenosis due to tumour. A 33-year-old female presented with acute paraparesis after spinal anaesthesia for caesarean section. Magnetic resonance imaging (MRI) revealed an intradural mass from posterior of T6 to T8-T9 interface. We operated the patient and after laminectomy of T6 to T9, dermoid tumour containing hairs was totally resected and cord was completely decompressed. After 6 months, the patient is without any neurological deficit. Puncturing the dura with cerebrospinal fluid (CSF) in the presence of an extramedullary mass could cause cord herniation through the blockade. In these cases, awareness about related signs even in absence of symptoms or complaints could help us to prevent post-SA neurological deficit.

Mailing Address: Dr. Arash Fattahi, Department of Neurosurgery, Faculty of Medicine, Iran University of Medical Sciences, Next to Milad Tower, Hemmat Highway, 1461886465, Tehran, Iran; Phone: +989 120 360 034; e-mail: fatahi.a@iums.ac.ir

Introduction

Spinal anaesthesia (SA), so called spinal block, is one of the most prevalent types of anaesthetic procedures, sometimes being superior to the general anaesthesia (Yüksek et al., 2020). In several comparable studies, SA had some superiority to the general anaesthesia (GA) in safety and in possible procedure-related complications (Visser et al., 2009; Mortazavi et al., 2022). Because of prevalent usage of this technique, knowing possible complications and pitfalls are crucial. In the literature, there are many reports of neurological deficits after SA and all of them discussed etiologies, direct toxic effect of injected drug to the spinal column, compressive hematoma in site of puncture, etc. (Nicholson and Eversole, 1946). However, very few reports of cord herniation through the site of spinal canal stenosis due to tumour could be found (Doh et al., 2001; Krishnan and Roychowdhury, 2013). Considering etiologies of these complications, it is important to know what pre-procedural data and exams could be helpful to prevent them.

Here, we present a rare case of thoracic spine dermoid cyst without any previous alarming symptoms that after SA, caused significant neurological deficits.

Case report

A 33-year-old female presented with acute paraparesis after spinal anaesthesia for caesarean section (C/S) without any previous complaints or problems, in October 2021. The patient was a primipara and because of obstetric problems she underwent C/S one week ago. She was unable to walk alone. She had also some degree of sphincter disturbance as difficulty in urination and constipation concomitant with distal paraesthesia of lower limbs. On neurological examination, she had symmetrical proximal and distal weakness of both lower limbs, 3 from 5 based on muscle strength grading (Naqvi and Sherman, 2020). We found decreased sensation below umbilicus, based on pinprick test (two point discrimination). Sphincter tone was normal. Examination revealed bilateral hyperreflexia with positive Babinski sign. After diagnosis of paraparesis in previous center, for excluding complications related to site of the intervention (lumbar puncture – LP), the patient underwent an emergency lumbosacral magnetic resonance imaging (MRI) that was normal (Figure 1A). Then after performing thoracic imaging, it revealed an intradural mass from posterior of T6 to T8-T9 interface (Figure 1B–G).

We decided to operate the patient in prone position. During T6 to T9 laminectomy, we found a stalk was invaginated into T9 lamina and then a bundle could be seen from it to the midline skin at level of T10. The stalk was connected to a dural defect at T9 level (Figure 2A). After opening of the dura, we could see a large yellow intradural mass containing of hairs that compressed thoracic cord to the anterior and left side (Figure 2B and C). The mass was debulked internally and its thin capsule was resected, as much as possible, excepting the pial interface with cord due to adherence (Figure 2D). We found also some osseous elements in the mass. Finally, dura was sutured in watertight manner and tract to skin was completely
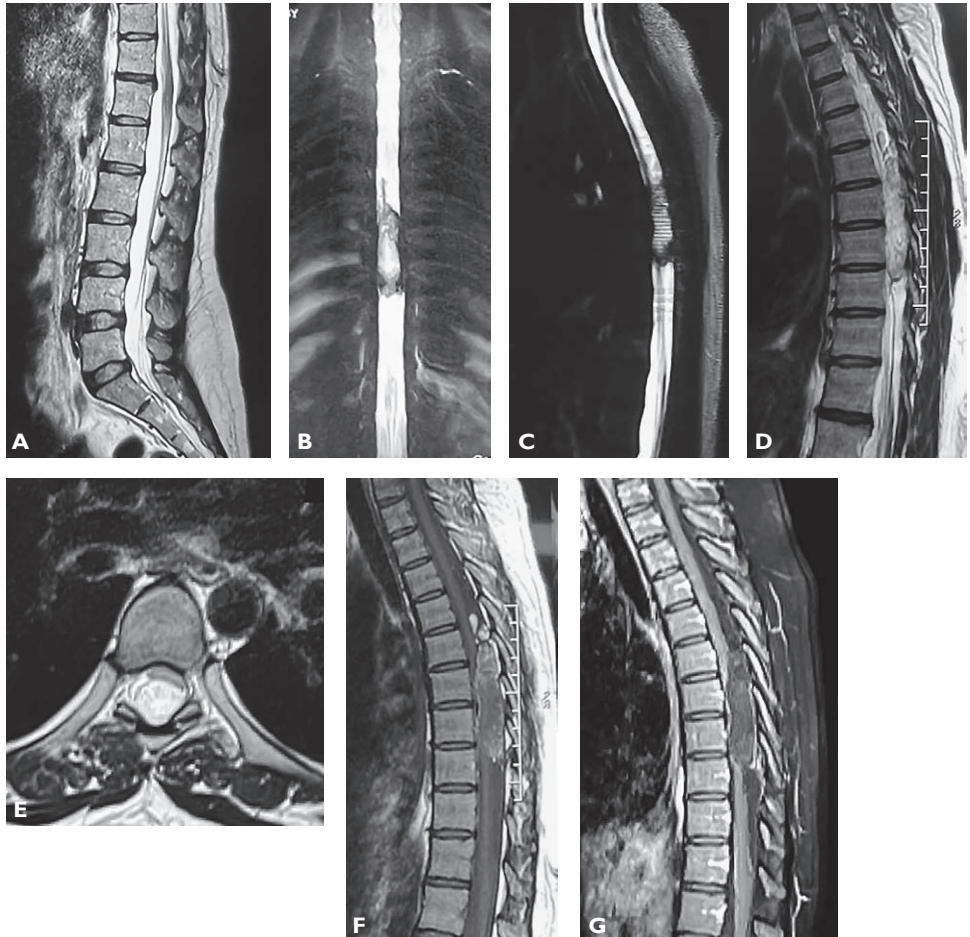
Figure 1 – Lumbosacral magnetic resonance imaging (MRI) (A) of patient showed no pathology but a complete cerebrospinal fluid (CSF) block can be seen in thoracic magnetic resonance myelogram (B, C). An hyperintense intradural extramedullary mass is present at T2, accompanied with severe cord compression and displacement (D, E). The lesion is also hypointense in T1 (F) with peripheral hyperintensity that after Gadolinium injection, is enhanced (G).

resected (Figure 2E). After 6 months, the patient is without any neurological deficit. Informed consent was obtained from the patient for this report.

Discussion
Throughout the literature, SA is safer and has less complications, in comparison with other anaesthetic options e.g., general anaesthesia (GA) (Yüksek et al., 2020). In spite this promising recommendations, occurrence of related neurological complications could be dangerous and knowing the ways to prevent them is crucial.
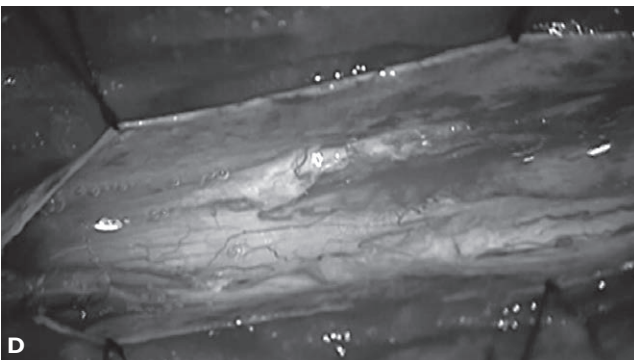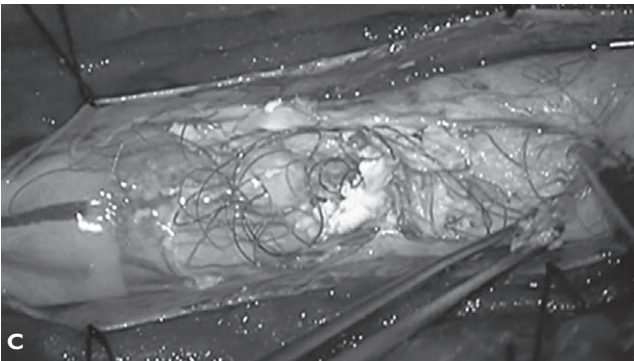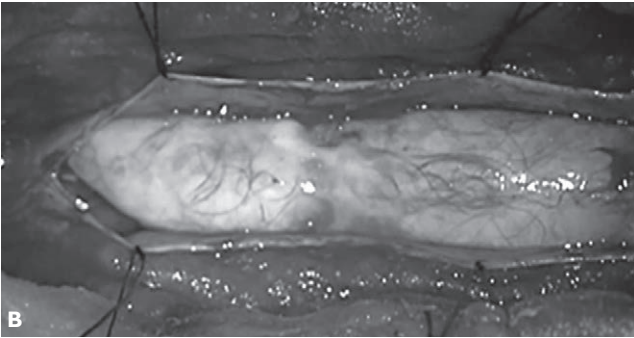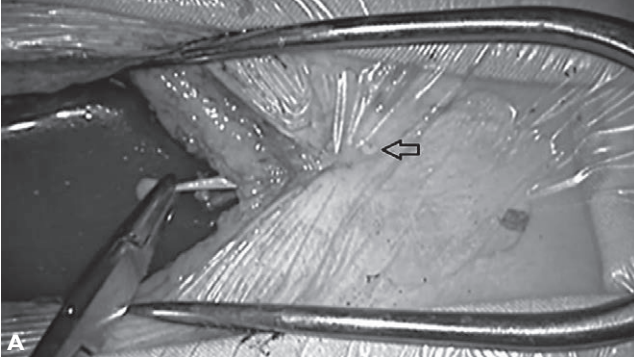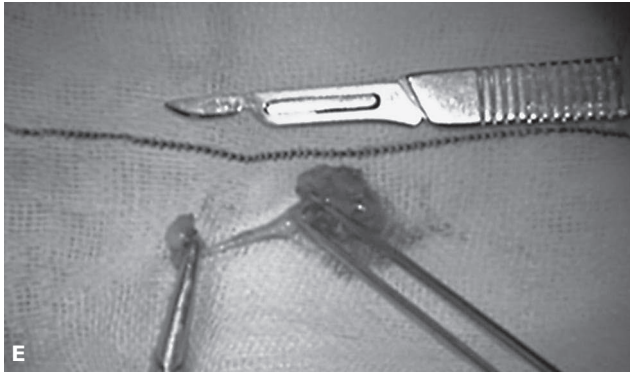
Figure 2 – Dermal sinus tract with its associated dimple is marked with arrow (A). After dural opening, we faced with a long, huge intradural mass with thin capsule containing fluid yellow matrix with hairs (B, C). The capsule was resected as much as possible (D) and finally, dermal sinus tract with its dimple were removed (E).

Some authors reported many neurological consequences after SA, with maximum prevalence of 1/1000; from post-dural puncture headache and drug related toxicity to cardiac arrest due to autonomic imbalance (Agarwal and Kishore, 2009). In general, the neurologic complications related to SA could be summarized to local intervention-site related (backache, hematoma, abscess, arachnoiditis, meningitis, etc.), direct neural elements injury (drug toxicity, autonomic cardiac arrest and direct cord tapping in cases of undiagnosed tethered cord) and cerebrospinal fluid (CSF) related (intracranial hypotension related headache, etc.) (Agarwal and Kishore, 2009; Kim et al., 2015).

Table 1 – Some clinical hints to avoid CNS herniation during SA

History taking and clinical presentation	Positive history for CNS disease (repeated meningitis, etc.); firstly, needs neurologist or neurosurgeon consultation	
	Positive familial history of midline CNS anomalies (dysraphism, etc.)	
	Presence of any neurological symptoms (cranial nerves palsies, paraparesis and other neurological deficits, severe ICP raising headache, disturbed vision, sphincter disturbance, etc.)	
Physical examination	Inspection	Search the midline from nasion to coccyx for dimple or any other surface anomalies; clues for dysraphism
	Examination	Presence of any neurological deficits; limbs and cranial nerves
		Presence of any neurological signs; altered DTRs, positive UMN signs (Hofmann's and Babinski's)
During SA	Reduce CSF volume taking as low as possible	
	In presence of acute paraparesis	Trendelenburg position must be considered
		Emergent neurologist or neurosurgeon consultation and imaging

CNS – central nervous system; SA – spinal anaesthesia; ICP – intracranial pressure; DTRs – deep tendon reflexes; UMN – upper motor neuron; CSF – cerebrospinal fluid

For the understanding of all possible neurologic consequences after SA, the CSF dynamic should be revealed. It is accepted that LP in concomitant with any intracranial mass could cause a lethal cerebral herniation through the foramen magnum (Su et al., 2002). Interestingly, this "sinking effect" after puncturing the dura accompanying CSF taking can develop in any location throughout the spinal canal, from foramen magnum to the sacrum (Doh et al., 2001; Krishnan and Roychowdhury, 2013; Mokri, 2013). Same as our case, dynamic of CSF circulation was changed and CSF circulated in two relatively separated compartments, above and below the canal stenosis due to the tumour. Now, tumour location resembles the foramen magnum and any puncturing of dura and taking CSF below the stenosis could cause intracanal hypotension below the stenosis and as a result, cord herniation through the tumour site and expected neurological deficits are inevitable.

Theoretically, any extramedullary lesions that cause stenosis and CSF block could represent the possible etiology for cord herniation during SA, especially if high amount of CSF is obtained; throughout the literature we can see very few cases in this subject (Doh et al., 2001; Krishnan and Roychowdhury, 2013). For intramedullary lesions, the mass must be as large as to completely block the circulation of CSF and put the spinal cord in close contact with spinal canal wall; that makes any vertical displacement of cord difficult and finally, dural puncture causes neurological deficit, as a result of pressure gradient between separated compartments above and below the stenosis after LP and resulting herniation of the cord through there. In fact, LP can deplete just the compartment below the stenosis. Some other possible causes could explain resulting neurological impairment after dural tap; emerged pressure differences in epidural venous plexus and possible new compression or swelling of the spinal cord adjacent to level of pathology, etc.

In general, such event is more common with concomitant large extramedullar mass (extradural or intradural), e.g., previously reported neurofibroma or large extruded cervical disc, than an expanded intramedullary mass (Doh et al., 2001; Krishnan and Roychowdhury, 2013). In some cases, when the hematoma is not causative and there is acute deficit after LP, we could put the patient in Trendelenburg position to relief herniation and if it is possible inject a sterile solution in the same amount as was taken CSF. In case of SA, this strategy is not appropriate because more prevalent causes of post procedural neurological deficits are other etiologies than cord herniation, this will not work or even be dangerous, e.g., in case of epidural hematoma (Nicholson and Eversole, 1946; Agarwal and Kishore, 2009).

A drawback in our case report is determining status of the neurological exam before SA that we do not know anything about that. Warning neurological status of the patient could possibly be helpful to prevent this complication. It is true that the patient had no complains or problems based on obtained history, but during the neurological exam it is possible to find some signs of involvement in central

nervous system (CNS); increases deep tendon reflexes (DTRs) and other upper motor neuron (UMN) signs, e.g., Hoffman's and Babinski signs even without any neurological deficits. Also in this case, if we were more accurate, we could see the dimple of the dermal sinus tract in midline of the skin over the spinal column that could be the alarming sign of a developing anomaly. As a result, anaesthesiologists has to be aware of signs and symptoms that revealed UMN disease such as compressing mass, hyperreflexia, positive Hoffmann's test and Babinski sign, history taking related to it, etc. It is possible these lesions, especially in developmental types or with insidious growth, do not have any symptoms even in presence of a large compressing mass. Table 1 explains some helpful hints to avoid possible complication during SA.

Conclusion

SA is safe and commonly used procedure for anaesthesia. Puncturing the dura associated with CSF taking and in presence of an extramedullary mass with significant compression of the cord could cause cord herniation through the blockade and resulting acute neurological deficits. In these cases, awareness about related manifestations even in absence of symptoms or complaints could help in preventing the post-SA neurological deficit.

References

Agarwal, A., Kishore, K. (2009) Complications and controversies of regional anaesthesia: a review. *Indian J. Anaesth.* **53(5)**, 543.

Doh, J. W., Hwang, S. C., Yun, S. M., Bae, H. G., Lee, K. S., Yun, I. G., Choi, S. K., Byun, B. J. (2001) Acute paraplegia following lumbar puncture in a patient with cervical disc herniation. *J. Korean Neurosurg. Soc.* **30(8)**, 1042–1046.

Kim, Y. Y., Song, J. W., Lim, J. H., Kim, Y. S., Kwon, Y. E., Lee, J. H. (2015) Nerve injury in an undiagnosed adult tethered cord syndrome patients following spinal anesthesia: A case report. *Anesth. Pain Med. (Seoul)* **10(3)**, 171–174.

Krishnan, P., Roychowdhury, S. (2013) Spinal coning after lumbar puncture in a patient with undiagnosed giant cervical neurofibroma. *Ann. Indian Acad. Neurol.* **16(3)**, 440.

Mokri, B. (2013) Spontaneous low pressure, low CSF volume headaches: Spontaneous CSF leaks. *Headache* **53(7)**, 1034–1053.

Mortazavi, M. M., Parish, M., Dorosti, A., Mohammadipour, H. (2022) Comparison of general anesthesia with spinal anesthesia on the quality of recovery of patients with selective abdominal hysterectomy in patients visiting the largest women's disease hospital in Northwestern Iran. *International Journal of Women's Health and Reproduction Sciences* **10(1)**, 25–30.

Naqvi, U., Sherman, A. I. (2020) Muscle strength grading. In: *StatPearls [Internet].* StatPearls Publishing, Treasure Island.

Nicholson, M. J., Eversole, U. H. (1946) Neurologic complications of spinal anesthesia. *J. Am. Med. Assoc.* **132(12)**, 679–685.

Su, T. M., Lan, C. M., Yang, L. C., Lee, T. C., Wang, K. W., Hung, K. S. (2002) Brain tumor presenting with fatal herniation following delivery under epidural anesthesia. *Anesthesiology* **96(2)**, 508–509.

Visser, W. A., Dijkstra, A., Albayrak, M., Gielen, M. J., Boersma, E., Vonsée, H. J. (2009) Spinal anesthesia for intrapartum Cesarean delivery following epidural labor analgesia: A retrospective cohort study. *Can. J. Anaesth.* **56(8)**, 577–583.

Yüksek, A., Miniksar, Ö. H., Honca, M., Öz, H. (2020) Incidence and causes of failed spinal anesthesia. *Dubai Med. J.* **3(2)**, 50–54.

Instructions to Authors

Prague Medical Report is an English multidisciplinary biomedical journal published quarterly by the First Faculty of Medicine of the Charles University. Prague Medical Report (Prague Med Rep) is indexed and abstracted by Index-medicus, MEDLINE, PubMed, EuroPub, CNKI, DOAJ, EBSCO, and Scopus.

Articles issued in the journal
a) Primary scientific studies on the medical topics (not exceeding 30 pages in standardized A4 format – i.e. 30 lines and 60–65 characters per line – including tables, graphs or illustrations)
b) Short communications
c) Case reports
d) Reviews
e) Lectures or discourses of great interest
f) Information about activities of the First Faculty of Medicine and other associated medical or biological organizations

Layout of the manuscript
a) Title of the study (brief and concise, without abbreviations)
b) Information about the author(s) in the following form:
   ■ first name and surname of the author(s) (without scientific titles)
   ■ institution(s) represented by the author(s)
   ■ full corresponding (mailing) author's reference address (including first name, surname and scientific titles, postal code, phone/fax number and e-mail)
c) Abstract (maximum 250 words)
d) Key words (4–6 terms)
e) Running title (reduced title of the article that will appear at the footer (page break), not more than 50 typewritten characters including spaces)
f) Introduction
   ■ The use of abbreviations should be restricted to SI symbols and those recommended by the IUPAC-IUB. Abbreviations should be defined in brackets on first appearance in the text. Standard units of measurements and chemical symbols of elements may be used without definition.
g) Material and Methods
h) Results
i) Discussion

j) Conclusion
k) References
- All the sources of relevant information for the study should be cited in the text (citations such as "personal communication" or "confidential data" are not accepted).
- It is not permitted to cite any abstract in the References list.
- References should be listed alphabetically at the end of the paper and typed double-spaced on separate pages. First and last page numbers must be given. Journal names should be abbreviated according to the Chemical Abstract Service Source Index. All co-authors should be listed in each reference (et al. cannot be used).
- Examples of the style to be used are:
   Yokoyama, K., Gachelin, G. (1991) An Abnormal signal transduction pathway in CD4–CD8– double-negative lymph node cells of MRL *lpr/lpr* mice. *Eur. J. Immunol.* **21**, 2987–2992.
   Loyd, D., Poole, R. K., Edwards, S. W. (1992) *The Cell Division Cycle. Temporal Organization and Control of Cellular Growth and Reproduction.* Academic Press, London.
   Teich, N. (1984) Taxonomy of retroviruses. In: *RNA Tumor Viruses,* eds. Weiss, R., Teich, N., Varmus, H., Coffin, J., pp. 25–207, Cold Spring Harbor Laboratory, Cold Spring Harbor, New York.
   References in the text should be cited as follows: two authors, Smith and Brown (1984) or (Smith and Brown, 1984); three or more authors, Smith et al. (1984) or (Smith et al., 1984). Reference to papers by the same author(s) in the same year should be distinguished in the text and in the reference list by lower-case letters, e.g. 1980a, or 1980a, b.
l) tables, figures, illustrations, graphs, diagrams, photographs, etc. (incl. legends)

Technical instructions
a) Manuscripts (in UK English only) must be delivered in the electronic form via Online Manuscript Submission and Tracking system (http://www.praguemedicalreport.org/). In case of problems, contact the Prague Medical Report Office (medical.report@lf1.cuni.cz). The online submission has to include the complete version of the article in PDF format, separately the manuscript as a MS Word file and a cover letter. The detailed version of the Instructions to Authors can be found at: http://www.praguemedicalreport.org/download/instructions_to_authors.pdf.
b) Text should be written in MS WORD only. We accept only documents that have been spell-checked with UK English as a default language.
c) Please, write your text in Times New Roman script, size 12, and line spacing 1.5.
d) Text should be justified to the left, with no paragraph indent (use Enter key only); do not centre any headings or subheadings.

e) Document must be paginated-numbered beginning with the title page.
f) Tables and graphs should represent extra files, and must be paginated too.
g) Edit tables in the following way: Make a plain text, indent by Tab (arrow key) all the data belonging to a line and finish the line by Enter key. For all the notes in table, use letter x, not *.
h) Make your graphs only in black-and-white. Deliver them in electronic form in TIFF or JPG format only.
i) Deliver illustrations and pictures (in black-and-white) in TIFF or JPG format only. The coloured print is possible and paid after agreement with the Prague Medical Report Office.
j) Mark all the pictures with numbers; corresponding legend(s) should be delivered in an extra file. Mark the position of every picture (photo) in the manuscript by the corresponding number, keep the order 1, 2, 3...

Authors' Declaration
The corresponding (or first author) of the manuscript must print, fill and sign by his/her own hand the Authors Declaration and fax it (or send by post) to the Prague Medical Report Office. Manuscript without this Declaration cannot be published. The Authors' Declaration can be found by visiting our web pages: http://pmr.lf1.cuni.cz or web pages of Prague Medical Report Online Manuscript Submission and Tracking system: http://www.praguemedicalreport.org/.

Editorial procedure
Each manuscript is evaluated by the editorial board and by a standard referee (at least two expert reviews are required). After the assessment the author is informed about the result. In the case the referee requires major revision of the manuscript, it will be sent back to the author to make the changes. The final version of the manuscript undergoes language revision and together with other manuscripts, it is processed for printing.
Concurrently, proofs are electronically sent (in PDF format) to the corresponding (mailing) author. Author is to make the proofs in PDF paper copy and deliver it back to the editorial office by fax or as a scanned file by e-mail. Everything should be done in the required time. Only corrections of serious errors, grammatical mistakes and misprints can be accepted. More extensive changes of the manuscript, inscriptions or overwriting cannot be accepted and will be disregarded. Proofs that are not delivered back in time cannot be accepted.

Article processing charge
Authors do not pay any article processing charge.

Open Access Statement
This is an open access journal which means that all content is freely available without charge to the user or his/her institution. Users are allowed to read, download, copy,

Editorial Office
Prague Medical Report
Kateřinská 32, 121 08 Prague 2, Czech Republic
e-mail: medical.report@lf1.cuni.cz
Phone: +420 224 964 570. Fax: +420 224 964 574

Prague Medical
REPORT
(Sborník lékařský)